CA1
DTC 801
85
T116
c.2

Department of Mechanical Engineering
University of New Brunswick
Fredericton, N.B.

TP 7519E

TANK CAR THERMAL RESPONSE ANALYSIS: VOLUME 6

PUBLISHED PAPERS

Prepared For:

TRANSPORT CANADA
TRANSPORTATION DEVELOPMENT CENTER
Montreal, Quebec H3A 2R3

Prepared By:

University of New Brunswick
Department of Mechanical Engineering
P.O. Box 4400
Fredericton, NB E3B 5A3

Library and Information Centre / Centre de documentation (BTLA)
RECEIVED / REÇU LE
AUG 14 1987
Transport Canada / Transports Canada

THE CONTENTS OF THIS REPORT REFLECT
THE VIEWS OF THE CONTRACTOR AND NOT
NECESSARILY THE OFFICIAL VIEWS OR
POLICIES OF THE TRANSPORTATION
DEVELOPMENT CENTER

REPORT DOCUMENTATION FORM

1. Transport Canada Report No.	2. TDC Project No.	3. Recipient's Catalogue No.
TP 7519E	4727	

4. Title and Subtitle	5. Report Date
Tank Car Thermal Response Analysis: Volume 6 Published Reports	
	6. Performing Organization Report No. UNB-ME-TF 29
7. Author(s)	8. Transport Canada File No.
J.E.S. Venart, A.C.M. Sousa, F.R. Steward, et al.	D1465-302-2
9. Performing Organization Name and Address	10. DSS File No.
Fire Science Centre University of New Brunswick P.O. Box 4400 Fredericton, N.B. E3B 5A3	11SD.T8200-2-2509
	11. DSS or Transport Canada Contract No. OSD82-00085
12. Sponsoring Agency Name and Address	13. Type of Report and Period Covered
Transportation Development Centre (TDC) Guy Favreau Complex 200 Dorchester Blvd. West, Suite 601, West Tower Montreal, Quebec H2Z 1X4	14. Sponsoring Agency Code TDC 4727
15. Supplementary Notes See also "Tank Car Thermal Response Analysis: Executive Summary", by J.E.S. Venart, March 1985, TP 6809E.	16. TDC Project Officer **D.W. Dibble**

17 Abstract

This collection of publications on the subject of Tank Car Thermal Response includes three abstracts, six technical papers, and one technical discussion:

1. "Fire and Explosion Loss Prevention and Safety Promotion in the Process Industries", 1983 - technical discussion.
2. "Thermal Modelling of LPG Rail Tank Cars Exposed to a Fire Environment", 1983 - abstract.
3. "Thermal Conductivity and Contact Conductance of EXPLOSAFE", 1983 - technical paper.
4. "The Physical Behaviour of LPG Tank Cars under Accident Conditions", 1984 - abstract.
5. "Radiative View Factors Associated with Rail Tank Car Fires", 1984 - abstract.
6. "Experiments on the Physical Modelling of LPG Tank Cars under Accident Conditions", 1984 - technical paper.
7. "Physical Behaviour of Pressure Liquified Fuel Tanks in Fire Accidents", 1984 - technical paper.
8. "Transient Thermal Stratification in Heated Partially Filled Horizontal Cylindrical Tanks", 1984 - technical paper.
9. "Incident Radiation from an Engulfing Pool Fire to a Horizontal Cylinder, Part I" and "Incident Radiation from a Flare to a Horizontal Cylinder, Part II", 1984 - technical papers.

18 Key Words	19. Distribution Statement
Accidents, BLEVE, Boiling, Fires, Pool, Propane, Railway, Tank Car, Thermal Response, Protection	Limited number of copies available from the Transportation Development Centre

20. Security Classification (of this report)	21. Security Classification (of this page)	22. No. of Pages	23. Price
Unclassified	Unclassified		---

TDC CDT 79-005

FORMULE DE DOCUMENTATION POUR RAPPORT

1. N° du rapport Transports Canada	2. N° de l'étude — CDT	3. N° de catalogue du destinataire
TP 7519E	4727	

4. Titre et sous-titre	5. Date du rapport
Tank Car Thermal Response Analysis: Volume 6 Published Reports	6. N° du rapport de l'organisme exécutant: UNB-ME-TF 29

7. Auteur(s)	8. N° de dossier Transports Canada
J.E.S. Venart, A.C.M. Sousa, F.R. Steward, et al.	D1465-302-2

9. Nom et adresse de l'organisme exécutant	10. N° de dossier — ASC
Fire Science Centre Université du Nouveau-Brunswick C.P. 4400 Fredericton, N.B. E3B 5A3	11SD.T8200-2-2509
	11. N° de contrat — ASC ou Transports Canada: OSD82-00085

12. Nom et adresse de l'organisme parrain	13. Genre de rapport et période visée
Centre de développement des transports (CDT) Complexe Guy-Favreau 200 ouest, boul. Dorchester, Suite 601, Tour Ouest Montréal, Québec H2Z 1X4	14. Code de l'organisme parrain: CDT 4727

15. Remarques additionnelles	16. Agent de projet — CDT
Voir aussi "Tank Car Thermal Response Analysis: Executive Summary", par J.E.S. Venart, mars 1985, TP 6809E.	D.W. Dibble

17. Résumé

Nomenclature de documents sur le thème du comportement thermique des wagons-citernes comprenant trois résumés, six mémoires et un exposé technique, comme suit:

1. "Fire and Explosion Loss Prevention and Safety Promotion in the Process Industries", 1983: exposé technique.
2. "Thermal Modelling of LPG Rail Tank Cars Exposed to a Fire Environment", 1983: résumé.
3. "Thermal Conductivity and Contact Conductance of EXPLOSAFE", 1983: mémoire.
4. "The Physical Behaviour of LPG Tank Cars under Accident Conditions", 1984: résumé.
5. "Radiative View Factors Associated with Rail Tank Car Fires", 1984: résumé.
6. "Experiments on the Physical Modeling of LPG Tank Cars under Accident Conditions", 1984: mémoire.
7. "Physical Behaviour of Pressure Liquefied Fuel Tanks in Fire Accidents", 1984: mémoire.
8. "Transient Thermal stratification in Heated Partially Filled Horizontal Cylindrical Tanks", 1984: mémoire.
9. "Incident Radiation from an Engulfing Pool Fire to a Horizontal Cylinder, Part I", et "Incident Radiation from a Flare to a Horizontal Cylinder, Part II, 1984: mémoires.

18. Mots-clés	19. Diffusion
Accidents, BLEVE, ébullition, flammes enveloppantes, propane, rail, wagon-citerne, comportement thermique, protection	Le Centre de développement des transports dispose d'un nombre limité d'exemplaires.

20. Classification de sécurité (de ce rapport)	21. Classification de sécurité (de cette page)	22. Nombre de pages	23. Prix
non classifié	non classifiée		—

TABLE OF CONTENTS

		PAGE
I	DISCUSSION: Paper I (A.F. Roberts) Fire and Explosion Loss Prevention and Safety Promotion in the Process Industries Proc. Sept. 12-16, (1983) Harrogate, IChemE.....	1-
II	ABSTRACT: "Thermal Modelling of LPG Rail Tank Cars - Exposed to a Fire Environment". 4th Int. Conf. on Mathematical Modeling, Zurich, (Aug. 15-17, 1983) p. 164-5.....	1-14
III	PAPER: "Thermal Conductivity and Contact Conductance of EXPLOSAFE", Proc. 18th Int. Thermal Conductivity Conf., Rapid City, South Dakota (Oct. 1983) in press.....	1-11
IV	ABSTRACT: "The Physical Behaviour of LPB Tank Cars under Accident Conditions", Comb. Inst. Can. Sect. Techn. Mtg. UNB *May, 1984.	1-5
V	ABSTRACT: "Radiative View Factors Associated with Rail Tank Car Fires", Comb. Inst. Com. Sect. Tech. Mtd., UNB, (May, 1984).....	1-6
VI	PAPER: "Experiments on the Physical Modeling of LPG Tank Cars under Accident Condition", Int. Symp. "Transport and Storage of LPG and LNG", Proc. Vol. 1 Royal Flemish Soc. of Engineers, Drugge (7-9th May 1984), p. 385-390.....	1-6
VII	PAPER: "Physical Behaviour of Pressure Liquefied Fuel Tanks in Fire Accidents". Proc. CSME 1984 Annual Conf. (May, 1984), Halifax, N.S., pp. 349-371.....	1-23
VIII	PAPER: "Transient Thermal Stratification in Heated Partially Filled Horizontal Cylindrical Tanks", ASME/AIChE National Heat Transfer Conference, Niagara Falls, N.Y., (Aug. 5-8, 1984), ASME Paper 84-HT-60.....	1-9
IX	PAPERS: "Incident Radiation from an Engulfing Pool Fire to a Horizontal Cylinder, Part I..	1-28
	"Incident Radiation From a Flare to a Horizontal Cylinder, Part II".....	1-31
	Fire Safety Journal (in press - accepted Feb. 6, 1984)	

EFCE Event No. 290

4th International Symposium on

Loss Prevention and Safety Promotion in the Process Industries

Organised by the Institution of Chemical Engineers in association with the Royal Institution of Naval Architects, held at Harrogate, England 12-16 September 1983

Supplementary Discussion Volume

THE INSTITUTION OF CHEMICAL ENGINEERS
SYMPOSIUM SERIES NOS. 80, 81 AND 82

ISBN 0 85295 159 0
ISBN 0 85295 160 4
ISBN 0 85295 161 2

FIRE AND EXPLOSION

I. Hymes

UKAEA

Paper 1: Dr. A. F. Roberts

Dr. S.J. Skinner, (Monsanto), asked if there had been any additional tests at Buxton to assess the durability of the various insulation materials used.

Dr. Roberts replied that in this series of trials there had been no such tests and that many properties in addition to thermal insulation needed to be taken into account when assessing the suitability of an insulation system.

Dr. Skinner, in a further question, asked if a steel shell had been used to hold the various insulants to the tank.

Dr. Roberts, who had indicated in his talk that he would be elaborating on the insulation, said that some of the insulation systems had been covered by a steel shell to give weather protection.

Replying to a question from Dr. J.E.S. Venart, (University of New Brunswick), Dr. Roberts said that the choice and size of PRV in the trials had been based upon the standard design requirements for the size of propane cylinder used. Valves of the same capacity had been used throughout the test series and as it emerged that the heat was affecting the performance of the valves,efforts had been made to steadily improve the insulation of the valve.

Dr. Venart then wanted to know if Dr. Roberts had a view on what caused the PRVs at Buxton to lift prematurely, i.e was it damage to the seat or softening of the spring? He would have expected film boiling to commence between 350 and 530 KW/m^2 yet Dr. Roberts' paper indicated about 250 KW/m^2. Could the transition to film boiling be due to the PRV performance?

Dr. Roberts replied that at Buxton there were clear indications of when film boiling had occurred and agreed that in some cases the pressure fluctuations when the PRV operated may have triggered the transition. More work to clarify the importance of this effect was probably merited.

Dr. Venart next asked if the percentage fill had been greater than 40% in any of the trials.

Dr. Roberts said the fill had been 40% in each case.

Dr. Venart then explained that he had conducted some experiments - not with propane but R11 and R12 - in which for the particular tank

used and heat inputs of > 100 Kk/m he had trouble with a two phase discharge from the PRV. Dr. Roberts said that in the Buxton trials as far as one could judge only vapour had been vented and that the tank always discharged in a safe manner.

Dr. I. Swift, (Fauske Associated USA), commented that many types of PRVs had been used in tests on railcars by Salat of the University of Maryland. None of these tests had proved very successful.

Dr. Roberts said he was aware of the work by Salat. In answer to a further question by Dr. Swift about the rate of temperature rise criteria for the insulants used at Buxton, Dr. Roberts said that in his trials the rate was as specified in the ASTM high rise test.

Paper 2: Mr. K. Palmer

Dr. A.V. Howard, (CEGB), noting the use of nitrogen as inert gas in the FRS trials asked whether the alternative use of chlorinated hydrocarbons had been considered. Mr. Palmer replied that alternative suppressants had not been looked for. Cholorinated hydrocarbons would be expensive and whilst their injection to about 10% v/v would suppress flaming, the extinction of smouldering would require the flooding of the test volume.

In a further question Dr. Howard enquired whether coal dust had been used in any of the FRS tests and if so what type of coal had been used and were the vapours analysed?

Mr. Palmer confirmed that coal dust had been used. A soft coal had been chosen for its ready smoking and smouldering characteristics. About 35% m/m volatiles were typically evolved. Analysis of the vapours would be complicated and had not been attempted.

Professor Napier commented that Finch of the BCURA had published some information on the composition of coal volatiles.

Mr. D. Chambers of Babcock Woodall Duckham asked if the FRS had experimented upon PVC cable insulation. Mr. Palmer thought it unlikely that PVC would exhibit the smouldering phenomenon since its unusual smoke gneration mechanism gives rise to large initial volumes of hydrogen chloride. Should the PVC be subjected to gross prior overheating there may be problems but no definitive opinion could be given.

Dr. I. Swift of Fauske and Associates, USA, asked whether any materials had been investigated in the FRS smouldering trials which hadn't given rise to flammable fumes.

Mr. Palmer explained that the aims of the trials had not included this point but certain substances having low calorific values may show such behaviour.

IV INT. CONF. ON MATHEMATICAL MODELING
Zurich, August 15-17, 1983.

IV ICMM	UNB	TITLE
1	22	

THERMAL MODELLING OF LPG RAIL TANK CARS EXPOSED TO A FIRE ENVIRONMENT

BY

A.C.M. SOUSA AND J.E.S. VENART
DEPARTMENT OF MECHANICAL ENGINEERING
UNIVERSITY OF NEW BRUNSWICK
FREDERICTON, N.B.
CANADA E3B 5A3

IV ICMM	UNB	INTRODUCTION I
2	22	

OBJECTIVE

To develop a mathematical model of heat transfer processes in a rail tank car under fire conditions

POTENTIAL USES OF THE MODEL

Prediction of tank car dynamic response with and without thermal protection

Analysis of test results

IV ICMM	UNB	INTRODUCTION II
3	22	

MOTIVATION

RAIL TANK CARS INVOLVED IN A RISING NUMBER OF ACCIDENTS, RESULTING IN DEATH, SERIOUS INJURY, EXTENSIVE PROPERTY DAMAGE AND DISRUPTIVE MAJOR EVACUATIONS.

EVALUATION OF NEW THERMAL PROTECTION SYSTEMS.

IV ICMM	UNB	PRE-MODELLING REQUIREMENTS
4	22	

UNDERSTANDING OF PARTICIPATING PHYSICAL PHENOMENA
THROUGH ANALYSIS OF EXPERIMENTAL DATA FROM:

FIELD TESTS, AND

LABORATORY OBSERVATIONS

IV ICMM	UNB	SUGGESTED MODEL EQUIVALENT THERMAL NETWORK
5	22	

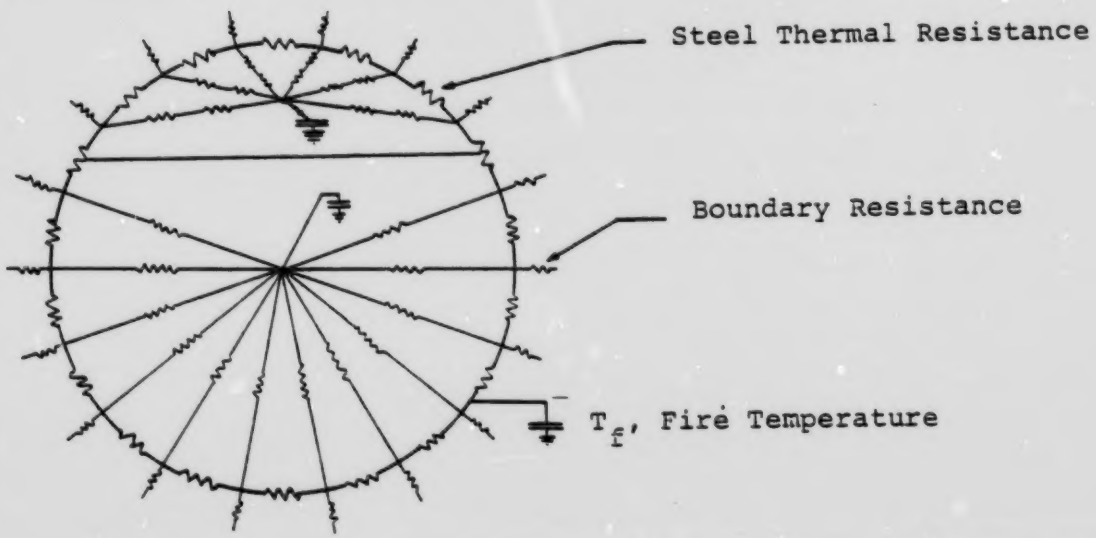

IV ICMM	UNB	MAIN FEATURES OF THE MODEL
6	22	

TRANSIENT CONDUCTION THROUGH THE TANK WALL WITH OR WITHOUT EXTERNAL PROTECTION

TWO-CONTROL VOLUMES WITH THE TANK, AT THE BOTTOM (LIQUID) AND AT THE TOP (VAPOUR) PORTIONS OF THE TANK

SELECTION OF THERMODYNAMIC STATE :

	TOP	BOTTOM
1.	SUPERHEATED	SATURATED
2.	SATURATED	SUBCOOLED
3.	SATURATED	SATURATED

IV ICMM	UNB	AUXILIARY FEATURES OF THE MODEL
7	22	

ADDITIONAL COMPUTATIONS

FLOW THROUGH THE PRESSURE RELIEF VALVE

SIMPLIFIED ANALYSIS OF THE STRESS STATES

SUPPLIED AS INPUT:

ANALYTICAL EXPRESSIONS FOR THE INTERNAL AND EXTERNAL HEAT TRANSFER COEFFICIENTS.

FIRE CONDITIONS VS. TIME.

LPG AND TANK MATERIAL PROPERTIES

PRESSURE RELIEF VALVE DATA

IV ICMM	UNB	CONSERVATION EQUATIONS
8	22	

MASS

VAPOUR $\dot{M}_G = - M_{G,Rv} + M_B$ (1)

LIQUID $\dot{M}_F = - M_{F,Rv} - M_B$ (2)

ENERGY

VAPOUR $\dot{U}_G = -(M.h)_{G,Rv} + M_B.h_F - P\dot{V}_G + \dot{Q}_G$ (3)

LIQUID $\dot{U}_F = -(M.h)_{F,Rv} - M_B.h_F - P\dot{V}_F + \dot{Q}_F$ (4)

DEFINITIONS

$\dot{U}_G = \dot{H}_G - \dot{(PV_G)}$; $\dot{U}_F = \dot{H}_F - \dot{(PV_F)}$; $H = (M.h)$

IV ICMM	UNB	COMPUTATIONAL STEPS OF THE MARCHING SOLUTION
9	22	

STEP 1: DETERMINE TOTAL HEAT SUPPLIED TO THE TANK.

STEP 2: CALCULATE HEAT TRANSFER COEFFICIENTS FOR LIQUID AND GAS REGIONS, RESPECTIVELY.

STEP 3: FIND $\dot{Q}_G$ AND $\dot{Q}_F$.

STEP 4: CHECK PRESSURE FOR RELIEF VALVE ACTION.

STEP 5: CALCULATE MASS OF RELEASE IF VALVE IS OPEN.

STEP 6: START ITERATION TO DETERMINE NEW PRESSURE LEVEL THAT SATISFIES ENERGY BALANCE.

IV ICMM	UNB	COMPUTATIONAL STEPS (CONTINUATION)
10	22	

STEP 6 (CONT.) SUPERHEATED VAPOUR PROPERTIES DETERMINED FROM:

EQ.(3) AND $v_G = v_G(h_G, P)$

SUBCOOLED LIQUID PROPERTIES DETERMINED FROM:

EQ.(4) AND $v_F = v_F(h_F, P)$

NEW MASSES FOR GAS AND LIQUID

$$M_{TOTAL} = M_F + M_G$$

$$M_F = M_F(M_{TOTAL}, v_F, v_G)$$

IV ICMM	UNB	COMPUTATIONAL STEPS (CONTINUATION)
11	22	

STEP 6 (CONT.)

ENERGY BALANCE

$$Q_{IN} = (M,h)_G^{(n+1)} - (M,h)_G^{n} + (M,h)_{G,Rv}^{n+\frac{1}{2}} - v_G^{n+\frac{1}{2}} \cdot$$

$$(P^{n+1} - P^{n}) + (M.h)_F^{n+1} - (M,h)_F^{n} + (M,h)_{F,Rv}^{n+\frac{1}{2}} -$$

$$V_F^{n+\frac{1}{2}}(P^{n+1} - P^{n})$$

STEP 7 CHECK FOR CONTENTS AND STRUCTURAL INTEGRITY OF THE TANK.

STEP 8 IF TANK HAS NOT FAILED AND LIQUID PHASE DOES EXIST IN THE TANK RETURN TO STEP 1.

IV ICMM	UNB	
12	22	FIG. 1 PRESSURE VS. TIME

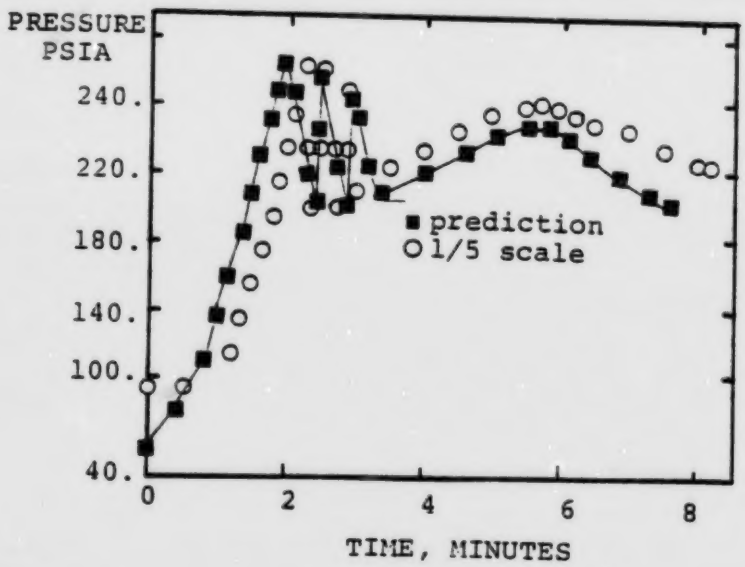

IV ICMM	UNB	FIG. 2 LIQUID TEMPERATURE VS. TIME
13	22	FIG. 3 WETTED AREA VS. TIME

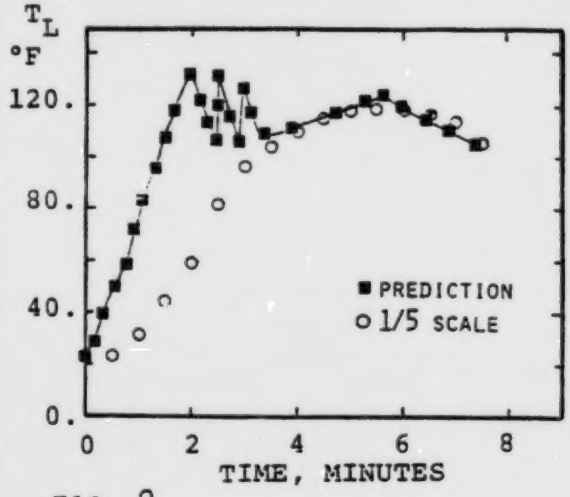

FIG. 2

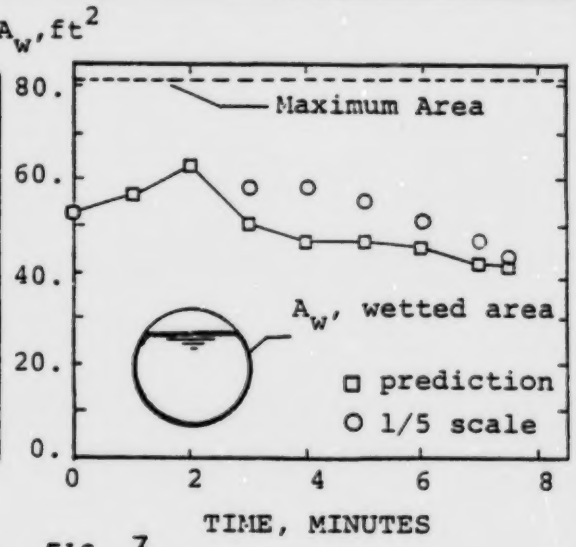

FIG. 3

IV ICMM	UNB	FINAL COMMENTS
14	22	

THE MODEL PREDICTS WITH REASONABLE ACCURACY THE MAIN PRESSURE - RELATED EVENTS, SUCH AS, VALVE OPENING AND TANK RUPTURE.

THE UNCERTAINTY OF THE SUPPLIED INPUT DATA, INCLUDING VALVE BEHAVIOUR, PRECLUDES AT THIS TIME FURTHER REFINEMENT OF THE MODEL AND A RELIABLE ACCURACY EVALUATION.

THERMAL CONDUCTIVITY AND CONTACT CONDUCTANCE OF EXPLOSAFE

J. E. S. Venart
University of New Brunswick, Fredericton, N. B., Canada

R. C. Prasad*
University of New Brunswick, Saint John, N. B., Canada

M. P. Callaghan
University of New Brunswick, Fredericton, N. B., Canada

ABSTRACT

The thermal conductivity of "EXPLOSAFE", an expanded aluminum foil used to augment the heat transfer in a pressure vessel, was measured experimentally over a temperature range of 5°-70° C. Measurements were obtained with different styles, orientations and thicknesses of EXPLOSAFE. In addition, the thermal contact conductance for an EXPLOSAFE matrix and wall interface was determined for one particular style as a function of pressure and a simple correlation developed.

A guarded hot-plate apparatus with an on-line Micro-Computer (Hewlett Packard-85) and the Hewlett Packard-3497 Data Acquisition System was used.

KEYWORDS

Thermal conductivity, EXPLOSAFE, contact conductance, contact resistance, expanded aluminum foil.

INTRODUCTION

"EXPLOSAFE" is an expanded aluminum foil which is used to augment the heat transfer in a pressure vessel and minimize or eliminate the possibility of explosion [1,2] . Programs are underway [3] for evaluating the effectiveness of using EXPLOSAFE for interior lining of railway tank cars and truck transport carrying liquid propane gas (LPG) as a protection against BLEVE (Boiling Liquid Expanding Vapor Explosion) under accident and/or fire conditions. The thermal conductivity of EXPLOSAFE and the conductance at the wall-interface are important parameters in such studies.

EXPERIMENTAL

A guarded hot plate apparatus (GHPA) was used to measure the thermal conductivity and contact conductance. The apparatus (Figure-1) consisted of a hot plate and two cold plates, one on either side of the hot plate. Two identical samples of EXPLOSAFE were clamped between the hot and cold plates. A guard heater surrounded the hot plate along the edge to prevent heat loss through the edges. The cold plates contained double-wall jacket through which cold fluid at controlled temperature was circulated. Four spring scales were affixed to the apparatus to measure the interfacial contact pressure between the hot/cold plates and the EXPLOSAFE sample. The guard heater, the main heater and the cold plate temperature were suitably adjusted to obtain a desired temperature difference (ΔT) or heat flux, Q. The steady state temperature difference across the EXPLOSAFE sample and the heat flux were measured to determine apparent thermal conductivity, λ_a, inclusive of the contact conductance effect. The true thermal conductivity, λ_t, of the sample was measured after application of a thermal contact grease (Wakefield Thermal Compound 120-8) at the contacting surfaces where the thermal conductance was assumed to be infinite.

$$Q = \lambda_t A \left[\frac{\Delta T_L}{\Delta X_L} + \frac{\Delta T_R}{\Delta X_R} \right] \qquad (1)$$

Using these results, the contact conductance, h_c, was calculated from the measurement in tests where thermal contact grease was not applied.

$$\frac{\Delta T_L}{(\Delta X_L/\lambda_a)} + \frac{\Delta T_R}{(\Delta X_R/\lambda_a)} = \frac{Q}{A} = \frac{\Delta T_L}{(2/h_c) + (\Delta X_L/\lambda_t)} + \frac{\Delta T_R}{(2/h_c)+(\Delta X_R/\lambda_t)} \qquad (2)$$

All data-acquisition and data-processing were performed with a Hewlett-Packard 3497 Data Acquisition System controlled by a Hewlett-Packard-85 Micro Computer.

TEST SAMPLES

EXPLOSAFE samples were supplied by the Vulcan Industrial Packaging Limited, Canada. The various styles (styles I, II, III) and orientations (V and H) in which they were tested, are shown in Figure-2. For styles I and II,V and H indicate the direction of the normal to the plane of the unit cell of the EXPLOSAFE mesh. For style III, V and H refere to the orientation of the major axis of the unit cell. Samples of thicknesses 25 mm and 50 mm were tested.

THEORETICAL PREDICTIONS

A theoretical model was developed to predict the thermal conductivity of EXPLOSAFE for styles I and III. It was assumed that heat was transferred across the EXPLOSAFE thickness only by conduction through the aluminum foil. Theoretical value of the thermal conductivity λ_{th} was obtained from

$$\lambda_{th} = \lambda_{al} \frac{\Delta X}{L_p} \cdot \frac{A_f}{A_e} \qquad (3a)$$

where $A_e = A_{vap} + A_l$

Path Length, L_p, and cross-sectional area, A_f, of the heat conduction path through aluminum foil as well as the effective cross-sectional area, A_e, of EXPLOSAFE per conduction path as shown in Figure-3 were obtained from the test samples by direct measurement.

RESULT AND DISCUSSION

The apparent thermal conductivity, λ_a, of all the samples were measured at mean sample temperatures of 5°-70°C (Figure-4).

The conductivity of styles II and III were lowest and highest respectively. Also, 25 mm thick sample of a given style and orientation consistently indicated an effective conductivity value lower than that for a 50 mm thick sample of the same style and orientation. This is attributed to the thermal contact resistance/conductance between test samples and hot/cold plates. As 25 mm and 50 mm samples both have the same contact resistance at constant pressure, it follows that the apparent conductivity of a thin sample will be less than that of a thick sample.

The samples were examined for any significant physical differences. It was found that 50 mm thick samples of style 3V were approximately 10 percent more dense than the 25 mm thick samples. The apparent conductivity of all 25 mm thick samples were thus normalized (Equation-4) to correct for the density differences.

$$\lambda_n = \frac{\rho_{3\text{-}50}}{\rho_{3\text{-}25}} \lambda_m \qquad (4)$$

True thermal conductivities for styles I and III were measured experimentally as well as estimated theoretically (Equation-3). The results are summarized in Table-1.

Table-1 True thermal conductivity of EXPLOSAFE

style	λ_t, $W.m^{-1}.K^{-1}$	
	Theoretical	Experimental
style I	0.409	0.45
style II	0.106	0.20
style III	2.414	2.25 H
		2.60 V

The apparent thermal conductivity, λ_a, as a function of pressure was measured for style III in the range of 1.69 to 4.65 k Pa (Figure-5). An increase in λ_a with increasing pressure resulted due to improved contact conductance at the EXPLOSAFE-place interface. Using the results of Figure-5 and equation (2), the thermal contact conductance was determined as a function of pressure. The following correlation was developed for h_c:

$$h_c = -1.236 + 183.011\ P - 22.146\ P^2 \qquad (5)$$

CONCLUSION

Thermal conductivity of EXPLOSAFE was measured for samples of three different styles, different orientations and thicknesses. A theoretical model is developed to estimate the thermal conductivity for styles I and III. The theoretical predictions are compared with experimentally measured values.

Thermal contact conductance of EXPLOSAFE-plate interface was estimated as a function of interfacial pressure and a simple correlation is proposed.

ACKNOWLEDGEMENTS

This work was performed under a program of studies funded by the Transport Canada under contract number OSD82-00085.

NOMENCLATURE

A Surface area of heater, m^2

A_1 Projected area of one conduction path (Figure-3), m^2

A_e Equivalent heat flow area, m^2

A_f Cross-sectional area of conduction path through the aluminum foil (= wt), m^2

A_{vap}	Area of vapor space between adjacent layers (Figure-2), m^2
a	Semi-major diagonal of the unit cell (Figure-3), m
b	Semi-minor diagonal of the unit cell (Figure-3), m
H	Horizontal
h_c	Thermal contact conductance, $W.\ m^{-2}.K^{-1}$
L	Length of one side of the unit cell (Figure-3), m
L_p	Path length for heat conduction through aluminum foil (Figure-3), m
P	Interface pressure, kPa, $kN.\ m^{-2}$
Q	Heat flow rate, W
t	Thickness of aluminum foil strand (Figure-3), m
V	Vertical
w	Width of aluminum foil strand (Figure-3), m
ΔT	Temperature difference across the thickness of the test sample, deg K
ΔX	Thickness of the test sample, m
λ	Thermal conductivity, $W.m^{-1}.K^{-1}$
ρ	Density of the test sample, $Kg.m^{-3}$

Subscripts:

a	apparent
al	aluminum
L	Left side
m	measured
R	Right side
t	true
th	theoretical
3-25	style III, 25 mm thick sample
3-50	style III, 50 mm thick sample
n	normalized

REFERENCES

1. R. D. Appleyard, "Testing and Evaluation of the EXPLOSAFE System as a Method of Controlling the Boiling Liquid Expanding Vapor Explosion (BLEVE)", Report #TP2740, EXPLOSAFE Division of Vulcan Industrial Packaging Ltd., Toronto, Canada, August 1980.
2. Financial Times - Markets, June 04, 1982.
3. J. E. S. Venart, "Tank Car Thermal Response Analysis", Interim Report for Transport Canada, Report # UNB-ME-TF18, August 1983.

a) GUARDED HOT-PLATE ASSEMBLY

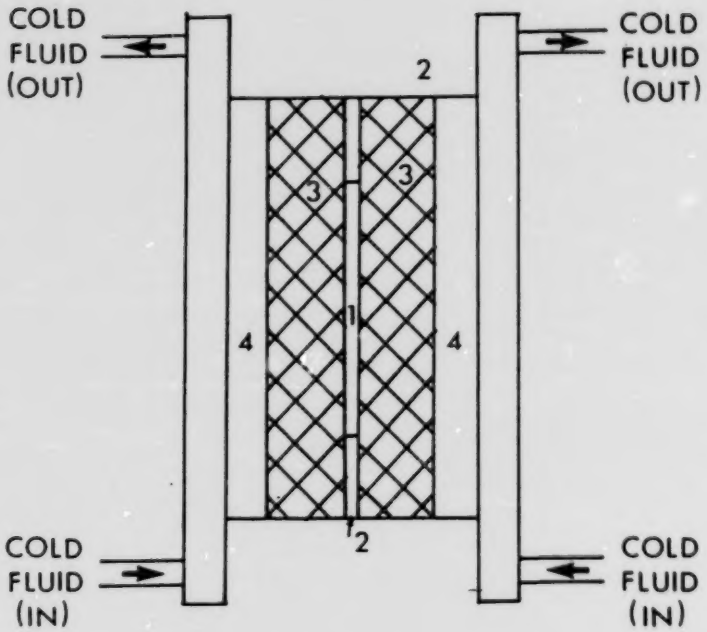

b) MAIN HEATER - GUARD HEATER ASSEMBLY

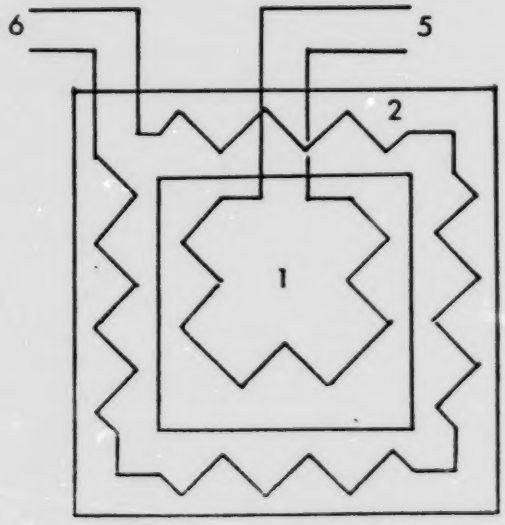

LEGEND

1. MAIN HEATER (MH)
2. GUARD HEARTER (GH)
3. TEST SAMPLE
4. COLD PLATE
5. MH POWER SUPPLY
6. GH POWER SUPPLY

Figure - 1 Guarded Hot Plate Apparatus.

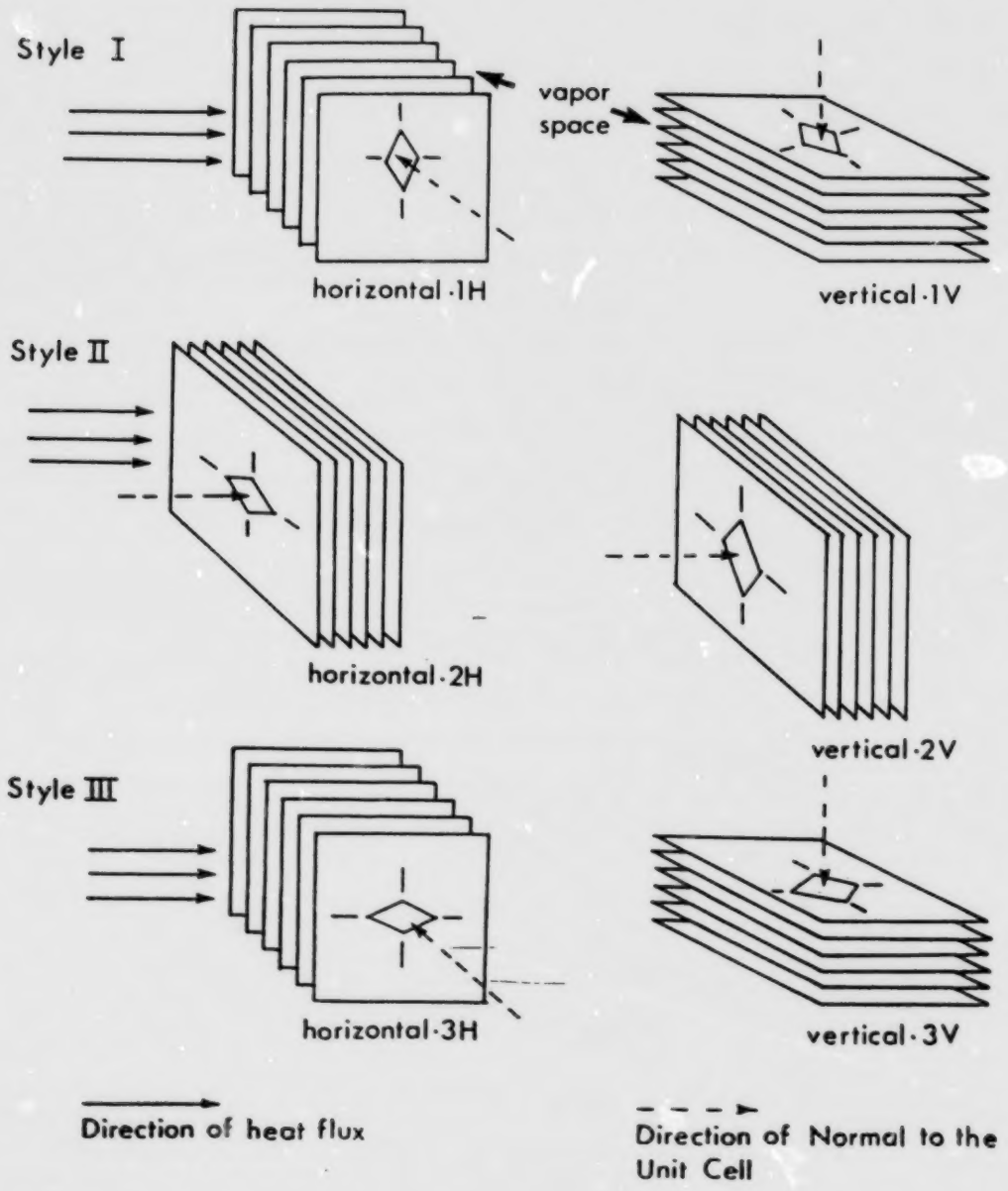

Figure - 2 EXPLOSAFE Styles and Orientations

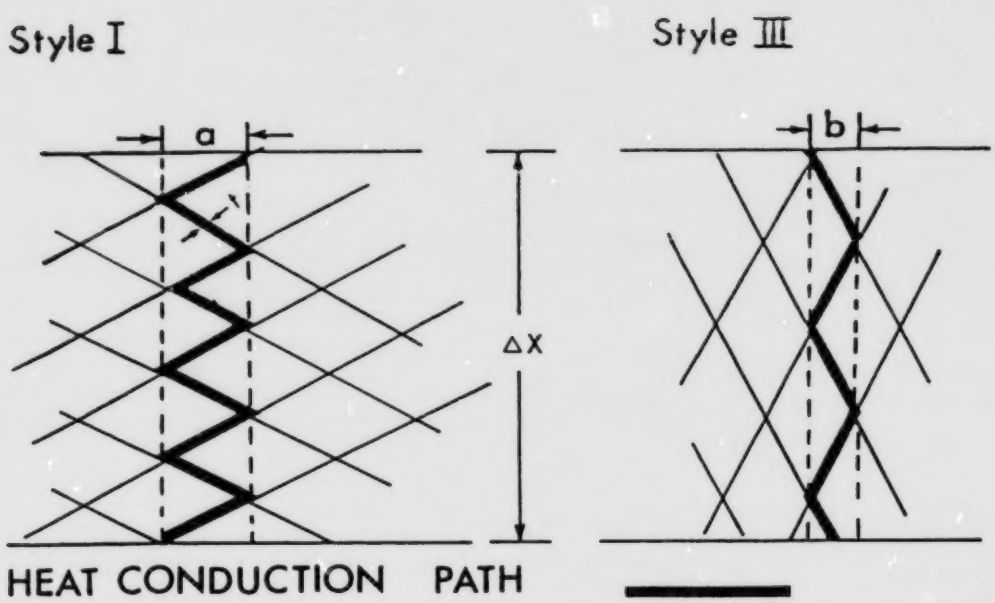

for above illustrations;

Style I $L_P = 9L$

$A_1 = a \times w$

Style III $L_P = 4.5$

$A_1 = b \times w$

Figure - 3 Heat transfer model for EXPLOSAFE

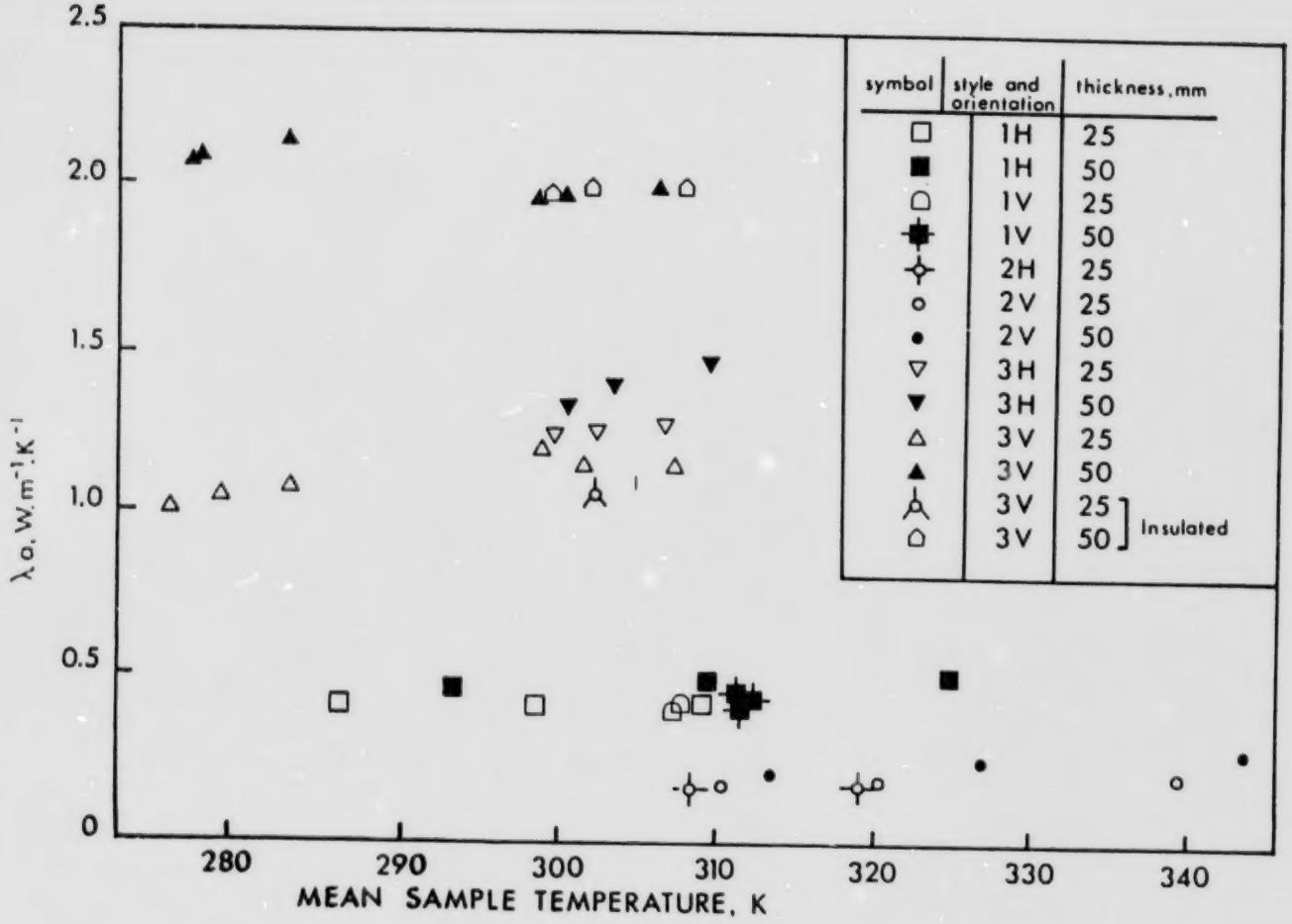

Figure - 4 Apparent thermal conductivity of EXPLOSAFE

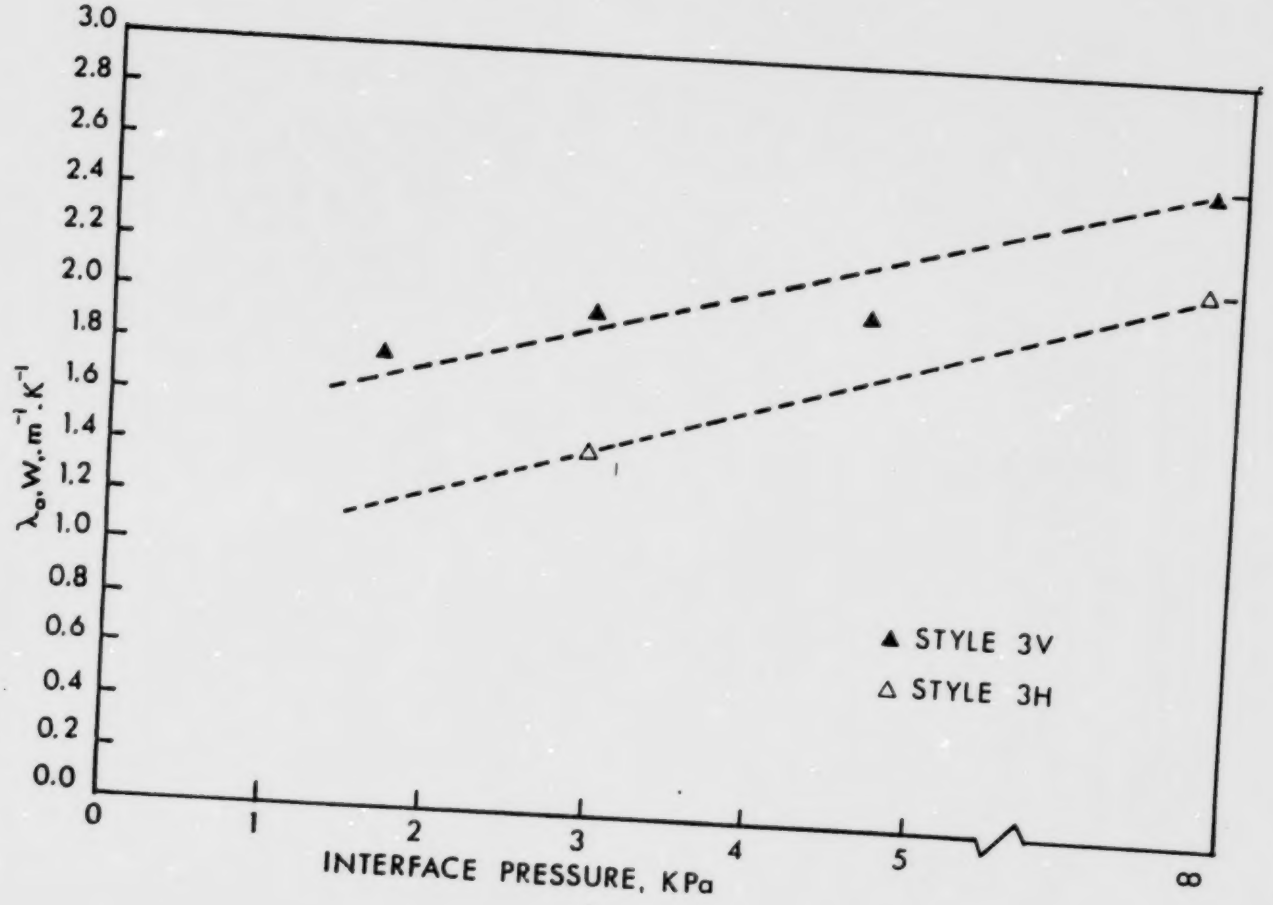

Figure - 5 Apparent thermal conductivity of EXPLOSAFE as a function of pressure

THE PHYSICAL BEHAVIOUR OF LPG TANK CARS UNDER ACCIDENT CONDITIONS

J.E.S. Venart, A.C.M. Sousa, F.R. Steward and R.C. Prasad
Fire Science Centre
University of New Brunswick
Fredericton, N.B.
Canada E3B 5A3

Introduction

Pressurized liquefied fuels are widely used in domestic, commercial and industrial installations. An increase in the consumption of such fuels within Canada is being encouraged by the Federal Government through its National Energy Program (1). The transportation of such fuels relies primarily on rail and road tank cars. A number of accidents involving such vehicles has produced extensive property damage, serious personal injury and a number of deaths in recent years. Major evacuations have also been necessary in some cases with one incident in Mississauga which caused the evacuation of almost a quarter of a million people for periods of up to five days (2).

In a typical accident, a tank car carrying a compressed flammable commodity, such as propane, LPG, is punctured due to a derailment or impact. The propane is released and subsequently ignited by sparks, or a hot car component (e.g., a hot brake). This results in a torch or a pool fire which may project onto or engulf other tank cars. These cars in turn are heated and unless properly vented by means of suitably sized relief valves, will fail and explode. The explosions are often extremely severe with major pieces of the exploding tanks and undercarriage being propelled up to 680 metres from their initial locations (2). Secondary fires frequently occur at and between the sites where the pieces come to rest. If significant amounts of fluid are released prior to ignition large vapour cloud explosions can occur with tragic loss of life and severe property damage.

In order to better understand this behaviour and to determine protection strategies the Transportation Development Center of Transport Canada has been supporting an experimental study at the Fire Science Centre of the University of New Brunswick (3). A laboratory test facility has been constructed to serve as a physical model of the internal fluid of such a tank car exposed to fire conditions. The test facility allows for data collection and visual observation in both the liquid and vapor phase during simulated fire conditions. This paper presents some preliminary results of the investigation.

Apparatus

The test facility was of a cylindrical steel tank with plexiglass end walls to allow visual observation during test runs.

The apparatus consists of an electrically heated horizontal double walled pressure vessel (40 l), a variable area pressure relief valve, PRV (6-25mm dia.), 25mm thick observation windows, and instrumentation, Fig. 1. R 11 and R 12 are used to simulate the LPG lading. The PRV is solenoid operated and may be controlled to open at 105 percent and close at 95 percent of tank pressure as for the real situation. The PRV may additionally be oriented at any angle from vertically upward to downward to emulate a variety of locations under accident conditions.

The instrumentation includes up to fifty shielded and stainless steel sheathed iron or copper constantan thermocouples and pressure transducers in the vessel and after the PRV. The time dependend mass of the lading is measured by four capacitance load cells which output frequency. An HP 85-3497A data acquisition and control system acts as overall system controller and data reduction, recording, and plotting unit. Time synchronized video records are made of all tests.

Heater power (0-65 kW/m^2) is maintained by use of manually controlled 220 V 3 phase variacs. There are nine individual heater elements located around the inner stainless steel tank between the mild steel argon cooled outer vessel. These elements may be controlled together or individually to simulate pool or torch fire heat flux distributions.

The test program, utilizing both R11 and R12, has been implemented using a variety of lading fills (78, 58 and 25 percent), power levels, (25, 50 and 65 kW/m^2) and pressure relief valve orifice sizes (6-25mm) for both subcooled and saturated initial conditions.

Results

To date the basic experiments have indicated the very complex nature and interdependence of the phenomena. The pressure, temperature, and mass temporal response as a function of heat flux, level, initial pressure (temperature, i.e. subcooling) are all necessary in order to be able to properly scale (3) the results to full size (4) or other situations (5).

The elements that have the most profound effect on the tank behaviour are the amount of thermal stratification and hence subcooling, the pressure-time and temperature-time responses of the PRV and the boiling and swelling phenomena.

Figure 2-4 give representative data obtained from the pressure vessel test facility.

Figure 2 gives the pressure in the vessel as a function of time during a typical run which ultimately led to sustained venting where the pressure relief valve remained open after two open-close ventings.

Figure 3 presents the vertical temperature distribution within the pressure vessel as a function of time before and shortly after the first vent by the pressure relief valve.

Figure 4 gives the vertical temperature distribution within the pressure vessel during and after the second vent by the pressure relief valve.

The test fluid was refrigerant 11, trichlorofluoromethane for the data presented.

Discussion

As the liquid and vapor ladding in the pressure vessel receives heat through the wall from the electrical heaters the pressure rises with time. The pressure within the vessel reaches the set point of the pressure relief valve which opens venting to the atmosphere until the depressurization allows the valve to close. In this particular experiment this cycle occurred twice. When the valve opened a third time the rate of heat added to the ladding was sufficient to maintain a sustained venting.

Figure 3 indicates that before the pressure relief valve opens the liquid gradually forms a warm stratified layer at the the surface. Visual observations indicate that the liquid heated at the wall rises to the surface and moves to the centre of the vessel. The warm surface layer gradually increases in thickness with time.

Once the pressure relief valve opens, Figure 4, the liquid flashes within this stratified layer cooling the liquid to a nearly uniform temperature. When the pressure relief valve closes the stratified temperature distribution was re-established.

A number of runs were made to evaluate the effect on the heat transfer within the vessel of an aluminium foil mesh, EXPLOSAFE, on the inside wall. While there was some difference in the heat transfer characteristics of the vessel with this material present it was concluded that the addition of this material would not yield a substantial improvement in preventing BLEVE's.

Conclusions

The most significant conclusions drawn from this study at this time are:

1) There is a complex heat transfer and fluid dynamic interaction within the pressure vessel during the heating and venting of simulated fire conditions.

2) There is significant stratification within the liquid phase prior to the opening of the pressure relief valve.

3) Venting by the pressure relief valve produces flashing in the warm surface layer of the liquid which cools the layer giving a more uniform temperature within the liquid phase.

4) The characteristics of the pressure relief valve significantly effect the later stages of the simulated fire conditions.

5) Simple thermodynamic and heat transfer models may be used to predict the pressure response of the vessel under test conditions.

References

1) National Energy Program Task 5; New Liquid Fuels; 5.5 Fuel in Transportation, Ottawa, Canada 1983.
2) Grange, S.G.M., "Report on the Mississauga Railway Accident Inquiry", Supreme Court of Ontario, TP2828, 1983.
3) Zuber, N., "The Problems in Modelling of Small Break LOCA", Heat Transfer in Nuclear Reactor Safety, Eds. Bankoff and Afgan, Hemisphere, New York, pp 3-48 (1982).
4) Anderson, C., Townsend, W., Zook, J. and Cowgill, G., "The Effects of a Fire Environment on a Rail Tank Car Filled with LPG", FRA-OR and D, 75-31, (1974).
5) Appleyard, R.D., "Testing and Evaluation of the EXPLOSAFE System as a Method of Controlling the Boiling Liquid Expanding Vapour Explosion (BLEVE)", TP 2740 Dept. of Res. and Dev. EXPLOSAFE Div., Vulcan Industrial Packaging Ltd., (1980).

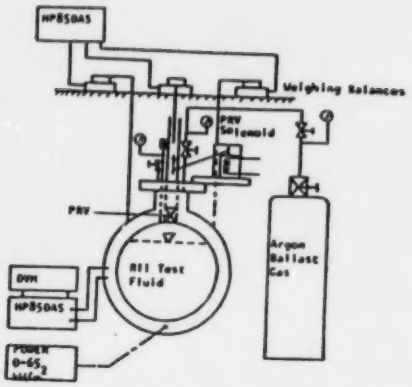

Fig. 1. Experimental Pressure Vessel to Simulate Fire Conditions of LPG Tank Car.

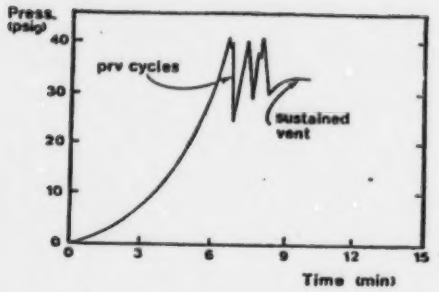

Fig. 2. Pressure Time Response for the Vessel with 78% Initial Fill, 6mm Diameter PRV and Heating Rate of 65 kW/m^2.

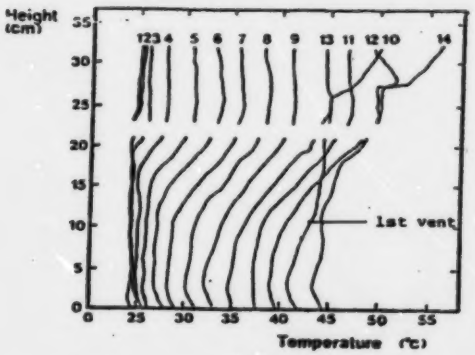

Fig. 3. Vertical Temperature Distribution within Pressure Vessel Before Opening of PRV, 58% Initial Fill, 6mm Diameter PRV and Heating Rate of 65 kW/m^2. Interval Between Scans 30 seconds.

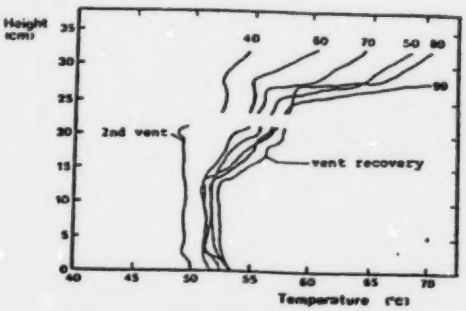

Fig. 4. Vertical Temperature Distribution within Pressure Vessel During and After Second Venting, 58% Initial Fill, 6mm Diameter PRV and Heating Rate of 65 kW/m^2, Interval Between Scans 30 seconds.

RADIATIVE VIEW FACTORS ASSOCIATED WITH RAIL TANK CAR FIRES

F.R. Steward, M. Tung, J.E.S. Venart and S. Wong
Fire Science Centre
University of New Brunswick
Fredericton, N.B.
Canada E3B 5A3

Introduction

An accident involving a number of rail tank cars carrying a liquefied gaseous fuel under pressure often results in a fire followed by an explosion. A part of the scenario of such an accident is a non-damaged tank car surrounded by burning fuel released from a ruptured tank nearby. As the non-damaged tank car is heated by the fire the pressure within the tank car rises until the pressure relief valve opens releasing a jet of fuel at high velocity which ignites forming a turbulent diffusion flame.

This paper is concerned with developing the relations for the interchange factors between the pool fire and the surface of the tank car, the turbulent diffusion flame and the tank car and the interaction of the radiation when the two fires exist simultaneously.

A laboratory apparatus has been constructed to study the interaction between the two flames and a simulated tank car experimentally.

Radiative Interchange Factors

Radiative interchange factors which are applicable to this problem have been calculated previously.

A compilation of radiative interchange factors associated with naturally occurring fires was made a number of years ago by Steward (1). Studies are available on the radiative interchange factors required for determining the radiative heat flux from a pool fire to the tank car surface (2-6). Two studies are also available on the radiative transfer from a turbulent diffusion flame to the tank car surface (7,8).

The radiative interchange factor between a pool fire and a surface within the fire can be determined from the triple integral.

$$\frac{d^2 g_s}{dA} = \int_0^Z \int_0^{R(z)} \int_0^{\pi} \frac{2k(z-h)e^{-kr}\rho d\theta d\rho dz}{\pi r^3} \qquad (1)$$

with the geometry defined in Figure 1.

The vector r between the element of gas volume and the surface can be determined as

$$r = (x^2+\rho^2+2x\rho\cos\theta+(z-h)^2)^{\frac{1}{2}} \tag{2}$$

The radius of the pool fire as a function of height was given by a polynomial based on experimental data (8)

$$R(z) = a_o+a_1z+a_2z^2+a_3z^3+a_4z^4 \tag{3}$$

with $a_o = 2.24$ m $\quad a_1 = -0.3806$

$a_2 = 0.6202\text{x}10^{-1}$ m^{-1} $\quad a_3 = 0.1219\text{x}10^{-1}$ m^{-2}

$a_4 = -0.3706\text{x}10^{-2}$ m^{-3}

Numerical evaluation of the above integral was carried out and the solution is presented in Figure 2.

The radiative interchange factor between a cone and a surface surrounding its base has been evaluated previously (1) by the evaluation of the triple integral.

$$\frac{d^2gs}{dA} = \int_0^Z \int_0^{az} \int_0^{\pi} \frac{2kz\ e^{-ks}\rho d\theta d\rho dz}{\pi r^3} \tag{4}$$

with the geometry defined in Figure 3.

The vector r between the element of gas volume and the surface can be determined as

$$r = (x^2+\rho^2+z^2+ 2x\rho\cos\theta)^{\frac{1}{2}} \tag{5}$$

The absorbing path length along the vector r is given by

$$s=r\left(1-\frac{x}{u^2-a^2z^2}\left((x+\rho\cos\theta) - \sqrt{a^2z^2-\rho^2\sin^2\theta}\right)\right) \tag{6}$$

when $u^2 \neq a^2z^2$

$$s=r\left(1 - \frac{x}{2(x+\rho\cos\theta)}\right) \tag{7}$$

when $u^2 = a^2z^2$

$$u^2 = x^2+\rho^2+2x\rho\cos\theta \tag{8}$$

The evaluation of the above integral yields the desired interchange factor presented in Figure 4.

The interchange factor which includes the interaction between the two flames is that shown in Figure 5. This calculation has not yet been performed at this time and is presently under development.

Apparatus

It was deemed desirable to have a direct measurement of the effect of the interaction of the propane jet flame on the heat transfer between a pool fire and a surface within the pool fire. Such an apparatus was constructed and is shown in Figure 6.

The pool fire is maintained at a steady state by continuously adding fuel into the centre of the liquid fuel pool. The flow rate of the propane into the burner producing the propane flame is controlled by a valve in the line.

Preliminary measurements taken on a cylindrical calorimeter inserted into the pool fire show only a small effect of the propane flame on the heat transfer to the calorimeter. However, these measurements were made for a propane flame to pool fire heat liberation rate of 0.52. The value of this ratio estimated from field tests is 3.5 to 4.0. This heat release rate of the propane flame is too great for the laboratory setup and the experiment will be relocated outside in the near future.

Conclusions

1) The radiative interchange factor between a pool fire and a surface within the fire has been evaluated.
2) The radiative interchange factor between a turbulent flame and a surface surrounding its base has been determined.
3) The interaction of a turbulent flame and the pool fire is being investigated. The major objective of this investigation is to determine the effect of the interaction on the heat transfer to a surface within the pool fire.

References

1) Steward, F.R., "Radiative Heat Transfer Associated with Fire Problems", Heat Transfer in Fires, Part IV, Scripta Book Company, Washington, D.C., (1974).
2) Fang, J.B. and Steward, F.R., "A Radiative Interchange Factor for Fire Propagation in a Porous Medium", Combustion Science and Technology, 4, 138-90, (1971).
3) Birk, A.M. and Oosthuizen, P.H., "Model for the Prediction of Radiant Heat Transfer to a Horizontal Cylinder Engulfed in Flames", ASME, 82-WA/H2-52, (1982).
4) May, W.G. and McQueen, W., "Radiation from Large Liquefied Natural Gas Fires", Combustion Science and Technology, 7, 51-6 (1973).

5) Mitsoulis, E.C., "Liquid Pool Fires", M.Sc. Thesis, Chemical Engineering Department, University of New Brunswick, Fredericton, N.B.
6) DeRis, J., "Fire Radiation - A Review", Seventeenth Symposium (International) on Combustion, The Combustion Institute, Pittsburgh, 1003-16, (1978).
7) Brzustowski, T.A., Gollahalli, S.R., Gupta, M.P., Kaptein, M. and Sullivan, H.F., "Radiative Heating from Flames", ASME, 75-H2-4 (1975).
8) Becker, R., "Mathematical Model of Luminous Flame Radiation for the Determination of Safety Zones", Ger. Chem. Eng., 3, 229-33, (1980).

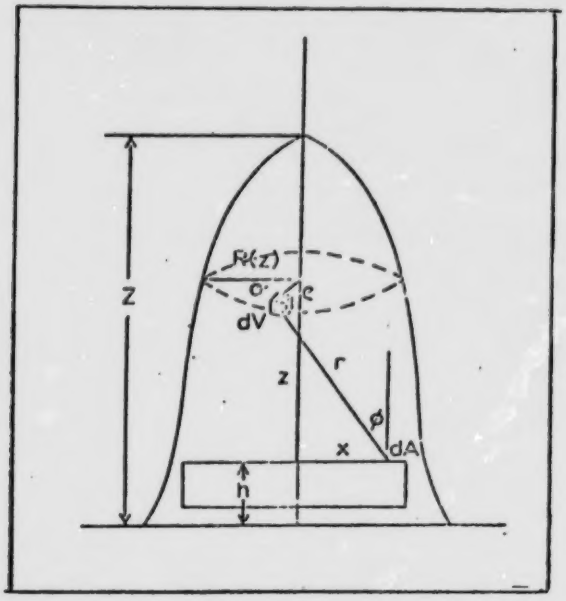

Fig. 1. Geometry of Radiative Interchange Factor Between a Pool Fire and the Surface of a Tank Car.

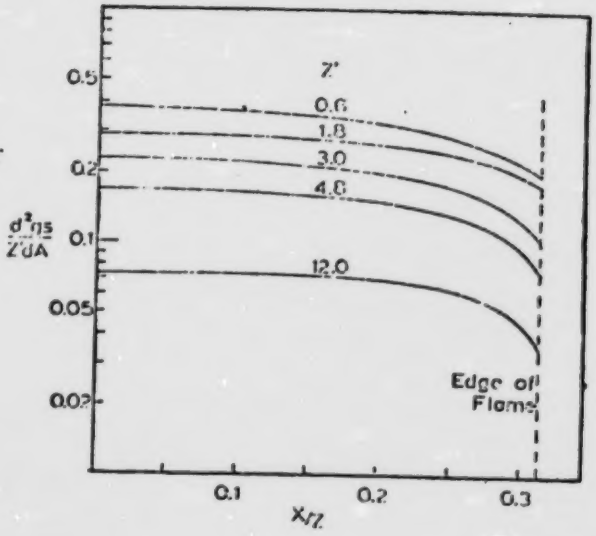

Fig. 2. Radiative Interchange Factor Between a Pool Fire and a Horizontal Surface with the Fire Located on a Tank Car. Height of Surface to Height of Flame Ratio = 0.15.

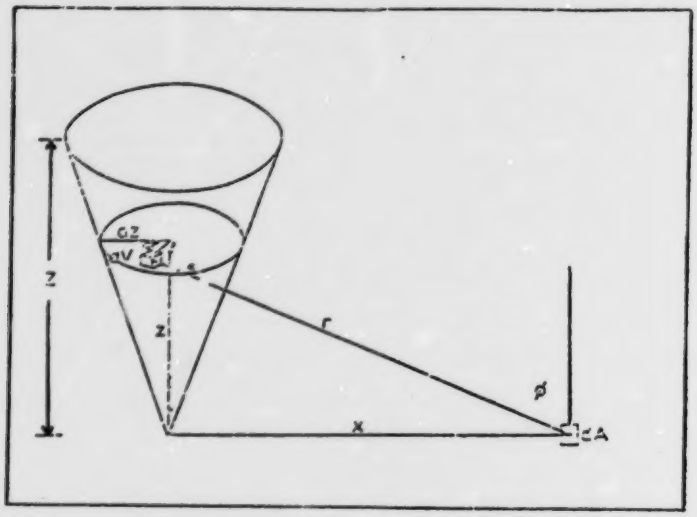

Fig. 3. Geometry of Radiative Interchange Factor Between Turbulent Jet Flame and a Horizontal Surface Surrounding Base of Flame.

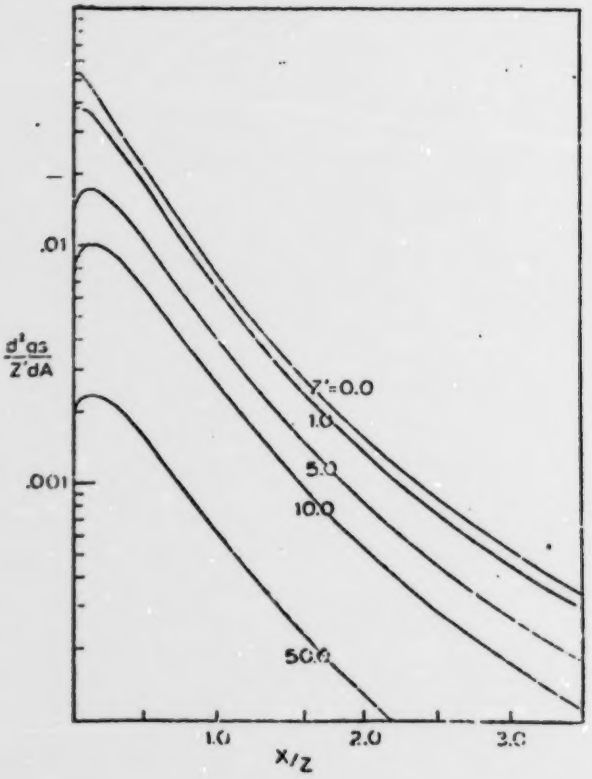

Fig. 4. Radiative Interchange Factor Between a Turbulent Jet Flame and a Horizontal Surface Surrounding Base of Flame.

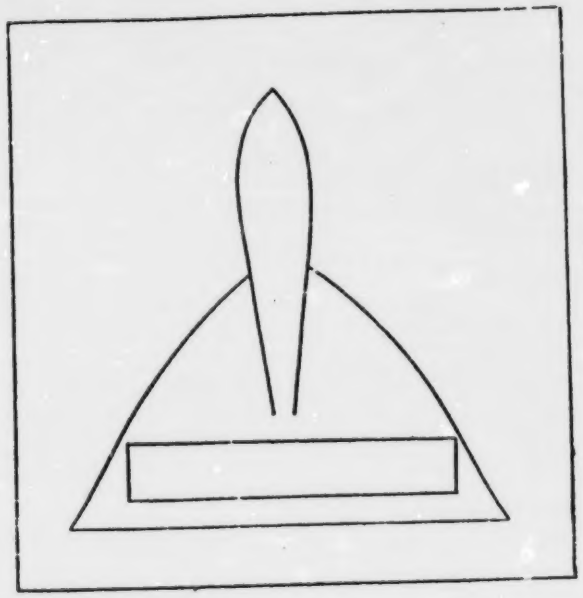

Fig. 5. Interaction of Turbulent Jet Flame with Pool Fire.

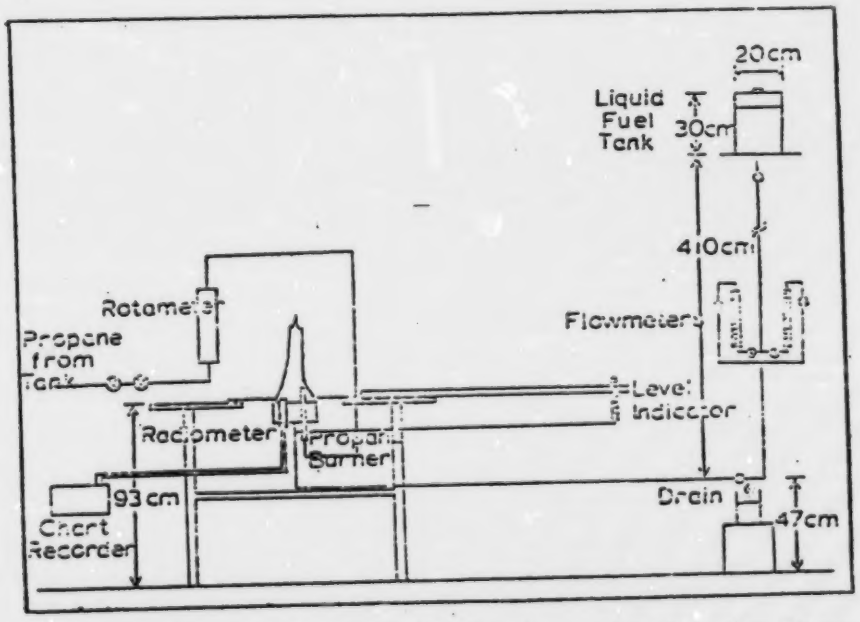

Fig. 6. Laboratory Apparatus for Investigating the Interaction of a High Velocity Turbulent Flame with a Pool Fire.

Proc. Int. Symp. Transport & Storage LPG / LNG Brugge May 7-10/84.

EXPERIMENTS ON THE PHYSICAL MODELLING OF LPG TANK CARS UNDER ACCIDENT CONDITIONS

J.VENART, A.SOUSA, F.STEWARD, R.PRASAD,
University of New Brunswick, Fire Science Centre,
Fredericton, N.B., Canada

ABSTRACT

The paper describes an experimental programme designed to show the influence of various fire accident conditions on the LPG lading and tank. The primary areas of interest identified and addressed in the paper are: i) tank, fluid, and pressure relief valve (PRV) temporal response with fire conditions; ii) liquid and vapour stratification, and iii) boiling and swelling behaviour.

Systematic experiments using R11 illustrate the influence of initial subcooling, boiling, fill level, relief cross section, and PRV characteristics on fluid behaviour.

INTRODUCTION

Railroad tank cars transporting such hazardous fluids as propane, butadiene, ammonia, ethylene, vinyl chloride and chlorine have been involved in a rising number of accidents. These accidents have caused death, serious injury, extensive property damage and disruptive major evacuations. In 1979 one Canadian incident, involving the derailment of twenty-one tank cars, nineteen of which were carrying dangerous commodities, caused the evacuation of almost a quarter of a million people for periods of up to five days (1).

In a typical accident, a tank car carrying a compressed flammable commodity, such as propane is punctured due to a derailment or impact. The propane is released and subsequently ignited by sparks, or a hot car component (e.g. a hot brake). This results in a torch or a pool fire which may project onto or engulf other tank cars. These cars in turn are heated and unless properly vented by means of suitably sized relief valves, will fail and explode. The explosions are often extremely severe with major pieces of the exploding tanks and undercarriage being propelled up to 680 meters from their initial locations. Secondary fires frequently occur at and between the sites where the pieces come to rest. If significant amounts of fluid are released prior to ignition large vapour cloud explosions can occur with tragic loss of life and severe property damage.

In order to better understand this behaviour and to determine protection strategies the Transportation Development Center of Transport Canada has been supporting a study at the Fire Science Center of the University of New Brunswick (2).

The results of this still preliminary investigation form the basis of a study of the thermohydraulic behaviour of real tanks in accident conditions. An understanding of the complex interactions between vessel, PRV, fire, and lading are necessary in order to develop a general computer code for design purposes and for safety analyses.

HEAT TRANSFER TO THE TANK AND LPG

The heat transfer to the LPG in the tank surrounded by a fire consists of:

1) radiation from the flames and convection from the combustion gases plus heated air to the walls of the tank, reradiation of the tank wall;
2) radial and circumferential conduction and thermal storage in the tank wall;
3) heat transfer to the LPG liquid and vapour.

Table 1 outlines the various sub-problems that must be addressed in order to fully describe the complete situation.

Table 1: Tank car sub-problems:

Thermal properties
Geometry
Pool fire PRV flare description and interaction
Pressure and temperature response
Vapour and liquid thermal stratification
PRV action
Boiling and liquid "swelling"
Internal and external protection systems

From the above the following will be briefly described here; i) Pool fire PRV flare interaction, ii) boiling and liquid swelling, and iii) pressure-temperature response, PRV action, and vapour and liquid stratification.

TEST FACILITY

The test facility for the above items consists of three experimental setups: i) heated pressure vessel, ii) small scale pool fire and PRV flare rig, and iii) boiling and swell determination apparatus.

Heated Pressure Vessel

The pressure vessel consists of an electrically heated horizontal double walled pressure vessel (40 l), a variable area PRV (6-25 mm dia.), 25 mm thick observation windows, and instrumentation, Fig. 1. R 11 and R 12 are used to simulate the LPG lading. The PRV is solenoid operated and may be controlled to open at 105 percent and close at 95 percent of tank pressure as for the real situation. The PRV may additionally be oriented at any angle from vertically upward to downward to emulate a variety of locations under accident conditions.

The instrumentation includes up to fifty shielded and stainless steel sheathed iron or copper constantan thermocouples and pressure transducers in the vessel and after the PRV. The time dependent mass of the lading is measured by four capacitance load cells which output frequency. An HP 85-3497A data acquisition and control system acts as overall system controller and data reduction, recording, and plotting unit. Time synchronized video records are made of all tests.

Heater power (0-65 kW/m^2) is maintained by use of manually controlled 220 V 3 phase variacs. There are nine individual heater elements located around the inner stainless steel tank between the mild steel argon cooled outer vessel. These elements may be controlled together or individually to simulate pool or torch fire heat flux distributions.

Systematic tests are performed wherein the fill level, initial temperature (pressure), PRV orifice area, and heat flux are varied (Table 2).

Table 2. Experimental Programme

Fill(%)	Power(kW/m^2)	PRV (dia.mm)	Fluid	Comment
85,55,25	25,50,65	6-25	R11,R12	subcooled, saturated

Pool Flare Interaction

The interaction between a pool fire and the turbulent [illegible]ame produced by the opening of the PR[illegible] [illegible]ject of some controversy. The [illegible] to the vapour space of the tank [illegible] determining factor as to the [illegible]accident. The question arises [illegible]he turbulent propane flame sig[illegible]nts or alters the heat trans[illegible] fire to the outside of the

A small scale propanol/kerosene pool fire 305 mm diameter with a water cooled sonic propane burner is being used. Measurements of the total heat flux to a cylindrical calorimeter as well as a water cooled radiometer will permit determinations of local and total heat fluxes. Temperatures are being measured by means of a small suction pyrometer and all these will permit this question to be answered (3).

Boiling and Swelling Apparatus

Tank storage and transport normally utilize large horizontal cylinders or spheres and hence the interior fluid sees a variety of surface inclinations and heat fluxes under accident conditions. A test apparatus is therefore designed to study the effects of heat flux, surface inclination, and pressure in both the nucleate and film boiling regions in R 11. Tests to 180 kW/m^2 at inclination angles from 0-180 degrees are reported in (4).

RESULTS

To date the basic experiments have indicated the very complex nature and interdependence of the phenomena. The pressure, temperature, and mass temporal response as a function of heat flux, level, initial pressure and temperature (ie. subcooling) are all necessary in order to be able to properly scale (5) the results to full size (6) or other situations (7).

The elements that have the most profound effect on the tank behaviour are the amount of thermal stratification and hence subcooling and superheat, the pressure-time and temperature-time responses, and the boiling and swelling phenomena.

Thermal Stratification

When the walls of the tank are heated the heat is initially conducted into the fluid core and vapour space. After a short time delay, buoyancy forces overcome gravitational forces and the fluid adjacent to the walls rises along the walls up to the free surface, forming thermally stratified layers in both the liquid and vapour regions. These layers in turn set the vapour pressure and hence initial PRV action.

An unstable boundary region exists at the bottom of the cylinder and this is responsible for the heating of the subcooled core. Both these phenomena are illustrated in Fig. 2, with some results of temperature-height at various time steps. An analysis (8) of these results has been quite successful as is also shown in the same figure.

Pressure-Time Response

The pressure continues to increase as heating continues eventually opening the PRV at the set pressure (typically 105% of relief pressure). The depressurization caused by this relief, after a brief delay, results in the homogeneous

flashing of that liquid in the stratified layer at or above the saturation temperature corresponding to the instantaneous pressure. Fig.3 illustrates the type of pressure record obtained for this along with the PRV's subsequent closure at the lower set pressure (typically 95% of relief pressure). Once closed the flashing ceases, stratification reestablishes itself and the pressure again rises. Subcooled boiling by now may well be established in the liquid boundary layers on the walls with its rate and mode being established by surface conditions (temperature and nucleation characteristics) and local heat flux. Valve action will continue as long as the rate of vapour generation in the boundary layer is less than that being relieved by the valve; this will be for as long as the liquid core and hence the boiling remains subcooled. Dependent upon the relief area, surface characteristics, and heat flux the valve may now remain open and the pressure remains essentially constant. In this stage there is both heterogeneous boiling at the tank wall in addition to the homogeneous boiling occurring in the bulk. Fig. 4 shows the change over in temperature distribution during this period. Fig. 5 illustrates the wall, vapour, and liquid temperatures for the same period.

The temporal temperature response of the thermocouple located at the top of the tank and at entry to the PRV indicates the initial discharge is superheated vapour followed by two phase fluid. The quantity and quality of this discharge decrease with decreasing fill level; with high lading fills (70-80%) the liquid entrained by the Bernoulli effect (5) causes the initial discharge of large liquid slugs. This fluid originates from the boundary layer and stratified layer boiling.

When the inside walls are covered with an aluminium foil mesh (EXPLOSAFE*) for the purpose of enhancing mixing, a more rapid but comparable thermal stratification occurs. This too can be modelled (8) as is shown in Fig. 6.

The opening of the pressure relief valve results in the rapid decrease of tank pressure. PRV closure is however usually effected prior to any pressure recovery as is noted for depressurization of steam generators, PWR's (9), or chemical reactors (10).

With large relief areas this pressure relief causes severe superheating of the liquid and results in massive heterogeneous and homogeneous vapour generation resulting in the bulk obtaining temperature uniformity faster than with smaller relief areas. As fill levels are lowered for the same relief area less liquid superheat occurs.

Once boiling occurs in the wall boundary layer the single phase stratification will no longer describe the local heat transfer coefficients and experimental data for nucleate or film pool boiling must be obtained as a function of heat flux and angle since fire engulfment tests have suggested that boiling in the tank may be either nucleate (6,7) or film (11).

Boiling and Liquid Swelling

There have been very few boiling experiments reported that utilize large surfaces coupled with variation in angle of inclination. Fig. 7 (4) illustrates the type of results obtained here. At low heat fluxes there is an increase in heat transfer coefficient as the angle of inclination is increased. As the heat flux increases and boiling commences the heat transfer coefficient becomes independent of angle for all but the highest angles. Use of "high flux" surfaces (Fig. 8) results in considerable improvement in heat transfer due to the increased number of active nucleation sites.

Although the above are steady state results their use may be justified in the transient heating model being developed here since pseudo thermodynamic equilibrium can be shown to apply after very short times (600 ms) (9).

General Model

The following model may therefor be postulated to describe the heat transfer process of the LPG liquid: i) the incidence of boundary layer boiling will be governed by a time dependent CTausius-Clapeyron relation, ii) for no boiling the transient stratified convection model will define the LPG-wall heat transfer, iii) with boiling empirical representations of the steady state boiling curves will be used, and iv) the effective two-phase fluid height may be defined in terms of a swell height that initially disregards the non-equilibrium effects of the flashing liquid.

A simplified version of such a model is in fact extremely successful in predicting the pressure response of certain tests (Fig. 9) (13). Modifications to this model are currently underway.

CONCLUSION

The most significant conclusions drawn from this study thus far are:

1. The transient data obtained has revealed the existence of a very complex interaction of lading fill, subcooling, PRV size and action, boiling, and both vapour and liquid thermal stratification with heat flux.
2. Prior to PRV action the primary vapour generation source originates in the liquid boundary layer. With PRV depressurization, flashing in the stratified layer assumes some importance on the rate of pressure recovery with PRV closure.

*Vulcan Industrial Packaging Ltd., Rexdale, Ontario, Canada

3. PRV closure in the early stages is affected by fill level; more complete fills entail larger surface areas and hence greater vapour generation and thus after an initial cycling period the rate of generation exceeds the relieving capacity of the valve and the unit remains open. With smaller fills the generation rate is lower and therefore the valve cycles.
4. Significant nonuniform void fraction distributions exist within the system during the early stages of PRV action due to the considerable amount of vapour and liquid thermal stratification.
5. Thermal stratification within the fluid and its subsequent flashing may be successfully modelled.
6. Simple thermodynamic and heat transfer models may be used to predict the pressure response of such vessels.

ACKNOWLEDGEMENT

Funding for this work was provided by the Natural Sciences and Engineering Research Council of Canada and Transport Canada, Transportation Development Center.

REFERENCES

(1) Grange, S.G.M. (Dec. 1980) "Report on the Mississauga Railway Accident Inquiry," Supreme Court of Ontario, TP2828.

(2) Venart, J.E.S., Sousa, A.C.M., Steward, F. R., and Lenard, J.G. (Oct. 1981) "Tank Car Thermal Modeling, a Proposal to Supply and Services Canada," DSS 09SDT8200-1-1540, UNB ME/TF-09.

(3) Tunç, M., Steward, F.R., and Venart, J.E. S. (May 1984) "A Pool Fire PRV Flare Interaction Model," Canadian Section Combustion Institute Meeting, Fredericton, N.B.

(4) Jung, D.S., Venart, J.E.S. and Sousa, A.C. M. (July 1984) "Nucleate and Film Boiling in R11: The Effects of Inclination Angle and Surface Enhancement," 1st U.K. National Heat Transfer Conference, Leeds.

(5) Zuber, N. (1982) "The Problems in Modeling of Small Break LOCA", Heat Transfer in Nuclear Reactor Safety, Ed. Bankoff and Afgan, Hemisphere, New York, pp. 3-48.

(6) Anderson, C., Townsend, W., Zook, J., and Cowgill, G. (Sept. 1974) "The Effects of a Fire Environment on a Rail Tank Car Filled with LPG," FRA-OR&D 75-31.

(7) Appleyard, R.D. (Aug. 1980), "Testing and Evaluation of the EXPLOSAFE System as a Method of Controlling the Boiling Liquid Expanding Vapour Explosion (BLEVE)," TP 2740 Dept. of Res. and Dev. EXPLOSAFE Div. Vulcan Industrial Packaging Ltd.

(8) Aydemir, N.U., Sousa, A.C.M., and Venart, J.E.S. (Aug. 1984) "Transient Thermal Stratification in Heated Partially Filled Horizontal Cylindrical Tanks," ASME/AIChE National Heat Transfer Conference, Niagara Falls.

(9) Hutcherson, M.N., Henery, R.E., and Wollersheim, D.E. (1983) "Two Phase Vessel Blowdown of an Initially Saturated Liquid - Part 1: Experimental," J. Heat Transfer (105) 687-693.

(10) Friedel, L. and Purps, S. (June 1982) "Experimental Analysis of Vessel Depressurisation by Top Venting," European Two Phase Flow Group Meeting, Paper D 2, Paris.

(11) Roberts, A.F., Cutler, D.P., and Billings, K. (1983) "Fire Engulfment Trials with LPG Tanks," Proc. 4th Int. Symp. Loss Prevention and Safety Promotion in the Process Industries, Vol. 3 p D1-D10, I ChemE Symposium Series 82.

(12) Singh, K.P. and Gupta, J.P., "Transient Swelling of Liquid Level During Pool Boiling in an Emergency Condenser," Letters in Heat and Mass Transfer 8, pp. 25-33.

(13) Sousa, A.C.M. and Venart, J.E.S. (1983) "Thermal Modelling of LPG Rail Rank Cars Exposed to a Fire Environment," 4th Int. Conference on Mathematical Modelling, August 15-17.

FIGURES

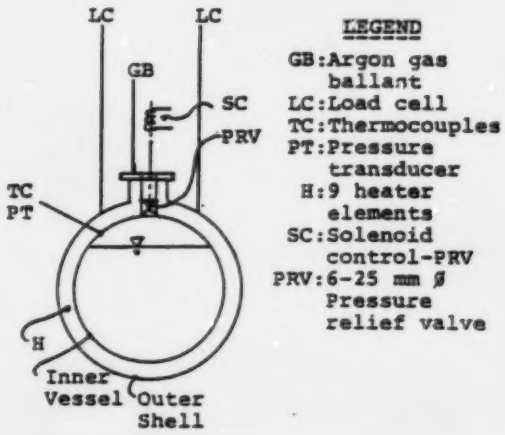

1. TEST FACILITY-HEATED PRESSURE VESSEL.

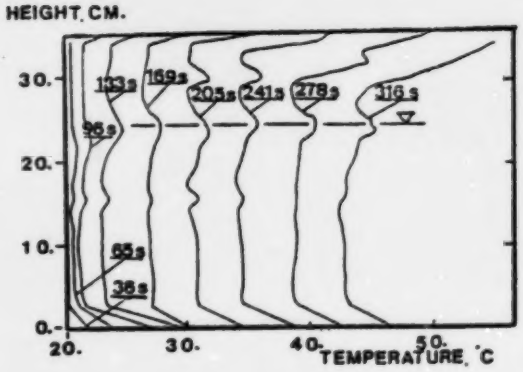

2. TEMPERATURE-HEIGHT-TIME: 78% FILL, 6 mm ⌀ PRV, 65 kW/m²

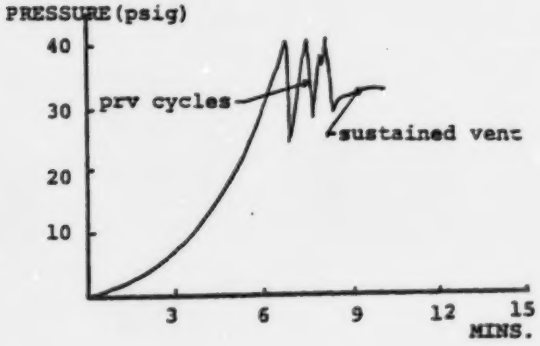

3. PRESSURE-TIME RESPONSE: 6 mm ⌀ PRV, 65 kW/m² a) 78% Fill b) 58% Fill.

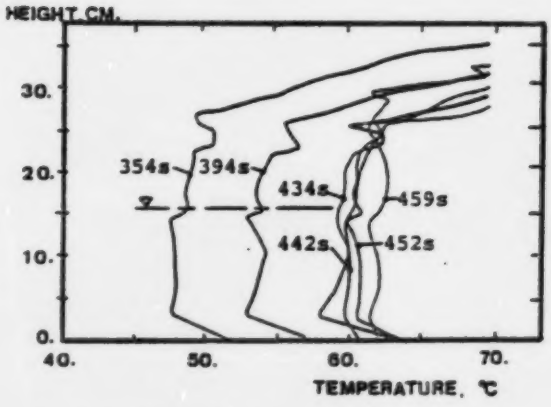

4. TEMPERATURE-HEIGHT-TIME: 58% Fill, 6 mm ⌀ PRV, 65 kW/m².

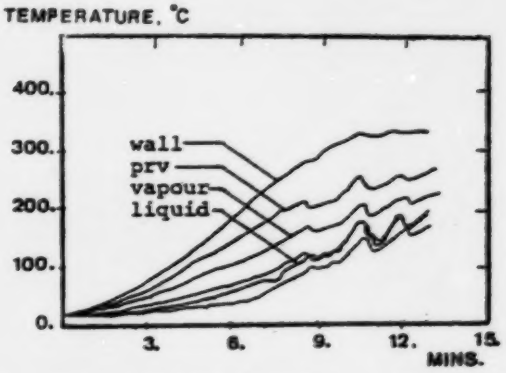

5. TEMPERATURE-TIME RESPONSE: % Fill, 6 mm ⌀ PRV, 65 kW/m²; WALL AND BULK TEMPERATURES IN VAPOUR AND LIQUID SPACES.

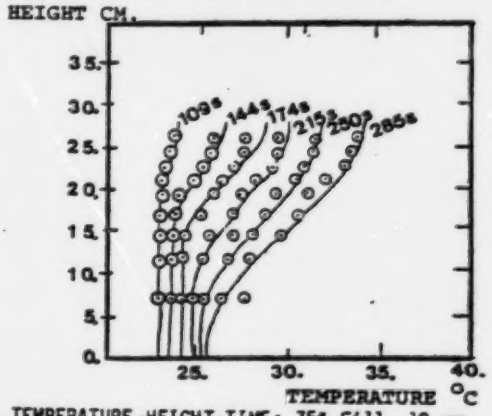

6. TEMPERATURE-HEIGHT-TIME: 75% Fill, 10 mm ⌀ PRV, 40 kW/m²; EXPLOSAFE.

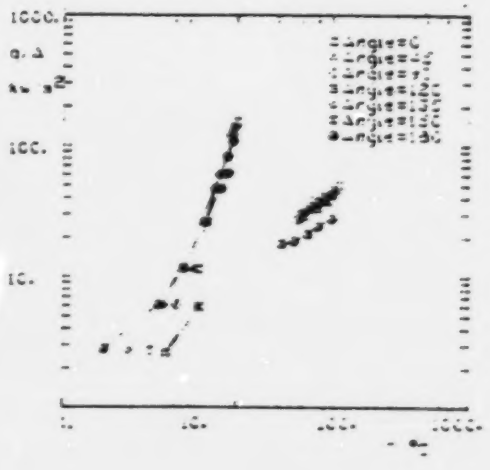

7. POOL BOILING HEAT TRANSFER WITH R 11: Effects of Surface Inclination.

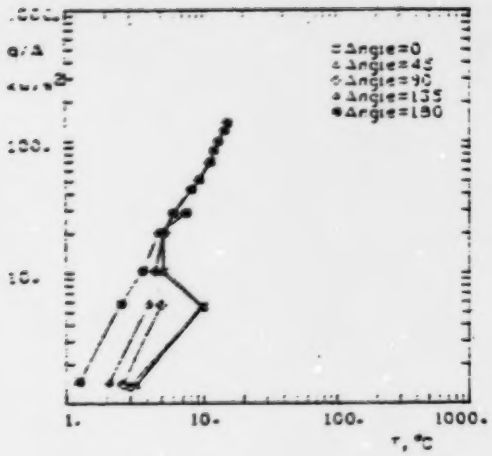

8. POOL BOILING HEAT TRANSFER WITH R 11: Effect of High Heat Flux Surface.

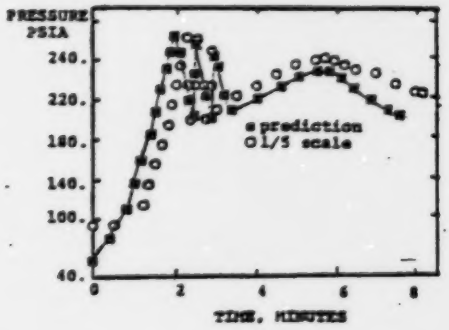

9. FIFTH SCALE PRESSURE TIME BEHAVIOUR.

THE PHYSICAL BEHAVIOUR OF PRESSURE LIQUEFIED FUEL TANKS UNDER ACCIDENT CONDITIONS

LA CONDUITE PHYSIQUE DES RESERVOIRS SOUS PRESSION POUR COMBUSTILES LIQUÉFIÉS EN CONDITIONS D'ACCIDENT

J.E.S. Venart, A.C.M. Sousa, F.R. Steward, R.C. Prasad
Fire Science Center
University of New Brunswick
Fredericton, N.B., Canada E3B 5A3

ABSTRACT

The paper reports on work concerned with the formulation, analysis modelling, simulation and verification of the fire induced heat transfer to tanks containing pressure liquefied fuels (LPG, LNG). The time dependent behaviour of the contents (pressure, temperature, and level (mass)), pressure relief valve(s) (open-close sequence, mass flow rate), and flare (strength and position), tank (temperatures and stresses), fire surrounds (intensity and location) and protection (both external and internal) has been simulated in order to determine whether full size tanks protected by a specific technique will explode or BLEVE when exposed to pool or torch fire environments.

RÉSUMÉ:

On rapporte l'étude concernant avec la formulation, l'analyse, le modélage, la simulation et la vérification du transfert de chaleur induit par le feu à des réservoirs contient combustibles liquéfiés et pressurisés. En fonction du temps la conduite du contenu (la pression, la température et le niveau (masse)), soupape de soulagement de pression (la succession de l'ouverture et la fermeture, le flux massique), et la flamme (la force et la position) , réservoir (les temperatures et les contraintes), environs du feu (l'intensité et la location) et protection (extérieur et intérieur) a été simulée pour determiner si un réservoir de grand format protecté par une technique specifique exposé a un milieu de feu de masse ou de torche va éclater ou BLEVE.

INTRODUCTION

Pressurized liquefied fuels are widely used in domestic, commercial and industrial situations, and expansion of their consumption is anticipated within the framework of the Energy National Program [1]. Their transportation relies extensively on rail and road tank cars, which, with the increased demand, have been involved in a rising number of accidents. These accidents have caused death, serious injury, extensive property damage and disruptive major evacuations. In 1979 one Canadian incident, involving the derailment of twenty-one tank cars, nineteen of which were carrying dangerous commodities, caused the evacuation of almost a quarter of a million people for periods of up to five days [2].

In a typical accident, a tank car carrying a compressed flammable commodity, such as propane is punctured due to a derailment or impact. The propane is released and subsequently ignited by sparks, or a hot car component (e.g., a hot brake). This results in a torch or a pool fire which may project onto or engulf other tank cars. These cars in turn are heated and unless properly vented by means of suitably sized relief valves, will fail and explode. The explosions are often extremely severe with major pieces of the exploding tanks and undercarriage being propelled up to 680 metres from their initial locations. Secondary fires frequently occur at and between the sites where the pieces come to rest. If significant amounts of fluid are released prior to ignition large vapour cloud explosions can occur with tragic loss of life and severe property damage.

In order to better understand this behaviour and to determine protection strategies the Transportation Development Center of Transport Canada has been supporting an experimental study at the Fire Science Center of the University of New Brunswick [3]. Several test facilities have been developed to investigate inclination effects in saturated nucleate and film pool boiling, the visual and physical study of lading height, valve aperture and action, heat flux, and the interaction of the pool fire and the pressure relief valve (PRV) flare.

The results of this still preliminary investigation form the basis of a study of the thermohydraulic behaviour of real tanks in accident conditions. An understanding of the complex interactions between vessel, PRV, fire, and lading is expected to provide the fundamentals of a general computer code, currently under development for design purposes and for safety analyses.

HEAT TRANSFER TO THE TANK AND LPG

The heat transfer to the LPG in the tank surrounded by a fire consists of:

i) radiation from the flames and convection from the combustion gases plus heated air to the walls of the tank, and reradiation of the tank wall,

ii) radial and circumferential conduction and thermal storage in the tank wall,

iii) heat transfer to the LPG liquid and vapour.

Figure 1 illustrates the internal fluid behaviour with a variety of protection schemes, such as external insulation and internal insulation (EXPLOSAFE*).

The various sub-problems that must be addressed in order to fully describe the complete situation may be outlined as:

i) Thermal Properties: For the possible potential ladings comprehensive sets of physical properties must be available. These must include both the thermodynamic and transport properties including speed of sound and surface tension. Tank material and insulation mechanical and thermal properties are also necessary.

ii) Geometry: A description of tank geometry must be able to incorporate the effects of tank pitch and attitude with respect to pressure relief valve (PRV) location(s) and fire location and intensity (torch or pool fire).

iii) Pool fire: PRV flare description and interaction. The PRV when open exhausts considerable quantities of lading under the influence of the tank internal pressure (lading vapour pressure). This material usually issues at sonic velocity due to the choked conditions of the flow and if flammable forms an intense turbulent flare capable of influencing both the structure and intensity of a surrounding pool fire as well as affecting the radiation loading on the tank vapour space.

iv) Vapour and liquid thermal stratification:

The flow inside the cylinder is recirculating in nature, but the magnitudes of velocities inside the bulk of the liquid are essentially very much smaller than the boundary layer velocities. The stratification developed in this form is stable and the shape of the temperature profile in the vertical direction does not change significantly as time progresses, although the circulatory motion accelerates. The pressure in the vapour space is at a saturation condition consistent with the interface temperature. That is, the interface temperature controls the pressure in the vapor space. Therefore, the determination of the amount of stratification is of importance.

* Vulcan Industrial Packaging, Rexdale, Ontario, Canada.

When the walls of the horizontal tank are suddenly exposed to uniform heating, heat is transferred to the fluid core mainly by conduction. After a short time delay, buoyancy forces overcome gravitational forces and the fluid adjacent to walls rises along the walls up to the free surface. The heated fluid spreads towards the centre as it reaches the surface and gradually forms a distinct warm layer in which a positive temperature gradient exists with a maximum at the interface.

An unstable region exists at the cylinder bottom. In this region, the heat transfer mechanism is similar to the case where a horizontal or nearly horizontal heated plate faces upwards. In this region mixing between heated and core fluid occurs contributing to the increase of the bulk temperature.

When the inside walls are covered with an aluminium foil mesh (EXPLOSAFE) for the purpose of enhancing mixing, comparable thermal stratification still takes place due to the flow in a now modified boundary layer.

When the PRV opens the liquid that is above the saturation temperature corresponding to the instantaneous relief pressure will flash causing a two-phase swell which will influence side wall heat transfer in both the former vapour and liquid spaces. Due to liquid swelling and vapour entrainment significant amounts of liquid in the form of fine droplets will be carried over into the PRV exhaust.

v) PRV action: Initial valve action will correspond to design except that dependent upon tank attitude and pitch and lading height the valve may exhaust, liquid, vapour or more usually a two phase mixture. If the latter case occurs design pressure relief may not be possible. As the time of fire exposure increases and the tank contents increase in temperature, the vapour space thermal stratification will expose the valve spring to ever higher temperatures resulting in a decrease in spring stiffness and relaxation. These effects will cause the PRV operating characterisitcs to change.

vi) Boiling and liquid swelling: The fire surrounds the tank and causes the lading fluid to be subjected to heating on a variety of inclinations. The heat transfer will initially be by free convection followed by subcooled nucleate or film boiling until such time as the fluid central core becomes saturated, at this point heat transfer is by saturated boiling.

Any heat transfer model must account for the effects of inclination in both these modes and in addition consider the reductions caused by vapour blanketing effects and the two-phase swelling noted earlier in item iv above.

vii) Internal and external thermal protection schemes : Modern tank cars now use external insulation with protective steel jackets. A variety of internal protection methodologies have been considered including EXPLOSAFE and two-phase thermo geysers.

Figure 1 illustrates the cross section of a tank with a variety of the above internal heat transfer mechanisms active along with several protection schemes including that of EXPLOSAFE.

From the above the following major areas of concern are to be described here; i) Boiling and liquid swelling, and ii) Pressure-temperature response, PRV action, and vapour and liquid stratification.

TEST FACILITY

The test facility for the above items consists of two experimental setups: i) Heated pressure vessel, and ii) Boiling and swell determination apparatus.

Heated Pressure Vessel

The pressure vessel consists of an electrically heated horizontal double walled pressure vessel (40 l), a variable area PRV (6-25mm dia.), 25mm thick observation windows, and instrumentation, Fig. 2. R 11 and R 12 are used to simulate the LPG lading. The PRV is solenoid operated and may be controlled to open at 105 percent and close at 95 percent of tank pressure as for the real situation. The PRV may additionally be oriented at any angle from vertically upward to downward to emulate a variety of locations under accident conditions.

The instrumentation includes up to fifty shielded and stainless steel sheathed iron or copper constantan thermocouples and pressure transducers in the vessel and after the PRV. The time dependend mass of the lading is measured by four capacitance load cells which output frequency. An HP 85-3497A data acquisition and control system acts as overall system controller and data reduction, recording, and plotting unit. Time synchronized video records are made of all tests.

Heater power (0-65 kW/m^2) is maintained by use of manually controlled

220 V 3 phase variacs. There are nine individual heater elements located around the inner stainless steel tank between the mild steel argon cooled outer vessel. These elements may be controlled together or individually to simulate pool or torch fire heat flux distributions.

The test program, utilizing both R11 and R13, has been implemented using a variety of lading fills (85-55 and 25 percent), power levels (25,50 and 65 kW/m^2) and pressure relief valve orifice sizes (6 - 25 mm) for both subcooled and saturated initial conditions. The results of these tests will be examined briefly later.

Boiling and Swelling Apparatus

Tank storage and transport normally utilize large horizontal cylinders or spheres and hence the interior fluid sees a variety of surface inclinations and heat fluxes under accident conditions. The test apparatus is therefore designed to study the effects of heat flux, surface inclination, and pressure in both the nucleate and film boiling regions in R11. Tests to 180 kW/m^2 at inclination angles from 0-180 degrees are reported in [5].

The experimental apparatus consists of 5 components (Fig. 3): an electric heater (including a holder for EXPLOSAFE and a copper surface), a reflux condenser, auxiliary heaters, thermocouples, a T-vessel and rotating system, and an HP-85/3497 computer and data acquisition system.

Electric heaters: There have been very few boiling experiments with large surface area. In order to model large systems similar to railway tank cars with reasonable confidence, a careful study with reasonably large surface areas must be undertaken. To meet this purpose an 8 cm diameter copper plate was used. A coil heater, located behind the plate, permitted an evenly distributed temperature field. A cross sectional view of the test section is shown in Fig.4a. To limit the heat transfer to one side of the heating plate, an insulation block made of lava was used. Thermal compound between the copper plate and the ground surface of the encapsulated heating element allowed good thermal contact so that the heat loss through the bottom was minimized. Numerical analysis and actual measurement of the temperature differences permitted assessment of the losses which did not exceed 15 percent at maximum heat flux (Fig. 4b).

In these tests the heat transfer surface was cleaned before testing with acetone. After assembly and charging of the system with R-11, the

liquid was preheated to bring the system up to the desired pressure, and the power to the main surface heating element initiated for the desired orientation angle. After steady state was obtained, (15-20 min.), all readings were taken and the power increased to the next desired level. The pressure in the T-vessel was maintained constant throughout the test.

At each data point the following items were determined; surface temperatures, liquid temperatures, temperatures in the insulation block and stainless steel and two voltage drops across the heating element and a standard resistor in order to calculate the power input to the heater. The heat flux associated with boiling from the copper plate was obtained by subtracting the heat loss through the insulation block from the power delivered to the heater. The detailed heat loss calculation method is described elsewhere [5].

RESULTS

To date the basic experiments have indicated the very complex nature and interdependence of the phenomena. The pressure, temperature, and mass temporal response as a function of heat flux, level, initial pressure (temperature, i.e. subcooling) are all necessary in order to be able to properly scale [6] the results to full size [7] or other situations [8].

The elements that have the most profound effect on the tank behaviour are the amount of thermal stratification and hence subcooling, the pressure-time and temperature-time responses, and the boiling and swelling phenomena.

Thermal Stratification

When the walls of the tank are heated the heat is initially conducted into the fluid core and vapour space. After a short time delay, buoyancy forces overcome gravitational forces and the fluid adjacent to the walls rises along the walls up to the free surface forming thermally stratified layers in both the liquid and vapour regions. These layers in turn set the vapour pressure and hence initial PRV action. An unstable boundary region exists at the bottom of the cylinder as mentioned previously and this is responsible for the heating of the subcooled core.

Data from experiments with Freon 11 are plotted in Figures 5 and 6. Figures 5a and b illustrate the temperature-height-time results obtained in representative tests at 82 percent fill. An integral technique describing the stratification [9] leads to very close agreement with an EXPLOSAFE fill, as shown in Figure 6. For filling ratios

below 30% by volume a lumped analysis can be made since there is no boundary layer formation due to the instability of the bottom layer and hence the amount of stratification is negligible.

Pressure-Time Response

The pressure increases as heating continues eventually opening the PRV at the set pressure (typically 105% of relief pressure). The depressurization caused by this relief after a brief delay, results in the homogeneous flashing of that liquid in the stratified layer at or above the saturation temperature corresponding to the instantaneous pressure. Figs. 7a and b illustrate the types of pressure records obtained for two different PRV relief areas. The relief in Fig. 7b illustrates the sustained vent obtained with a smaller relief area than in Fig. 7a. Once closed the flashing ceases, stratification reestablishes itself and the pressure again rises. Subcooled boiling may now as well be established in the liquid boundary layers on the walls with its rate and type being set by surface conditions (temperature and nucleation characteristics) and local heat flux. Valve action will continue as long as the rate of vapour generation in the boundary layer is less than that being relieved by the valve; this will be for as long as the liquid core and the boiling remain subcooled. Dependent upon the relief area, surface characteristics, and heat flux the valve may remain open with the pressure remaining essentially constant. In this stage there are both heterogeneous boiling at the tank wall in addition to the homogeneous boiling occurring in the bulk. Figs.8 show the changeover in temperature distribution during this period for two initial fills. Fig. 9 illustrates the wall, vapour, and liquid temperatures for the same time levels and demonstrates the severe effects of stratification, venting, and recovery after venting for an initial fill of 58% (Fig. 8b).

The time temperature response of the thermocouple located at the top of the tank and at entry to the PRV indicates the initial discharge is superheated vapour followed by two phase fluid. The quantity and quality of two phase discharge decreases with decreasing fill levels. At high ladings fills (70-80%) the quantity of liquid entrained by the Bernoulli effect [6], as a result of swelling, is large causing a significiant reduction in the temperature of the exiting fluid.

When the inside walls are covered with an aluminium foil mesh (EXPLOSAFE), for the purpose of enhancing mixing, a more rapid but comparable thermal stratification occurs. This too can be modelled [9] as has been shown in Fig. 6.

The opening of the pressure relief valve results in a rapid decrease of tank pressure. PRV closure is, however, usually effected prior to any substantial pressure recovery as is noted for the depressurisation of steam generators, PWR's [10], or chemical reactors [11].

With large PRV areas this pressure relief causes severe superheating of the liquid and results in massive heterogeneous and homogeneous vapour generation resulting in the bulk fluid obtaining temperature uniformity faster than with smaller relief areas. As fill levels are lowered for the same relief area less liquid superheat occurs.

Once boiling occurs in the wall boundary layer the single phase stratification model will no longer describe the local heat transfer coefficients and experimental data for nucleate or film pool boiling must be obtained as a function of heat flux and angle since fire engulfment tests have suggested that boiling in the tank may be either nucleate [7,8] or film [12].

Boiling and liquid swelling

There have been very few boiling experiments reported that consider the variation in angle of inclination coupled with the use of a large surface. Fig. 10 [5] illustrates the type of results obtained here for smooth and enhanced boiling surfaces in R11. At low heat fluxes there is an increase in heat transfer coefficient as the angle of inclination is increased. As the heat flux increases and boiling commences the heat transfer coefficient becomes independent of angle for all but the highest angles. Use of a "high flux" surface (Fig. 10b) results in considerable improvement in heat transfer due to the increased number of active nucleation sites.

The effect of orientation on nucleate boiling has been reported in [13]. Here comparisons were made of boiling heat transfer for three different surface orientations of a strip heater in R-11; facing upward, downward and vertical. The results show that for the orientations of facing upward and vertical, the boiling curves obtained are typical for nucleate boiling heat transfer; that is a pronounced increase of heat transfer rate with

surface temperature after the onset of nucleation and the existence of a burnout point. For the case of facing downward, however, the curve differs very significantly from the other two with a very much reduced heat transfer capability but still with a burnout point. Ti-Ting Chen [14] performed similar experiments and pointed out that the orientation effect is important in the region of 150 to 180 degrees. The test section areas used by the previous workers are however very small (9.25 cm^2 and 3.17 cm^2 respectively) so that edge effects may dominate the heat transfer performance from their surfaces. For very large surfaces edge effects, bubble agglomeration, and bubble acceleration/retardation effects may become apparent.

A detailed study has been conducted as part of this work in the region 150 - 180 degrees. Figure 10a and 10b show the effect of the orientation of the surface. At low heat fluxes, below 30 kWm^2, the temperature difference decreases continuously as the angle increases. Heat transfer performance is thus increased by increasing the angle of inclination. At high heat fluxes however (above 45 kW/m^2 to 70 kW/m^2), even though the angle increases, the temperature difference does not change significantly. It is evident that in this range of heat flux, heat transfer performance is not dependent upon the orientation of the surface. At higher heat fluxes, above 80 kW/m^2, as the angle increases, temperature differences increase slowly but steadily and in the vicinity of 170 degrees the temperature difference increases to very large values resulting in burnout.

Heat transfer performance for the 180 degree (facing downward) case is, of course, the poorest except at very low heat fluxes (2 or 3 kW/m) in the natural convection region. As seen in Fig. 10a there is an inflexion point around 8 - 9 kW/m^2. For the downward facing case, due possibly to edge effects, heat transfer performance continuously decreases so that at around 80 kW/m^2 it yields the poorest heat transfer performance.

It is observed that once the suface is inclined there are strong convection currents promoted by bubble motion; these enhance surface heat transfer. When the heating surface is facing downward bubbles agglomerate and are apt to collect on the underside so that the gross convection currents are not sufficient to sweep the bubbles away. As a consequence, bubble

motion does not add to the convection mechanism as it does when the surface is in any other position.

Effect of EXPLOSAFE

To improve the heat transfer in railway tank cars under accident conditions EXPLOSAFE, which is a honeycomb type expanded aluminum mesh, has been proposed as an internal protection device. In order to study the effects of this, six small studs and wire were used to hold down the 19, 25, and 50 mm thick EXPLOSAFE samples in good contact with the surface. Fig.10b illustrates that EXPLOSAFE does not cause any appreciable enhancement in nucleate boiling. As the thickness increases, heat transfer is retarded. This can be explained by the introduction of a thermal contact resistance. At first it was thought that this material will function as a fin to promote heat transfer from the surface. From these results however, it can be shown that even though EXPLOSAFE is in good contact, there is a micro layer between the EXPLOSAFE and the surface. This layer therefore acts as a thermal resistance to prevent the liquid from having a good access to the surface, wetting the surface and taking the heat away as a result. Dhir and Catton [15] have analyzed boiling in porous media. In deep beds, the vapour channels extend only part way into the bed while in shallow beds these channels are well formed throughout the bed. As the thickness of EXPLOSAFE increases, it acts as a deep bed and accordingly retards the heat transfer.

Although the above are steady state results their use may be justified in the transient heating model under development here since pseudo thermodynamic equilibrium can be shown to apply after very short times (600 ms) [9,11].

General Model

The following model may therefore be postulated to describe the heat transfer process to the LPG liquid: i) the incidence of boundary layer boiling will be governed by a time dependent Clausius-Clapeyron relation, ii) for no boiling the transient stratified convection model will define the LPG-wall heat transfer, iii) with boiling empirical representations of the steady state boiling curves will be used, and iv) the effective two-phase fluid height may be defined in terms of a swell height that initially disregards the non-equipibrium effects of the flashing liquid.

A simplified version of such a model is in fact extremely successful in predicting the pressure response of certain tests (Fig. 11)[16]. Modifications to this model are currently underway.

CONCLUSION

The most significant conclusions drawn from this study thus far are:

1. The transient data obtained has revealed the existence of a very complex interaction between lading fill, subcooling, PRV size and action, boiling, and both vapour and liquid thermal stratification with heat flux.

2. Prior to PRV action the primary vapour generation source originates in the liquid boundary layer. With PRV depressurization flashing in the stratified layer assumes some importance on the rate of pressure recovery with PRV closure.

3. PRV closure in the early stages is affected by fill level; more complete fills entail larger surface areas and hence greater vapour generation and thus after an initial cycling period the rate of generation exceeds the relieving capacity of the valve and the unit remains open. With smaller fills the generation rate is lower and therefore the valve cycles.

4. Significant nonuniform void fraction distributions exist within the system during the early stages of PRV action due to the considerable amount of vapour and liquid thermal stratification.

5. Thermal stratification within the fluid and its subsequent flashing may be successfully modelled.

6. Simple thermodynamic and heat transfer models may be used to predict the pressure response of such vessels.

ACKNOWLEDGEMENT

Funding for this work was provided by the Natural Sciences and Engineering Research Council of Canada and Transport Canada, Transportation Development Center.

REFERENCES

1. National Energy Program Task 5; New Liquid Fuels; 5.5 Fuel in Transportation, Ottawa, Canada, 1983.

2. Grange, S.G.M. (Dec. 1980), "Report on the Mississauga Railway Accident Inquiry," Supreme Court of Ontario, TP2828.

3. Venart, J.E.S., Sousa, A.C.M., Steward, F.R., and Lenard, J.G. (Oct 1981), "Tank Car Thermal Modeling, A Proposal to Supply and Services Canada," DSS 09SDT8200-1-1540, UNB ME/TE-09.

4. Tunç, M., Steward, F.R., Venart, J.E.S. and Wong, S., (May 1984), "A Pool Fire PRV Flare Interaction Model," Canadian Section Combustion Institute Meeting, Fredericton, N.B.

5. Jung, D.S., M.Sc.E. thesis, Department of Mechanical Engienering, UNB (in preparation Feb. 1984).

6. Zuber, N. (1982), "The Problems in Modeling of Small Break LOCA," Heat Transfer in Nuclear Reactor Safety, Eds. Bankoff and Afgan, Hemisphere, New York, pp. 3-48.

7. Anderson, C., Townsend, W., Zook, J., and Cowgill, G., (Sept. 1974), "The Effects of a Fire Environment on a Rail Tank Car Filled with LPG," FRA-OR&D 75-31.

8. Appleyard, R.D. (Aug. 1980), "Testing and Evaluation of the EXPLOSAFE System as a Method of Controlling the Boiling Liquid Expanding Vapour Explosion (BLEVE)," TP 2740 Dept. of Res. and Dev. EXPLOSAFE Div., Vulcan Industrial Packaging Ltd.

9. Aydemir, N.U., Sousa, A.C.M., and Venart, J.E.S. (Aug. 1984), "Transient Thermal Stratification in Heated Partially Filled Horizontal Cylindrical Tanks," ASME/AIChE National Heat Transfer.

10. Hutcherson, M.N., Henry, R.E., and Wollersheim, D.E. (1983), "Two-Phase Vessel Blowdown of an Initially Saturated Liquid - part 1: Experimental," J. Heat Transfer (105) 687-693.

11. Friedel,L. and Purps, S. (June 1982), "Experimental Analysis of Vessel Depressurisation by Top Venting," European Two Phase Flow Group Meeting, Paper D2, Paris.

12. Roberts, A.F., Cutler, D.P., and Billings, K. (1983), "Fire Engulfment Trials with LPG Tanks," Proc. 4th Int. Symp. Loss Prevention and Safety Promotion in the Process Industries, Vol. 3, p.D1-D-10, IChemE Symposium Series 82.

13. Githinji, P.M. and Sabersby, R.H., (1963), "Some Effects of the Orientation of Heating Surfaces in Nucleate Boiling," ASME Journal of Heat Transfer, vol. 85, p. 379.

14. Li-Ting Chen (1978),"Heat Transfer to Pool Boiling Freon from Inclined Heating Plate," Letters in Heat and Mass Transfer," vol. 5, pp. 111-120.

15. Dhir, V.K. and Catton, J. (1982),"Boiling in a Porous Bed, Applied Scientific Research,"vol. 38, pp. 69-76.

16. Sousa, A.C.M. and Venart, J.E.S. (1983), "Thermal Modelling of LPG Rail Tank Cars Exposed to a Fire Environment," 4th Int. Conference on Mathematical Modelling, Zürich, August 15-17.

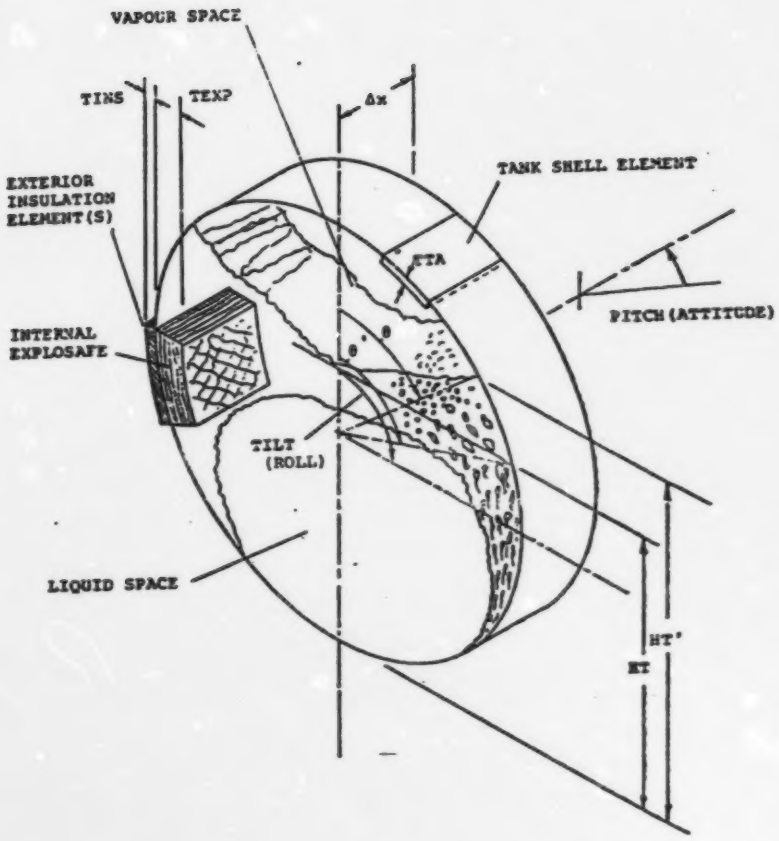

Figure 1. Typical Tank Car Section
TINS: thickness of insulation;TEXP: thickness of EXPLOSAFE; TTA: thickness of tank shell; HT: liquid level;HT': swelling height;θ': fill angle;θ: swell angle

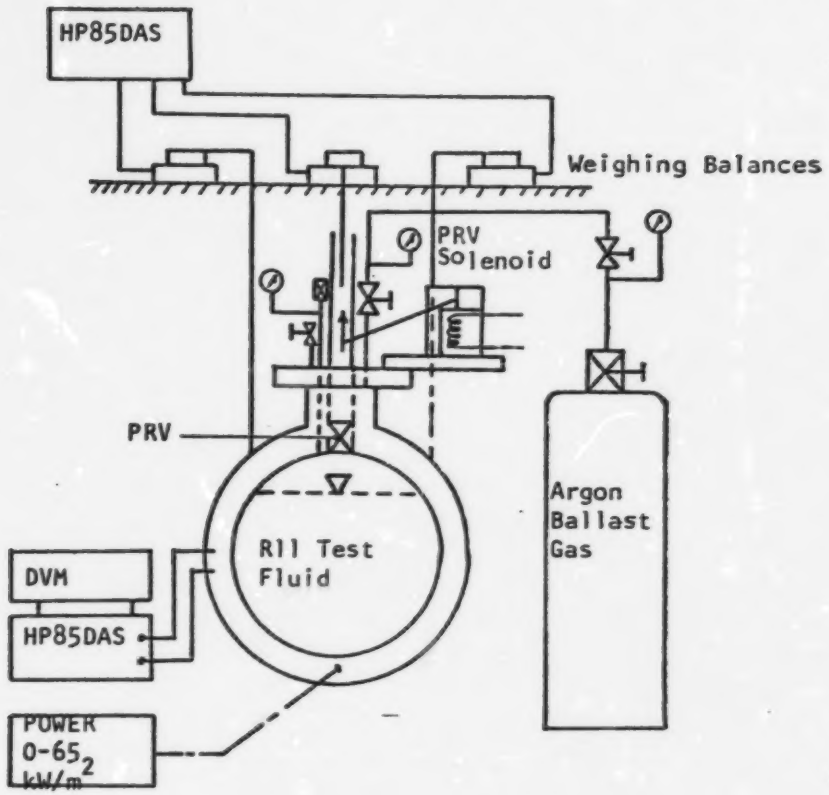

Figure 2. Experimental Facility for Tank/Fluid Behaviour

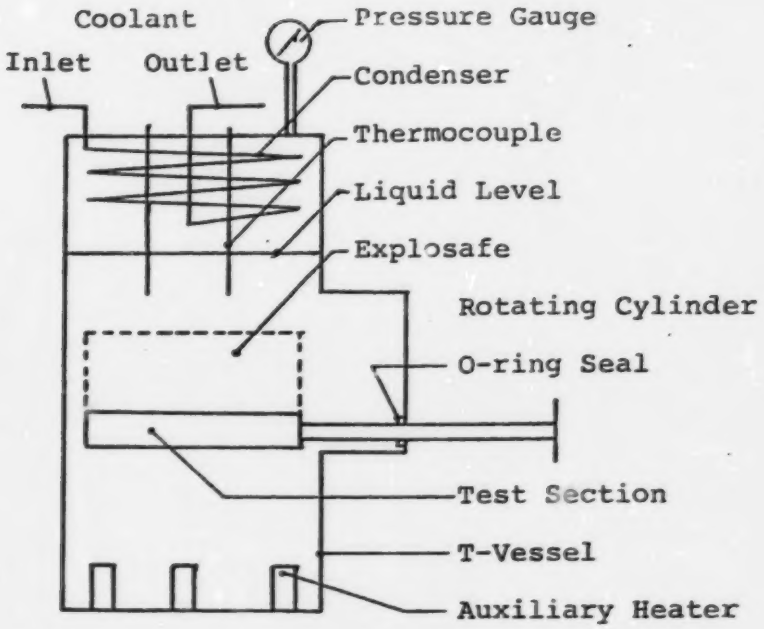

Fig. 3 Boiling and Swelling Apparatus

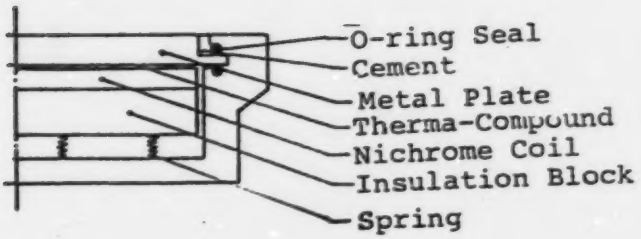

Fig.4(a) Boiling Heater Details

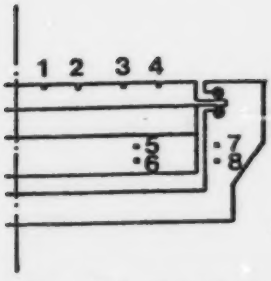

1-8: Iron-Constantan
9-11: Copper-Constantan

$T_{surf.} = (T_1 + T_2 + T_3 + T_4)/4$

$T_{liq.} = (T_9 + T_{10} + T_{11})/3$

Fig.4(b) Thermocouple Details

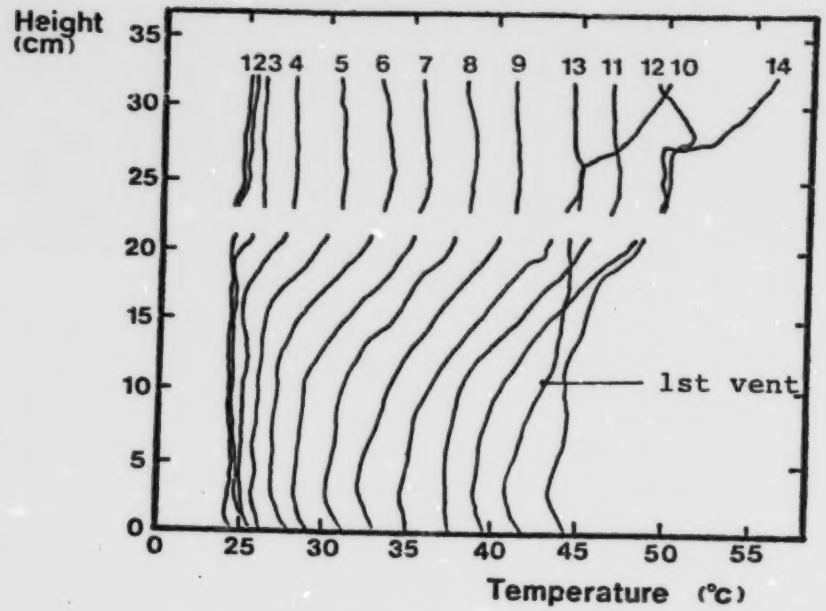

Fig. 5(a) Temperature-height-scan number; 70% fill
6 m ϕ PRV; 65 kW/m^2, Scan interval 30 s.

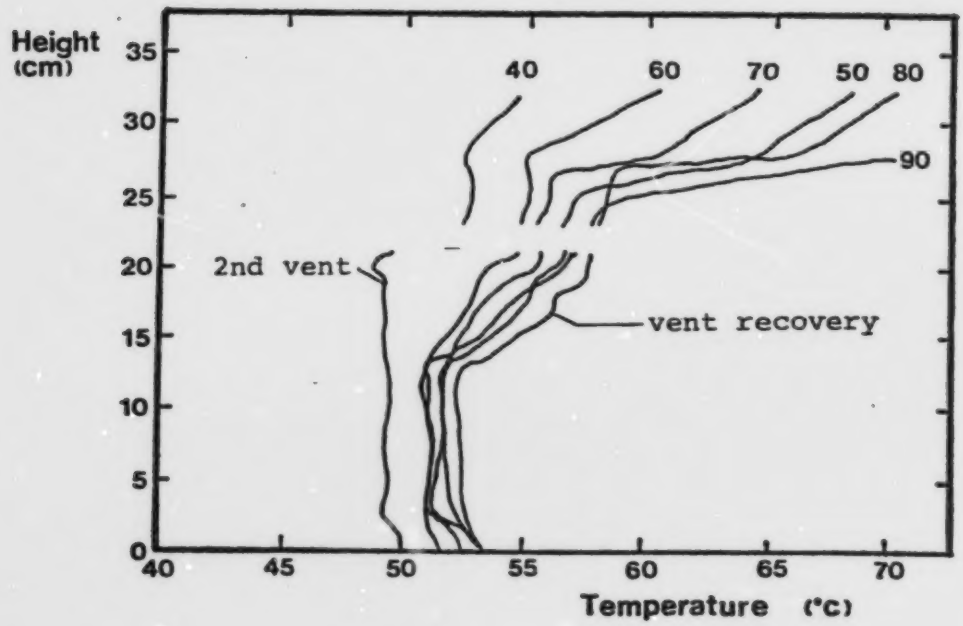

Fig. 5(b) Temperature-height-scan number, 70% fill
6 mm ϕ PRV, 65 kW/m^2, Scan interval 30 s.

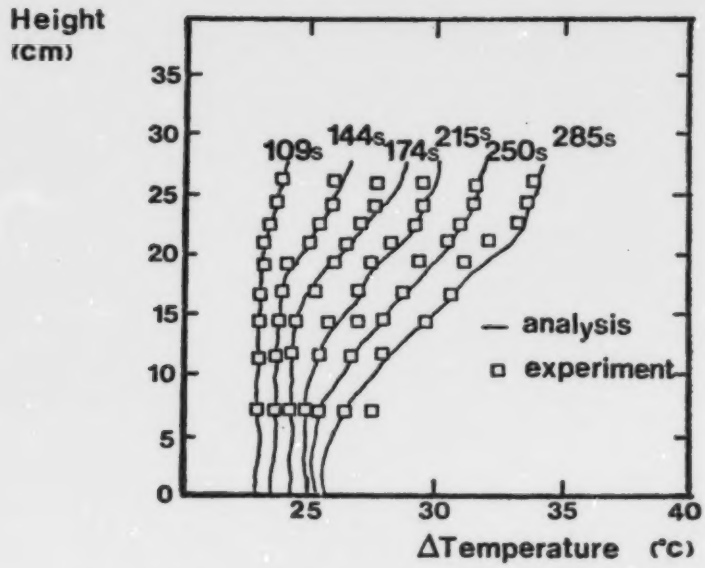

Fig. 6 Temperature-Height-Time; 75% Fill, 10 mm ϕ PRV, 40 kW/m^2; EXPLOSAFE

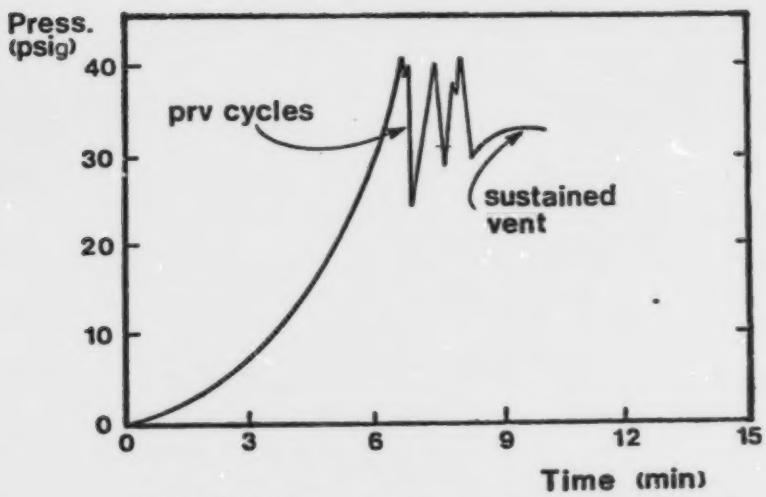

Fig. 7(a) Pressure Time Response 78% Fill, 6 mm ϕ PRV 65 kW/m^2

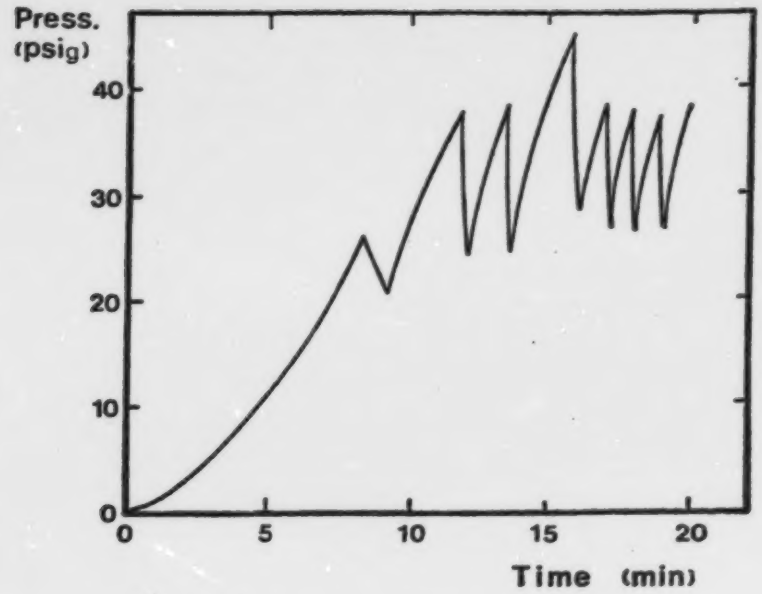

Fig. 7(b) Pressure Time Response; 78% Fill
6 mm ϕ PRV 65 kW/m^2

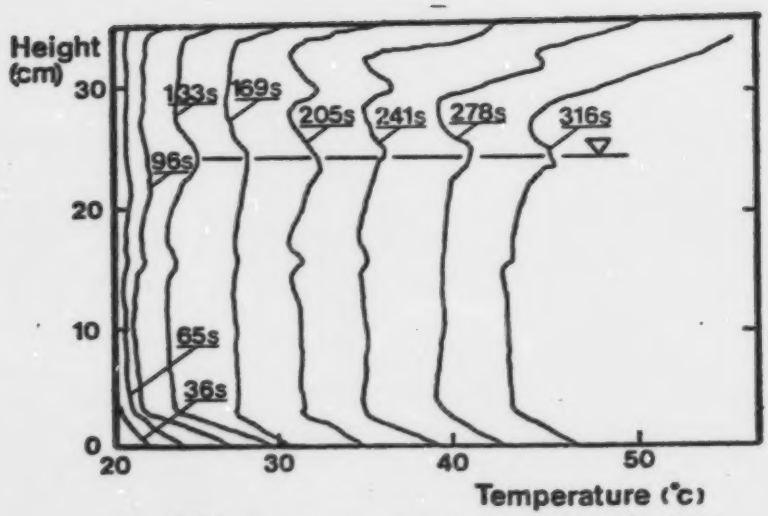

Fig.8(a) Temperature-height-time, 78% Fill
6 mm ϕ PRV 65 kW/m^2

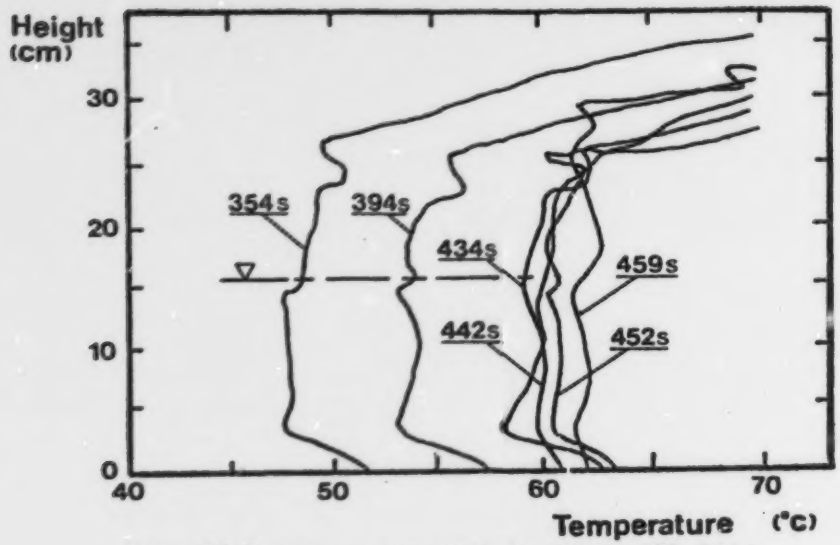

Fig. 8(b) Temperature-Height-Time: 58% Fill, 6 mm ϕ PRV, 65 kW/m^2.

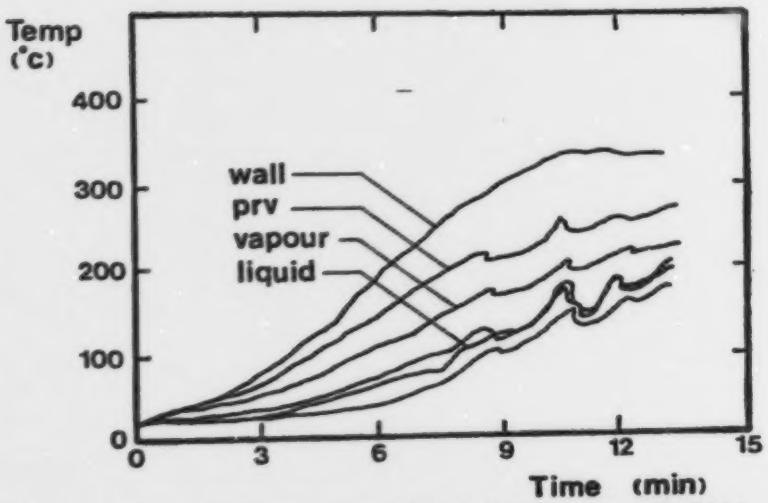

Fig. 9 Temperature-Time Response: 58% Fill, 6 mm ϕ PRV, 65 kW/m^2; Wall and Bulk Temperatures in Vapour and Liquid Spaces

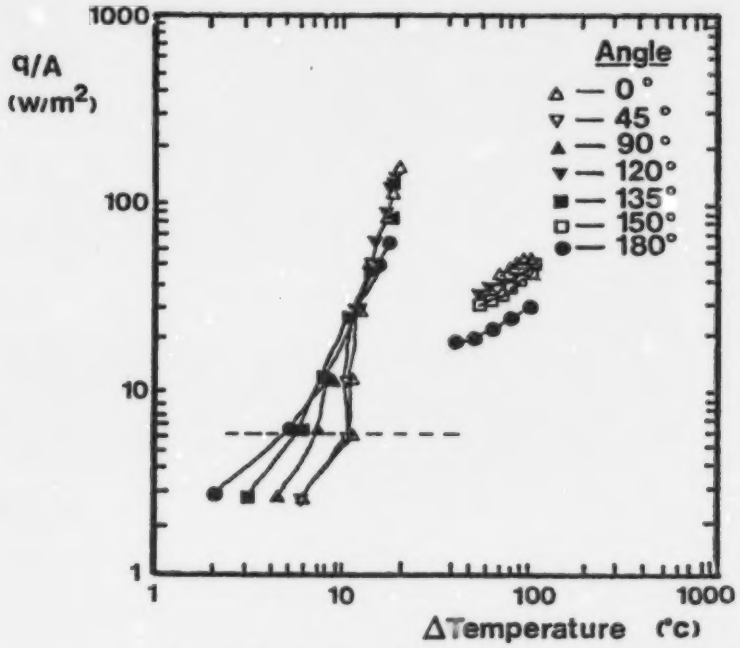

Fig. 10(a) Pool Boiling Heat Transfer With R 11: Effects of Surface Inclination.

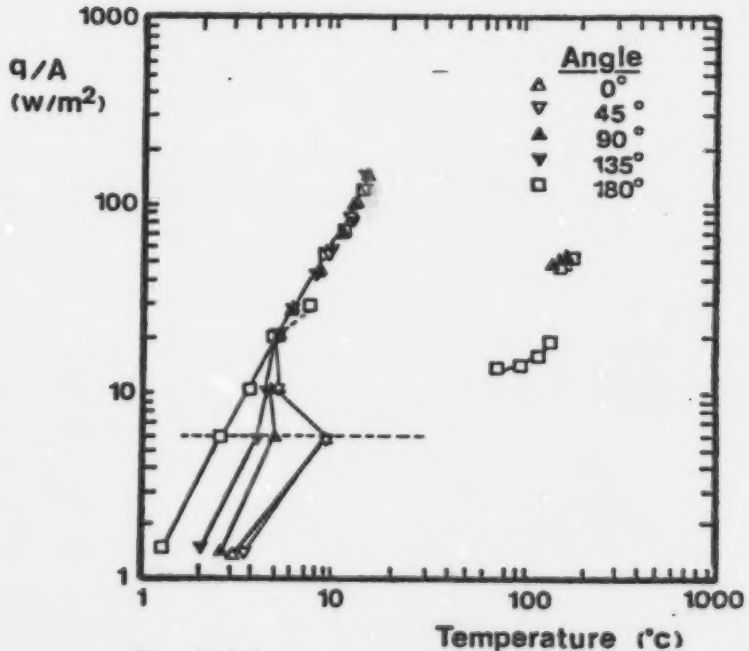

Fig. 10(b) Pool Boiling Heat Transfer with R 11: Effect of High Heat Flux Surface.

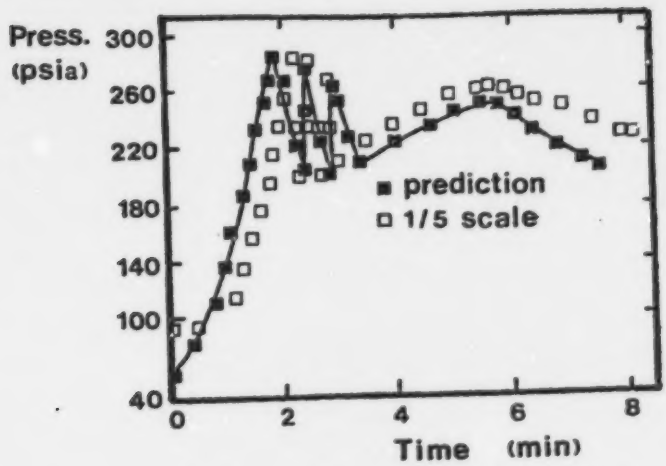

Fig.11 Fifth Scale Pressure Time Behaviour

THE AMERICAN SOCIETY OF MECHANICAL ENGINEERS
345 E. 47 St., New York, N.Y. 10017

84-HT-60

The Society shall not be responsible for statements or opinions advanced in papers or in discussion at meetings of the Society or of its Divisions or Sections, or printed in its publications. Discussion is printed only if the paper is published in an ASME Journal. Released for general publication upon presentation. Full credit should be given to ASME, the Technical Division, and the author(s). Papers are available from ASME for nine months after the meeting.
Printed in USA.

TRANSIENT THERMAL STRATIFICATION IN HEATED PARTIALLY FILLED HORIZONTAL CYLINDRICAL TANKS

N.U. AYDEMIR, A.C.M. SOUSA AND J.E.S. VENART

DEPARTMENT OF MECHANICAL ENGINEERING
UNIVERSITY OF NEW BRUNSWICK
FREDERICTON, N.B. CANADA E3B 5A3

ABSTRACT

Thermal stratification is investigated for fluids contained in partially filled horizontal cylindrical tanks with uniform wall heat flux. The convective instability at the bottom of the tank is formulated by using a new approach, and closed form expressions for the boundary layer commencing after the instability are obtained by an integral analysis. The analytical technique is extended to include the physical situation in which the inside walls are covered with an aluminium foil mesh (EXPLOSAFE). Results with and without EXPLOSAFE are presented and compared with experimental data for R-11. Fairly good agreement is shown between the analytical and experimental results.

NOMENCLATURE

c_p specific heat, J/kg°C
D inner diameter of the cylindrical tank, m
E energy integral, J/m°C
$Fo_R = \frac{\alpha t}{R^2}$ Fourier number
$Gr_L^* = \frac{g\beta q L^*}{k\nu^2}$, Modified Grashof number; L=D for laminar flow, L=R for turbulent flow
g acceleration due to gravitational force, m/s^2
k thermal conductivity, W/m°C
$\dot{m}_{b\ell}$ rate of mass flow in the boundary layer, kg/s
$\dot{m}_{s\ell}$ stratified layer mass increase rate, kg/s
Nu_ϕ Nusselt number based upon the distance $x=\phi R$
$Pr = \nu/\alpha$, Prandtl number
q wall heat flux, W/m^2
R inner radius of the cylindrical tank, m
r radial distance in r-ϕ plane, m
t time, s
T temperature, °C
T_∞ reference temperature, °C
u tangential velocity, m/s
U non-dimensional tangential velocity, $U=u/(\nu/R)$
x,y coordinate system of a fluid element in the boundary, $x=R\phi$, $y=R-r$
Z thickness of stratified layer, m
A dimensionless stratification profile
α $k/c_p\rho$, thermal diffusivity, m^2/s
α_s fill angle
β coefficient of thermal expansion
δ free-convective boundary layer thickness
δ_ℓ laminar sublayer thickness
ξ,η dimensional and non-dimensional distances in the growth direction of stratified layer
Θ temperature difference, $T-T_\infty$
Θ_w wall temperature difference, T_w-T_∞
$\Theta^* = \Theta/(qR/k)$
ν kinematic viscosity, m^2/s
ρ density, kg/m^3
τ_w shear stress at the wall
ϕ angle measured from the bottom of the cylinder
$\bar{\phi}$ the limiting angle for stability
Ψ volume of stratified layer per unit depth
Δ non-dimensional boundary layer thickness, $\Delta=\delta/R$
Ω equivalent external boundary layer velocity, m/s
ω stratification angle

INTRODUCTION

The present study is part of a research program investigating the thermal response, under fire accident conditions, of tank cars carrying hazardous liquefied gases [1], such as LPG.

In the early stages of fire exposure the transient thermal stratification of the contained fluid determines the escalation of vapor pressure, which in turn may dictate the eventual rupture of the tank. As a first approximation to the fire conditions, a uniform heat flux distribution is assumed.

Observations have been carried out by the authors in a fully instrumented computer controlled experimental rig consisting of a 380 mm-diameter stainless steel tank loaded with R-11. The tank is provided with plexiglass end walls, which permit a clear visualization of the flow. A brief literature survey and qualitative description of the physical phenomena are outlined in the next sections. The instrumentation control hardware and software and experimental procedures

are discussed elsewhere [2] and only sufficient detail is given here to support the measurements reported.

BRIEF LITERATURE SURVEY

Over the years natural convection in enclosures has been the object of extensive research efforts. A careful literature survey, however, reveals that a great proportion of this effort has been devoted to natural convection in rectangular configurations;while the important area of natural convection in partially-filled horizontal cylinders has been somewhat neglected. For instance the experimental studies reported in [3], [4], [5] and [6] are performed using fully filled horizontal cylinders for different boundary conditions, namely: in [3] the two sides are maintained at distinct uniform temperatures, whereas in [4] a sawtooth distribution is used. In both cases a single rotating central core region is present. In [5] the cylinder is heated circumferentially and the flow pattern observed shows two counter rotating large cells carrying heat along the boundary up to the surface. Similar experiments for a uniformly heated cylinder and related extensive data are reported in [6]. An analytical solution valid for high Prandtl number fluids is given by [7]. All of the above mentioned studies are for fully filled cylinders and to the authors' knowledge no experimental or analytical study exists for partially filled horizontal cylinders.

Owing to the geometry of the solution domain an exact analytical method is out of the question and even some difficulties may be encountered when a numerical method is used. This particular point is addressed in [8], where a special coordinate transformation is outlined and utilized to study similar problems.

The present paper aims to demonstrate the capabilities of an integral approach in predicting the amount of stratification in the tank although no information on the complete flow field can be obtained.

The use of an integral analysis may be justified based on the following experimental observations:

i. There exists a thin boundary layer where the velocities are much higher than the downward core velocities,
ii. the fluid layers are nearly isothermal in each horizontal plane,
iii. the core is quasi-isothermal below the stratified layer, its temperature increases with time due to the uniform mixing with fluid from the base of the cylinder.

The transient results presented in this paper are for time intervals of less than seven minutes since the pressurized vessel simulating the tank car will be allowed to discharge via a pressure relief valve (PRV). Typical height versus temperature data obtained from the experimental facility to be described is shown in Figure 1 indicating the transient stratification taking place in the cylinder. At t=420 seconds the tank vents at a predetermined pressure resulting in uniform mixing in the stratified layer. The purpose of the present analysis is essentially to predict the time for the vessel to reach the preset pressure for vent, which is a function of the interface temperatures as will be discussed in the following section. The behaviour of the flashing liquid inside the vessel is beyond the scope of this paper and will not be discussed here.

Integral methods have been successfully applied to the stratification problem in vertical cylinders due to its significance in hydrogen fueled rocket vehicles; [9] and [10] note that the bottom heating is responsible for the increase of the core temperatures. The significance of this is demonstrated in [9] where a comparison of side versus bottom and side heating is performed. The effect of side heating, although small, has a contribution in the increase of core temperatures, and it may be attributed to the turbulent eddies diffusing into the bulk of the fluid from the boundary layer as observed in [11] for a rectangular tank.

Both [9] and [10] have assumed the commencement of the boundary layer at the vertical walls, stating that complete mixing takes place near the conical bottom of the cylinder. For a horizontal cylinder, however, it is difficult to estimate the region of complete mixing or in other words to decide where the free-convective boundary layer starts. It has been confirmed by the experiments of [5] and [6] as well as by the authors' experimental observations that a region of convective instability exists at the bottom of the cylinder and the boundary layer starts for $\phi \gg 0$.

The physical model developed to determine the region of mixing and required modification of the integral method is described later.

DESCRIPTION OF PHYSICAL PHENOMENA

When the walls of the horizontal tank are suddenly exposed to uniform heating, heat is transferred to the fluid core mainly by conduction. After a short time delay, buoyancy forces overcome gravitational forces and the fluid adjacent to walls rises along the walls up to the free surface, as depicted in Figure 3. The heated fluid spreads towards the centre as it reaches the surface and gradually forms a distinct warm layer in which a positive temperature gradient exists with a maximum at the interface. The flow inside the cylinder is recirculating in nature, but the magnitudes of velocities inside the bulk of the liquid are essentially very much smaller than the boundary layer velocities. The stratification developed in this form is stable and the shape of the temperature profile in the vertical direction does not change significantly as time progresses, although the circulatory motion accelerates. The pressure in the vapor space is at a saturation condition consistent with the liquid interface temperature. That is, the interface temperature controls the pressure in the vapor space. The determination of the time dependent stratification is, therefore, of corsiderable importance.

Another observation made from the experiments is that of an unstable region at the cylinder bottom. In this region, the heat transfer mechanism is similar to the case where a horizontal or nearly horizontal heated plate faces upwards. In this unstable region mixing between heated and core fluid occurs contributing to the increase of the bulk temperature. It is necessary, therefore, to predict the initiation of the stable wall boundary layer after this region and modify the integral analysis accordingly.

When the inside walls are covered with an aluminium foil mesh (EXPLOSAFE[1]) for the purpose of enhancing mixing, it was observed that a comparable thermal stratification still takes place due to the flow in the now modified boundary layer. The vertical temperature gradient, however, shows a marked difference from that for the unprotected tank (Figure 6) in that the core temperature response and thermal stratification are more rapid.

EXPERIMENTAL FACILITY

The apparatus consists of an electrically heated horizontal double walled pressure vessel (40 l), a variable area PRV (6-25mm dia.), 25mm thick observation windows, and instrumentation, Fig. 2. R 11 and R 12 are used to simulate the LPG lading. The PRV is solenoid operated and may be controlled to open at 105 percent of tank pressure as for the real situation. The PRV may additionally be oriented at any angle from vertically upward to downward to emulate a variety of locations under accident conditions.

The instrumentation includes up to fifty shielded and stainless steel sheathed iron or copper constantan thermocouples and pressure transducers in the vessel and after the PRV. The time dependent mass of the lading is measured by four capacitance load cells which output frequency. An HP 85-3497A data acquisition and control system acts as overall system controller and data reduction, recording, and plotting unit. Time synchronized video records made of all tests.

Heater power (0-65 kW/m^2) is maintained by use of manually controlled 220 V 3 phase variacs. There are nine individual heater elements located around the inner stainless steel tank between the mild steel argon cooled outer vessel. These elements may be controlled together or individually to simulate pool or torch fire heat flux distributions.

The test program, utilizing both R11 and R12 has been implemented using a variety of lading fills (85-55 and 25 percent), power levels (25,50 and 65 kW/m^2),protection schemes, and pressure relief valve orifice sizes (6 - 25 mm) for both subcooled and saturated initial conditions.

ANALYSIS

Boundary Layer Model

The experimental observations reveal a thin laminar or turbulent boundary layer along the wetted walls of the experimental tank, commencing after the unstable region located at the tank bottom. An integral analysis is used to obtain closed form expressions for the tangential velocity and boundary layer thickness in the usual manner incorporating modifications when the flow is turbulent.

Using the transformation $x=R\phi$, $y=R-r$, the integral equations of motion for a curved boundary become identical to those of a flat plate;[6] has arrived at the same set of equations with the exception of a transient term. Here a quasi-steady state is assumed because as shown later, the core temperature, T_∞, is considered as time dependent and the time rate of change of temperature is relatively small. Using continuity, the Boussinesq approximation and the above transformation, the equations of motion and energy are as follows:

Motion.
$$\frac{\partial}{\partial x}\int_0^\delta u dy = \int_0^\delta \beta g (T-T_\infty)\sin\phi dy - \frac{\tau_w}{\rho} \qquad (1)$$

Energy.
$$\frac{\partial}{\partial x}\int_0^\delta u(T-T_\infty)dy = -\alpha \left.\frac{\partial T}{\partial y}\right|_{y=0} \qquad (2)$$

with the boundary conditions

$$u = \frac{\partial u}{\partial y} = \frac{\partial T}{\partial y} = 0 \; ; \; y = \delta \qquad (3.a)$$

$$u = 0, -k\frac{\partial T}{\partial y} = q \; ; \; y = 0 \qquad (3.b)$$

The above set of equations can be easily solved by standard techniques if the assumption of a power law variation is made for the velocity and the boundary layer thickness. It should be noted that the effect of external stratification is not included due to its insignificance in the present problem. In Figure (1) the growth of the thermal layer is indicated with dashed lines below which the core fluid can be considered isothermal. On the other hand, the boundary layer flow rate is integrated up to the lower end of the stratified layer in which a characteristic temperature gradients exists. Thus, it is assumed that the external region next to the boundary layer is always isothermal. This stems from the good mixing between the core liquid and the convective currents due to the instability initiated at the bottom of the vessel. In the case of a rectangular tank heated from the sides, this effect is absent and appreciable gradients occur in the liquid core. [16] In this reference this effect was explicitly included in the energy equation.

For laminar flow, with constant heat flux at y=0, the temperature and velocity profiles used for integration are

$$\theta = \frac{q\delta}{2K}(1-y/\delta)^2 \qquad (4.a)$$

$$\frac{u}{\Omega} = \frac{y}{\delta}(1-y/\delta)^2 \qquad (4.b)$$

respectively, with δ and Ω given by power law relations. Substituting Eqs. 4.(a) and (b) in Eqs. (1) and (2), neglecting the variation in the buoyancy term in Eq.(1) due to change in sin θ results in

$$\Delta = 2.7\left[\frac{1/Pr^2 + 1.25/Pr}{Gr_D^* \sin\phi}\right]^{1/5} \phi^{1/5} \qquad (5)$$

$$\Omega = 4.1\left[\frac{1/Pr^2 + 1.25/Pr}{Gr_D^* \sin\phi}\right]^{-2/5} \phi^{3/5} \qquad (6)$$

The justification for the above approach is easily understood when the differential equations of motion are solved by expanding the $\sin\phi$ term in series form (Appendix A.) This method uses the technique of successive approximation utilizing the forms suggested by [12] for the stream function and the temperature field. These solutions are obtained using a modified form of Nachtsheim-Swigert Scheme [13]. The second order solution predicts similar trends to those above in Eqs. (5) and (6) where values of Ω (for laminar flow) are slightly lower. This favourable comparison is the basic motivation for their use. For the turbulent regime the profiles given by [14] are

$$\theta = \theta_w\left[1 - (y/\delta)^{1/7}\right] \qquad (7)$$

and
$$\frac{u}{\Omega} = \left(\frac{y}{\delta}\right)^{1/7}(1 - y/\delta)^4 \qquad (8)$$

Since Eq. (7) yields an infinite gradient at y=0, a linear temperature profile in a laminar sublayer is assumed. The thickness of this sublayer is given by [15] as

$$\delta_\ell = 15\,\nu\sqrt{\delta/\tau_w} \qquad (9)$$

---

† Vulcan Industrial Packaging Ltd., Rexdale, Ontario, Canada

with the heat flux being specified at the edge of the sublayer.

By assuming similarity between forced and buoyancy induced flows, the shear stress at the wall, τ_w, may be represented [10,14,16,17] by

$$\tau_w = 0.0225\ \rho\Omega^2 \left(\frac{\nu}{\Omega\delta}\right)^{1/4} \tag{10}$$

Therefore the boundary condition

$$\left.\frac{\partial\theta}{\partial y}\right|_{y=0} = -\frac{q}{k} \quad \text{is changed to} \quad \left.\frac{\partial\theta}{\partial y}\right|_{y=y_\ell} = -\frac{q}{k}$$

where $y_\ell = \delta_\ell$. The new temperature profile is then,

$$\theta = 44\,\frac{q}{\rho c_p}\left(\frac{\delta}{\Omega\delta^2}\right)^{1/4}\left[1 - \left(\frac{y}{\delta}\right)^{1/7}\right]. \tag{11}$$

Before integrating Equations (1) and (2) using (8) and (11) it will be assumed that the contribution of the laminar sublayer to the integrated momentum and energy equations is negligible as has been suggested by [18].

Finally, it can be shown that integration of (1) and (2) with a power law assumption yields,

$$\Delta = 0.525\left(\frac{Pr^*}{Gr_R^* \sin\phi}\right)^{1/4} \phi^{5/7} \tag{12}$$

$$\Delta = 3.84\left(\frac{Pr^*}{Gr_R^* \sin\phi}\right)^{-5/14} \phi^{3/7} \tag{13}$$

Stratification model. In [19] and [20] the integral method is applied to thermal stratification in vertical cylinders. In [19] it is assumed that all incident heat on the tank walls is carried directly to upper regions of the fluid through the boundary layer, allowing no increase of temperature in the bulk of the liquid. While [20] uses temperature profiles valid for a constant wall temperature which can be justified due to the low values of heating in liquid hydrogen. In the present constant heat flux case, however, the modified profiles given by Eqs. (4) and (11) are required.

In what follows an outline of the stratification model is given. The rate of mass flow in the boundary layer should be equal to the rate of increase of mass in the stratified layer i.e. $\dot{m}_{b\ell} = \dot{m}_{s\ell}$ where,

$$\dot{m}_{b\ell} = \int_0^\delta \rho u\,dy \tag{14}$$

$$\dot{m}_{s\ell} = \rho\,\frac{dV}{dt} \tag{15}$$

Using the notation of Figure 4 substitution of Eq.(4-b) (or Eq. (8) for turbulent flow) in Eq. (14) and equating it to Eq. (15) results in

$$\int_{\bar\theta}^{\pi-\alpha_s} \frac{\cos2\phi-1}{\phi^{0.8}\sin^{0.2}\phi}\,d\phi = 1.85\ Fo_R\,\P(Pr,Gr_D^*) \tag{16.a}$$

where

$$\P(Pr,Gr_D^*) = \left(\frac{1/Pr^2 + 1.25/Pr^*}{Gr_D^*}\right)^{-1/5}, \text{ and}$$

for turbulent flow

$$\int_{\bar\theta}^{\pi-\alpha_s} \frac{\cos2\phi-1}{\phi^{8/7}\sin^{2/7}\phi}\,d\phi = 0.588\ Fo_R Pr^*\P(Pr,Gr_R^*) \tag{16.b}$$

where $\P(Pr,Gr_R^*) = (Pr/Gr_R^*)$

Equation (16) can be integrated for several values of Fo_R to obtain the growth of the thermal layer.

In order to determine the temperature variation the total energy carried in the boundary layer will be equated to the integrated energy in the stratified layer

$$D(\pi-\alpha_s)\int_0^t \dot{q}\,dt = \rho c_p \int_{\pi-\alpha_s}^{\bar\theta} (T-T_\infty)L(\xi)\,d\xi = \rho c_p E \tag{17}$$

The experimental data for moderate heat fluxes in the range of 0-40 kW/m^2 show that the temperature profile in the thermal layer has an inflection point, suggesting a third order polynominal fit. In addition there appears to be very little heat/mass transfer across the interface, i.e.

$$\theta = \frac{T-T_\infty}{T_s-T_\infty} = \alpha_1 + \alpha_2\eta + \alpha_3\eta^2 + \alpha_4\eta^3 \tag{18}$$

subject to

$$\theta = 1;\ \eta=0$$

$$\theta = 0;\ \frac{d\theta}{d\eta}=0,\ \eta=1 \quad \text{where } \eta=\zeta/z \tag{19}$$

These give

$$\theta = (2\eta+1)(1-\eta)^2 \tag{20}$$

Using Equation (20) in Equation (17) results in

$$T_s - T_\infty = \frac{(\pi-\alpha_s)\dot{q}t}{\rho c_p E z} \tag{21}$$

where E is the energy integral on the right handside of Eq. (17).

Equation (16) is used to predict the growth of the thermal layer while Equation (21) predicts the temperature. The two equations are linked through the energy integral, E. The horizontal cylinder geometry presents and additional problem which to the authors' knowledge has not been discussed previously: the hydrodynamic instability of the boundary layer near the bottom of the cylinder.

Approximate Analysis of Hydrodynamic Stability of a Boundary Layer on a Concave Surface. The buoyancy induced instability of the boundary layer can be analysed once the effective forces on a fluid element are considered (Figure 5). In addition to the body force and the force due to the difference in hydrostatic pressure at the ends of the control volume, another force exists due to the presence of curvature. This is the centrifugal force, which acts in a direction opposite to the projection of the buoyancy force on a normal axis to the fluid element therefore preventing boundary layer separation. In the following analysis, any force perpendicular to the normal axis is not considered since it has no contribution in the stability of the element (eg. the wall shear force); the algebraic sum of forces on this axis thus yields a sufficient criterion for

stability. Projection of the body and hydrostatic forces on the normal axis is (per unit length),

$$F_{BH} = \int_0^{\delta} g(\rho-\rho_\infty)\cos\phi dy = \int_0^{\delta} \beta g\rho(T-T_\infty)\cos\phi dy \qquad (22)$$

The centrifugal force is

$$F_c = \int_0^{\delta} \rho \frac{u^2}{R} dy \qquad (23)$$

For stability, the centrifugal force must be equal to or greater than the body and hydrostatic force. Integrating and equating Eqs. (22) and (23) using the appropriate laminar temperature and velocity profiles results in

$$\frac{221\ \tilde{\phi}\ \tan\tilde{\phi}}{1 + 1.25Pr} \geq 1 \qquad (24)$$

The turbulent analog of Equation (24) can be derived similarly using turbulent profiles. Equations (16) and (21) can therefore be rewritten as,

$$\int_{\tilde{\phi}}^{\pi-\alpha_s} \frac{\cos 2(\phi-\tilde{\phi})-1}{(\phi-\tilde{\phi})^{0.8}[\sin(\phi-\tilde{\phi})]^{0.2}} d\phi = 1.85 Fo_R^{*}(Pr, Gr_D^{*}) \qquad (25)$$

$$T_s - T_\infty = \frac{(\pi-\alpha_s-\tilde{\phi})t}{\rho c_p E z} \qquad (26)$$

With this modification, one can now determine the increase in the temperature of the core fluid as there is direct mixing in the region determined by Eq. (24).

Extended Analysis for EXPLOSAFE. To deal with the physical situation in which EXPLOSAFE covers the inside walls of the tank, the following modifications to the fluid properties have been made: a - the thermal conductivity is calculated based on the configuration of the aluminum mesh immersed in Freon 11 at stagnation conditions, b - the heat capacity and thermal expansion are unchanged, c - the density of the mesh/fluid combination is the weighted average, d - the kinematic viscosity is 1.8 times larger than that of Freon 11 based on the assumption of similarity between heat and momentum diffusion which was also used in the integration of Eqs. (1) and (2).

External Stratification. The effect of external stratification shows itself by the ejection of warm fluid from the boundary layer into the bulk liquid, hence causing a thinning in the thickness of the momentum layer [16]. In the stratified layer the temperature difference between the wall and average fluid temperature for that horizontal plane decreases with increase in height. Since q is constant the heat transfer increases, fig. 8 . An analysis similar to that of Appendix A (Appendix B) has calculated the momentum and thermal boundary layers for the simplest case of thermal stratification, $\lambda = \phi + \phi^2/2$. Figs. 9 a and b respectively illustrate the variation of these varibles with the temperature distribution outside the boundary layer.

RESULTS AND DISCUSSIONS

Data from experiments with R11 for two different fill heights are plotted along with the analytical predictions in Figs. 6 and 7 with and without the internal protection material EXPLOSAFE. The proposed approach leads to very close atreement despite the simplifying assumptions utilized in its development. The third order profile given in Eq. (18) appears to represent the thermal stratification profile adequately for both cases. For filling ratios, below 30 percent by volume, a lumped analysis can be made since this angle approximately represents the stability for side wall boundary layer commencement.

In the present analysis the liquid-vapour interface is assumed adiabatic due to the experimentally observed temperature profiles (Fig. 1) and the very small amount of condensation taking place resulting from the vapour being compressed due both to heating and from the liquid thermal expansion.

Unlike the circumstances in vertically walled and side heated tanks, the heat transfer significantly differs in that analysis for these cases yields large discrepancies between experimental and integral solutions [16]. This perhaps is due to the mixing of the low velocity eddies generated in these boundary layers with the downward moving core fluid. This process is self sustaining as the core velocities are appreciable and create a reverse shear in the outer boundary region causing further enhancement of the turbulent mixing. If this mixing is neglected, the interface temperatures are over predicted as in [10] or [16].

The heat loss in the boundary layer due to external stratification and that due to eddy mixing is quite distinct. The first is due to the decrease in buoyancy forces due to the decreasing temperature difference between boundary layer and core and the second is due to the existence of the reverse shear layer between core and boundary layer.

In the partially filled horizontal cylinder large downward core velocities are absent due to the mixing of the core fluid with the fluid issuing from the unstable region located on the concave bottom of the cylinder. In this region the heated fluid moves directly vertically upwards to mix with the downward moving fluid from the stratified layer, reducing the effect of reverse shear and enhancing mixing to provide a near isotheral but time dependent core temperature.

This latter effect is accounted for quite separably in the present analysis by the instability analysis since it provides the primary energy content to the core. In the previous sections a simple force balance was utilized to provide criteria for the end of this unstable region so to mark the formation of the stable boundary layer. Once this layer is formed the usual equations of motion (Eqs. 1 and 2) govern the flow since the centrifugal force acts in a direction perpendicular to the flow. It should also be mentioned that the present analysis neglects the buoyancy terms in the ϕ direction since the perturbation analysis (Appendix A) shows that the second order results predict similar but only slightly larger velocities. Also due to the influence of direct mixing caused by the unstable region no account is made for thermal stratification in Eqn. 2 unlike that used in [16].

The model with EXPLOSAFE assumes that is main effect in the flow is to conduct heat normal to the surface with negligible influence in the boundary layer flow direction due to its very low void fraction (~0.03).

In addition to the experimental evidence above, comparison to a numerical solution obtained using a coordinate transformation and the coupled equations of motion and energy [8] yields the centerline vertical temperature profiles shown in Figure 10. The shape of

the stratification curves obtained with this method compares favorably, however the integral method does not fully predict the detail of bulk liquid temperature since uniform mixing was assumed. The computed isotherms for this case shown in Figure 11 are nearly horizontal except in the near wall/interface region thus justifying the assumption of a uniform temperature at any given height; a condition which was preassumed in the integral stratification analysis.

CONCLUDING REMARKS

An integral method has been presented for the prediction of thermal stratification inside a partially filled, horizontal cylinder subjected to uniform side heating. A new approach was developed to determine the boundary layer instability due to buoyancy forces on a concave surface. The model has been modified for a case where the cylinder walls are covered with an aluminum mesh commercially available as EXPLOSAFE.

Good agreement with experimental data for both protected an unprotected cylinders was obtained. The integral method was compared with a numerical integration and some limitations of the former were discussed. It can be concluded that the integral method yields good predictions with modest computational requirements for the stratification problem in a horizontal cylinder.

ACKNOWLEDGEMENT

This work was supported by the Natural Science and Engineering Research Council of Canada and The Transportation Development Centre, Transport Canada.

REFERENCES

[1] Venart, J.E.S., Sousa, A.C.M., Steward, F.R. and Lenard, J.G., "Tank Car Thermal Modeling," a Proposal to Supply and Services Canada: DSS File No. 09 SDT 8200 - 1 - 1540, October 23, 1982, 52 pages.

[2] Venart, J.E.S., Sousa, A.C.M., Steward, F.R. and Prasad, R.C., "Experiments on the Physical Modeling of LPG Tank Car Under Accident Conditions," Symposium "Transport and Storage of LPG and LNG." Brugge, 7-9 May, 1984. (To appear).

[3] J.D. Hellums, S.W. Churchill, "Transient and Steady State, Free and Natural Convection, Numerical Solutions: Part I," AIChE J, 8, 690 (1962).

[4] I. Brooks, S. Ostrach, "An Experimental Investigation of Natural Convection in a Horizontal Cylinder," J. Fluid Mech., Vol. 44, part 3, p. 545 (1970).

[5] L.B. Evans, N.E. Stefany, "An Experimental Study of Transient Heat Transfer to Liquids in Cylindrical Enclosures," Chemical Engineering Progress Symposium Series, p. 209 (1965).

[6] H.G. Maahs, "Transient Natural Convection Heat Transfer in a Cylinder," Ph.D. Thesis, University of Washington, Seattle (1964).

[7] S. Ostrach, "Natural Convection in Enclosures," Advances in Heat Transfer, p. 161 (1972).

[8] Aydemir, N.U., Venart, J.E.S., Sousa, A.C.M., "Natural Convection in Partially Filled Horizontal Cylinders," to appear.

[9] J.W. Tatom, W.H. Brown, L.H. Knight, E.F. Coxe, "Analysis of Thermal Stratification of Liquid Hydrogen in Rocket Propellant Tanks," Adv. in Cryogenic Engineering, vol. 9, p. 265 (1963).

[10] G.C. Vliet, J.J. Brogan, T.S. Sheppard, F.H. Morse, F.L. Hines, "Stratified Layer Flow Model: A Numerical Approach to Liquid Temperature Stratification," J. Spacecraft, vol. 1, No. 6, p. 666 (1964).

[11] J.W. Tatom, "Transient Turbulent Free Convection in a Closed Container With Heating At The Sides Only," Proc. Heat Trans. and Fluid Mech. Inst., Northridge, Calif., p. 321 (1972).

[12] Koh, J.C.Y., Price, J.F., "Laminar Free Convection from a non-isothermal cylinder," J.H. Transfer, May, 1965, p. 237.

[13] J.A. Adams, D.F. Rogers, "Computer Aided Heat Transfer Analysis," McGraw-Hill, 1973, p. 401.

[14] Eckert, E.R.G., Jackson, T.W., "Analysis of Turbulent Free Convection Boundary Layer on Flat Plate," NACA Report 1015, (1951).

[15] Zijnen, Van Der Hegge, "Measurements of the velocity distribution on the boundary layer along a plane surface,"abstracted in McAdams, Heat Transmission, p. 104, McGraw-Hill (1942).

[16] O. Suzuki, A. Mizukami, "Unsteady Turbulent Natural Convection in a Tank," 1983 ASME.WAM, Paper No. 83-WA/HT-2.

[17] L.B. Evans, R.C. Reid, E.M. Drake, "Transient Natural Convection in a Vertical Cylinder," AIChE J., vol. 14, No. 2, p. 251, (1968).

[18] T. Fujii, "An Analysis of Turbulent Free Convection Heat Transfer from a Vertical Surface," JSME, Vol. 2, No. 8, pp. 559-563 (1959).

[19] J.M. Ruder, A.D. Little, "Stratification in a Pressurized Container with Sidewall Heating, AJAA, Vol. 2, No. 1, p. 135 (1964).

[20] T. Bailey, R. Vande Koppel, G. Skartvedt, "Cyrogenic Propellant Stratification Analysis and Test Data Correlation," AIAA Journal, Vol. 1, No. 7, p. 1657 (1963).

APPENDIX A

Perturbation Analysis

The governing equations are

$$u\frac{\partial u}{\partial x} + v\frac{\partial u}{\partial y} = \beta g(T-T_\infty)\sin\phi + \nu\frac{\partial^2 u}{\partial y^2}$$

$$u\frac{\partial T}{\partial x} + v\frac{\partial T}{\partial y} = \frac{\nu}{Pr}\frac{\partial^2 T}{\partial y^2}$$

$$\frac{\partial u}{\partial x} + \frac{\partial v}{\partial y} = 0 \qquad (A.1)$$

with u and v streamwise and cross-stream velocity components, respectively.

The general approach is to expand the velocity and temperature in terms of the stream function and a non-dimensional temperature. The velocity and temperature variations in the boundary layer can be represented by

$$u = \frac{\partial \psi}{\partial y} = G(\phi,\eta) \text{ and } \theta = \theta^*(\phi,\eta) \qquad (A.2)$$

where ψ is the stream function and

$$\phi = \frac{x}{R},\ \eta = \frac{y}{R}\left[\frac{Gr_R^*}{\frac{1}{Pr} + \frac{1.25}{Pr^2}}\right]^{1/5} \qquad (A.3)$$

$$\theta^* = \frac{k(T-T_\infty)}{qR}\left[\frac{Gr_R^*}{\frac{1}{Pr^2} + \frac{1.25}{Pr}}\right]^{1/5},\quad \psi = \alpha\left[\frac{Gr_R^*}{\frac{1}{Pr^2} + \frac{1.25}{Pr}}\right]^{1/5} f(\phi,\eta)$$

The above non-dimensionalization is chosen so to be consistent with the results of the integral analysis.

The power series expansion suggested by Koh and Price [12] is used with a constant heat flux boundary

condition

$$f(\phi,\eta) = \phi f_o + \phi^3 f_1 + \phi^5 f_2 + \phi^7 f_3 + \ldots. \qquad (A.4)$$
$$\theta^*(\phi,\eta) = \theta_o + \phi^2 \theta_1 + \phi^4 \theta_2 + \phi^6 \theta_3 + \ldots.$$

substituting Eq. (A-3) in Eq. (A-1) and performing the differentiation, noting that $f_o, f_1 \ldots, \theta_o, \theta_1 \ldots$ are functions of η only,

$$f_\eta f_{\eta\phi} - f_\phi f_{\eta\eta} = f_{\eta\eta\eta} + \theta^* \sin\phi \qquad (A.5)$$
$$f_\eta \theta^*_\phi - f_\phi \theta^*_\eta = \theta^*_{\eta\eta}/Pr$$

Substituting Eq.(A-4) in Eq.(A-5) and expanding $\sin\phi$ in a power series, the first two sets of equations corresponding to ζ and ζ^3 are

$$f_o''' + f_o f_o'' - f_o'^2 + \theta_o = 0 \qquad (A.6)$$
$$\theta_o'' + Pr\, \theta_o' f_o = 0$$

and

$$f_1''' + f_o f'' - 4f_o' f_1' + 3f_o'' f_1 + \theta_1 - \frac{\theta_o}{6} = 0 \qquad (A.7)$$
$$\theta_1'' + Prf_o\theta_1' - 2Prf_o'\theta_1 + 3Prf_1\theta_o' = 0$$

with the boundary conditions

$$\eta = 0;\ f_o = f_o' = f_1 = f_1'' = 0,\quad \theta_o' = -1$$

$$\eta \to \infty;\ f_o' \to 0,\ f_1' \to 0,\ \theta_o \to 0,\ \theta_1 \to 0$$

Finally, using a second order Runge-Kutta method. f_o and f_1 are computed. Nachtsteim-Swigert method was used to satisfy the asymptotic boundary conditions. The solution for U can be expressed as

$$\frac{u}{\frac{\nu}{R^2}\left[\frac{Gr_R^*}{\frac{1}{Pr^2} + \frac{1.25}{Pr}}\right]^{-2/5}} = \phi f_o' + \phi f_1' + \ldots$$

where $|f_o'|_{max} = 0.3402$, $|f_1'|_{max} = 0.02$

being the maximum values of f_o and f_1 in the direction of η for a fixed ϕ.

APPENDIX B

Effect of External Stratification

The governing equations are as before (Appendix A) with the exception of energy equation where the Effect of external stratification is accounted for, namely:

Energy equation:

$$u\frac{\partial\theta}{\partial x} + v\frac{\partial\theta}{\partial y} = \frac{\nu}{Pr}\frac{\partial^2\theta}{\partial y^2} - u\frac{dA}{dx} \qquad (B.1)$$

where $A(x) = \frac{k}{qR} Gr_R^{*1/5} T_\infty(x)$, $\phi = x/R$

Equations (A.5) take the form

$$f_\eta f_{\eta\phi} - f_\phi f_{\eta\eta} = \theta\sin\phi + f_{\eta\eta\eta} \qquad (B.2)$$
$$f_\eta\theta_\phi - f_\phi\theta_\eta = \frac{1}{Pr}\theta_{\eta\eta} - f_\eta A'$$

where $A(\phi)$ is the external temperature variation outside the boundary layer.

Assuming a series solution as in Appendix A and substituting it in (B.2) and assuming

$A(\phi) = \phi + \phi^2/2$, the simplest form that will incorporate the effects of external stratification, after collecting of the same order of magnitude we obtain

$$f_o''' = (f_o')^2 - f_o f_o'' - \theta_o \qquad (A-6)$$
$$\theta_o'' = -Pr\, f_o\theta_o'$$
$$f_1''' = 4f_o' f_1' - f_o f_1'' - 3f_1 f_o'' - \theta_o/6 - \theta_1$$
$$\theta_1'' = Pr[2f_o'\theta_1 - f_o\theta_1' - 3f_1\theta_o' + f_o'] \qquad (B.3)$$
$$f_2''' = 6f_o' f_2' + 3(f_1')^2 - f_o f_2'' - 3f_1 f_1'' - 5f_o'' f_2 - \frac{\theta_o}{120} + \frac{\theta_1}{6} - \theta_2 \qquad (B.4)$$
$$\theta_2'' = Pr[4f_o'\theta_2 + 2f_1'\theta_1 - f_o\theta_2' - 3f_1\theta_1' - 5f_2\theta_o' + f_1']$$

These three ordinary differential equations were solved with the same method as in Appendix A, subject to the following boundary conditions;

at $\eta = 0$; $f_o = f_o' = f_1 = f_1' = f_2 = f_2' = 0$;

$\theta_o' = -1$, $\theta_1' = \theta_2' = 0$

as $\eta \to \infty$; $f_o' \to 0$, $f_1' \to 0$, $f_2' \to 0$;

$\theta_o \to 0$, $\theta_1 \to 0$, $\theta_2 \to 0$.

FIGURES

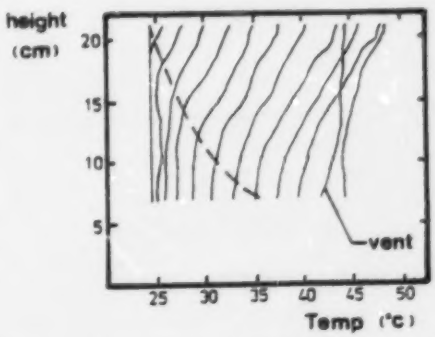

Figure 1. Transient development of vertical temperature profiles for q=20Kw/sq.m, 92% fill, without EXPLOSAFE. (each profile is 35 s apart)

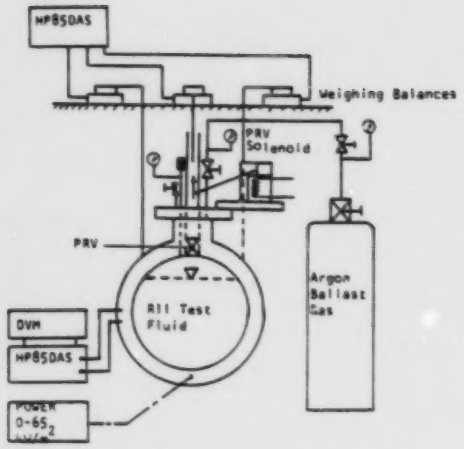

Figure 2. Experimental facility for tank/fluid behaviour

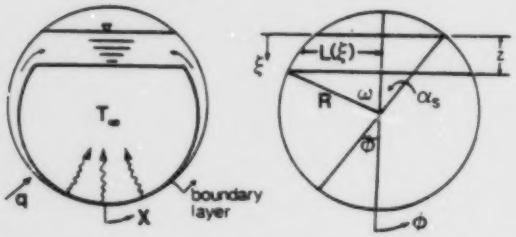

Fig. 3.Physical picture Fig. 4.Notation diagram

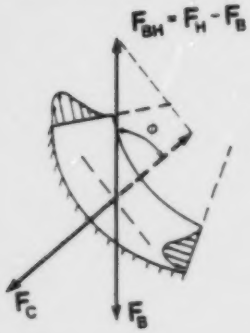

Figure 5. Normal forces on a fluid element

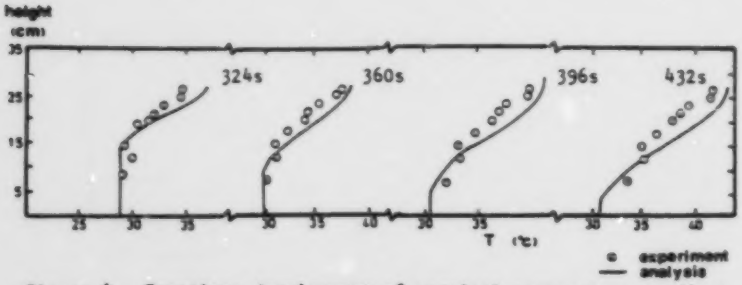

Figure 6. Transient development of vertical temperature gradient 80% fill, with 1" EXPLOSAFE, q=40 Kw/m^2.

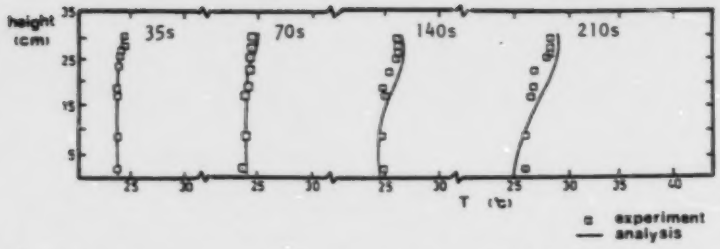

Figure 7. Transient development of vertical temperature gradient, 85% fill, without EXPLOSAFE, q=20Kw/m^2.

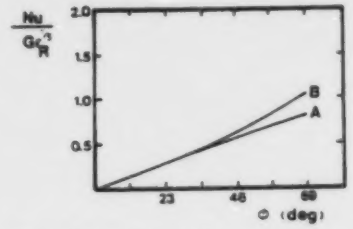

Figure 8. Variation of Nusselt No. from the leading edge. (A-no stratification, B- $\lambda = \phi + \phi^2/2$)

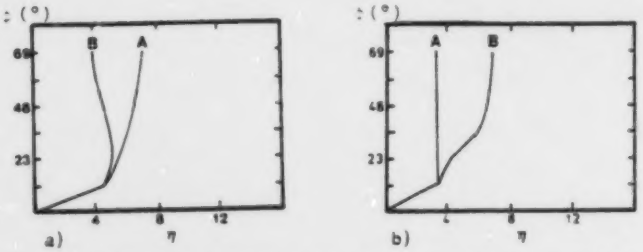

Fig. 9. a) Momentum boundary layer. b) Thermal boundary layer (A-no external stratification. B- $\lambda = \phi + \phi^2/2$)

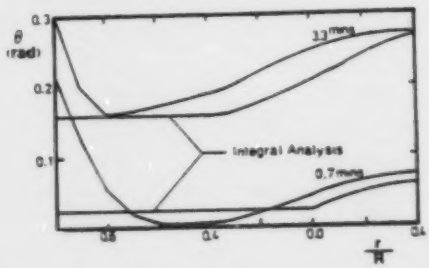

Fig. 10. Transient vertical temperature profiles for Pr=6380, Gr_R=114, Φ=90°.

Fig. 11. Isotherms for Pr=6380, Gr_R=114

INCIDENT RADIATION FROM AN ENGULFING POOL FIRE TO A HORIZONTAL CYLINDER

PART I

M. Tunc*

J.E.S. Venart

Department of Mechanical Engineering,

U.N.B., Fredericton, N.B., Canada

*Address after Oct. 1, 1983

Technical University of Istanbul
Thermodynamics Department
Mechanical Eng. Faculty
Gumussuyu, Istanbul, Turkey

ABSTRACT

A three dimensional formulation has been utilized to determine the incident radiant heat flux on a cylinder surface which is engulfed in flames. The model has been developed as a part of a study concerned with thermal protection systems for railway tank cars carrying hazardous materials. The circumferential and longitudinal variation of heat fluxes on the cylinder surface are determined.

The effect of wind on the inclination of the flame and the location of the points of maximum radiant heat flux on the cylinder have been determined.

NOMENCLATURE

A	surface area, m^2
a	the distance between the point under consideration and the top center point on the cylinder surface, m
D	the diameter of the cylinder, m
H	the height of the combustion zone, m
h_1	the distance between the top of the cylinder and the ground, m
h_3	the distance between the center of the cylinder and the ground, m
k	the mean absorption coefficient of the combustion gases, m^{-1}
L	the length of the cylinder, m
Q	the radiant flux exchanged between an element of volume and a surface element, W
q	the radiative flux density on a surface received from a finite source, W/m^2
r	the radius of the cylinder, m
R(z)	flame radius, m
s	the absorbing path length, m
T	temperature, K
U	wind speed, m/s
V	volume, m^3
W	the width of the pool fire, m

x horizontal axis

z vertical axis

Greek Symbols

β drag coefficient ratio, dimensionless [6]

δ the wall thickness of the cylinder, m

θ angular coordinate, rad

θ_1 the angle between the vertical vector and the vector between the center of the cylinder and the point of interest on the circumference of the cylinder, rad

θ_2 the inclination angle of the pool fire, rad

ρ radial coordinate, m

ρ_a air density, kg/m^3

ρ_f flame density, kg/m^3

σ Stefan Boltzmann constant, 5.66×10^{-8} W/m^2K^4

ϕ the angle between the connecting vector and the vector normal to the surface element, rad

INTRODUCTION

Under certain accident conditions, cylindrical tanks containing liquified gases, in particular LPG, may be exposed to enveloping pool fires. The primary objective of this paper is to determine the variation of the incident radiant heat flux along the length and around the circumference of the tank, portrayed as a cylinder, engulfed in flames. The effect of wind velocity on the incident radiant heat flux on the cylinder surface is also investigated.

There are numerous studies concerned with the properties of pool fires and the resulting radiant heat flux to external targets and to the pool surface. A mathematical model was developed by Masliyah and Steward [1] to calculate the radiative emission from the flame. The radiative interchange between the flame and the plane surrounding its base was determined by assuming the flame to be a gray emitter. To compute the radiative heat flux from a luminous pool fire to an arbitrarily located target surface, either within or external to the fire, a general calculation procedure has been presented by Modak [2]. Recently Birk and Oosthuizen [3] estimated the radiant heat transfer to a long horizontal cylinder engulfed in flames. In their two dimensional analysis the cylinder is considered to be of infinite length and the combustion gases which surround the cylinder, occupy

a space which can be represented by a rectangle. The walls of this rectangle are represented by an infinite but stagnant media. The model estimates the various surface to surface and surface to volume exchange factors as a function of position around the circumference of the cylinder. This method is not able to determine the radiant heat flux variation along the length of the cylinder.

The present study presents a three dimensional formulation to determine the variation of incident radiant heat flux on the cylinder surface. The effect of wind on the flame is also considered.

ANALYSIS

The following assumptions are made:

(1) The emission from the flame is independent of wave length, i.e., the emitting flames are grey [4].

(2) The scattering of radiation is negligible [1].

(3) The effect of convective heat transfer is neglected [2].

(4) The cylinder surface is a black body.

(5) The effective radiation temperature and the flame's grey absorption coefficient are constant throughout the flame volume [2].

The shape of flame is an important parameter and controls the radiative heat flux coming to the cylinder surface. This analysis avoids arbitrary assumptions regarding shapes (such as conical, rectangular or cylindrical flames, etc.)

and instead characterizes the flame shape by means of axi-symmetric flame contours obtained from actual photographs and other experimental evidence from large ($W \geq 4.5$ m) JP-4 jet fuel pool fires [5]. In this work a fourth order polynomial is fitted to the contours of the flame to describe the radius of the flame as a function of height:

$$R(z) = a_0 + a_1 z + a_2 z^2 + a_3 z^3 + a_4 z^4 \qquad (1)$$

The flame shape corresponding to Eq. (1) is shown in figure 1.

(a) The longitudinal radiant heat flux variation

The radiation interchange between an elemental volume dV of radiating gas in the flame and an arbitrary surface element dA on the top line of the cylinder, is depicted in figure 1. The emission of radiation of a gas volume is 4 kdV with the fraction heading toward the surface element dA equal to

$$\cos\phi \cdot dA/4\pi s^2 \qquad (2)$$

The amount transmitted over an absorbing path length s is given by $e^{-k \cdot s}$. The total radiant heat flux received by the element dA, originating at dV is thus

$$Q = \sigma T^4 \left[\cos\phi \frac{dA}{4\pi s^2}\right] 4\, kdV \cdot e^{-k \cdot s} \qquad (3)$$

From Fig. 1 the following relationships may be obtained:

$$dV = \rho d\theta d\rho dz \tag{4a}$$

$$\cos\phi = \frac{z-h_1}{s} \tag{4b}$$

$$s^2 = a^2 + (z-h_1)^2 + \rho^2 + 2a\rho\cos\theta \tag{4c}$$

Substituting the above quantities into equation (3) and integrating over the proper limits yields the total flux denxity received by the area element dA from the flame.

$$q = \int_0^{R(z)} \int_{h_1}^{H} \int_0^{\pi} \frac{2\sigma k T^4 \rho (z-h_1) e^{-ks}}{\pi s^3} \, d\theta dz d\rho \tag{5}$$

The triple integral above was solved numerically using Simpson's rule.

(b) The circumferential radiant heat flux variation

The radiation interchange between an elemental volume dV of the radiating gas and the surface element dA located on the yz plane with an arbitrary angle θ_1, is shown in Figure 1.b. Here

$$\cos\phi = \frac{z - (h_3 + r\cos\theta_1)}{s} \tag{6a}$$

$$s^2 = \rho^2 + (r\sin\theta_1)^2 + [z - (h_3 + r\cos\theta_1)]^2 + 2(r\sin\theta_1)\,\rho\cos\theta \tag{6b}$$

The circumferential heat flux variation was obtained by substituting the above quantities into equation (3) and carrying out the necessary integration. The limits of integration cover that portion of the pool fire which is above a tangent plane to the point of interest on the cylinder surface.

(c) The variation of incident radiant heat flux on the top surface line of the cylinder due to the inclination of pool fire under cross wind conditions

Omer and Cedomir [6] have calculated the angle of tilt by which a wind bends the flame from the vertical. They checked their analytical results, with their own small scale experiments. The angle of tilt for very large scale flames was stated to be

$$\theta_z = \frac{0.787\,\beta\,U^2}{W} \qquad (7)$$

where $\beta = 0.7$ [6].

The variation of this angle with wind velocity is shown in the Figure 2. Experimental results obtained from analysing film of 4.5 m diameter JP.4 from a pool fire are also included in this figure.

In order to model the maximum possible radiation for the wind bent flame (Figure 3) the centerline of the pool fire volume is assumed to be in the xz plane. For this case

$$\cos\phi = \frac{z - \{\frac{h_1}{\cos\theta_2} \pm a\sin\theta_2\}}{s} \qquad (8)$$

$$s^2 = \rho^2 + a^2\cos\theta_2^2 + \{z - (\frac{h_1}{\cos\theta_2} \pm a\sin\theta_2)\}^2 + 2(a\cos\theta_2)\rho\cos\theta$$

In order to determine the variation of incident heat flux, the above quantities again are substituted into equation (3). In equation (8) the ± sign corresponds to the appropriate side of the centerline of the pool fire volume.

(d) In many practical circumstances the centerline of pool fire does not necessarily coincide with the xz plane.

For this most general case a three dimensional computer model for the pool fire and the cylinder has been generated (Fig. 4). By using this model, the points on the cylinder surface which, within the limitations of the assumption made, receives the maximum amount of radiant heat flux, for several inclination angles, have been determined and are shown in Fig. 5.

RESULTS

The heat flux on the top centerline surface has been obtained for two tank sizes which approximate those of full and fifth scale fire tests conducted on propane filled tanks [5, 7].

The results shown in Figures 6-9 correspond to a fifth scale rail tank car.

Figure 6 shows the variation of incident radiant heat flux longitudinally on the top surface of the cylinder for different k values. The flame temperature and the wall temperature are assumed to be 1100K and 580K respectively. It is clear from Figure 6 that the radiant flux density from the flame to the cylinder becomes maximum toward the center of the pool and decreases markedly toward the edges.

The effect of flame temperature on the incident radiant heat flux is shown in Figure 7. Figure 8 presents the circumferential variation of incident radiant heat flux for several k values. The incident heat flux varies considerably around the circumference of the cylinder. The shape of the pool fire changes under crosswind conditions (Figure 3).

The incident radiant heat flux from the inclined pool fire to the top cylinder surface shown in Figure 9 for several inclination angles.

The points which receive maximum amount of radiation on the cylinder surface change for different θ_2 values. For instance when $\theta_2 = 60$ (the angle between the vertical and the centerline of the pool fire volume) the point which receives the maximum amount of radiation, is located approximately at the far end of the top of the 1/5 scale cylinder.

Figure 10 and Figure 11 refer to a full scale pool fire whose dimensions are given in Table 1.

Figure 10 presents the variation of the incident radiant heat flux on the top cylinder surface for several flame temperatures.

The variation of incident heat flux circumferentially is shown in Figure 11. In the second part of this study experiments will be described with 1/5 and full scale propane filled tanks as will be explained in detail there [5, 7]. In order to verify the results obtained from this study, however, we will describe only one of these experiments dealing with the incident radiation from the luminous flame resulting from a 3 m × 5.45 m JP-4 pool fire engulfing a 1/5 linear scale tank containing 0.681 m^3 liquid propane. During the experiment there was an 11 kmph breeze along the axis of the vessel from the NNW. Approximately 15 minutes after ignition all the propane had been vented and the test terminated. The east upper portion of the vessel was found to be severely bulged.

From Figure 2 an 11 kmph wind speed approximately corresponds to an inclination angle, $\theta = 50°$. The parts of the tank surface which receive maximum radiative heat flux, can be determined for an inclination angle of $\theta = 50°$ from Figure 9. From this figure it can be seen that this surface element is located approximately 1.1 ÷ 1.3 m from the center of flare; this corresponds roughly to the surface area of the tank which has been bulged.

TABLE 1

Quantity	Full Scale	Fifth Scale
a_0 (m)	8.488	2.24
a_1	-0.3733	-0.3806
a_2 (m^{-1})	$0.1424.10^{-1}$	$0.6202.10^{-1}$
a_3 (m^{-2})	$0.1021.10^{-2}$	$0.1219.10^{-1}$
a_4 (m^{-3})	$-0.7240.10^{-4}$	$-0.3706.10^{-2}$
D (m)	3.05	0.61
H (m)	22	6
h_1 (m)	4.575	0.915
h_3 (m)	3.05	0.61
L (m)	18.3	3.66
W (m)	17	4.5
δ (m)	$1.59.10^{-2}$	$0.64.10^{-2}$

CONCLUSION

The circumferential and longitudinal variation of the incident radiant heat flux on a cylindrical surface engulfed in flame has been determined. Those parts of the cylinder surface which receive the maximum amount of radiant heat flux during cross wind conditions were evaluated. The obtained results have been compared with existing experimental results and reasonable agreement was found.

REFERENCES

1. Masliyah, J.H., and Steward, F.R., "Radiative Heat Transfer from a Turbulent Diffusion Buoyant Flame With Mixing Controlled Combustion." Combustion and Flame, Vol. 13, 1969, pp. 613-625.
2. Modak, A.T., "Thermal Radiation from Pool Fires." Vol. 29, 1977, pp. 177-192.
3. Birk, A.M. and Oosthhuize, P.H., "Model for the Prediction of Radiant Heat Transfer to a Horizontal Cylinder Engulfed in Flames." ASME Paper 82-WA/HI-52.
4. Hottel, H.C. and Sarofim, A.D., "Radiative Transfer." McGraw-Hill, 1967.
5. Appleyard, R.D., "Testing and Evaluation of EXPLOSAFE System as a Method of Controlling the Boiling Liquid Expanding Vapour Explosion." Transport Canada Report No. TP 2740, 1980.
6. Omer, A.D. and Cedomir, M.S., "Effect of wind on buoyant diffusion flames." I & EC Fundamentals, Vol. 3, No. 2, 1964, pp. 147-154.
7. Charles, A., "The effects of a fire environment and rail tank car filled with LPG." U.S. Department of Transportation, PB-241358, 1974.

LIST OF FIGURES

Figure 1a, 1b - Pool fire and the cylindrical tank car.

Figure 2 - The variation of the pool fire inclination versus wind velocity.

Figure 3 - Inclination of the pool fire under cross wind conditions.

Figure 4 - The three dimensional presentation of the pool fire and the rail tank car.

Figure 5 - The maximum radiation heat flux receiving points for several inclination angles.

Figure 6 - The variation of incident radiant heat flux longitudinally on the top surface of the cylinder for different k values (1/5 scale).

Figure 7 - The effect of flame temperature on the incident radiant heat flux (1/5 scale).

Figure 8 - The circumferential variation of incident radiant heat flux on the cylinder surface for several k values (1/5 scale).

Figure 9 - Effect of the inclination of the pool fire on the incident radiant heat flux on the cylinder surface for several inclination angles.

Figure 10 - The effect of flame temperature on the incident radiant heat flux (full scale).

Figure 11 - The circumferential variation of incident radiant heat flux on the cylinder surface for several k values (full scale).

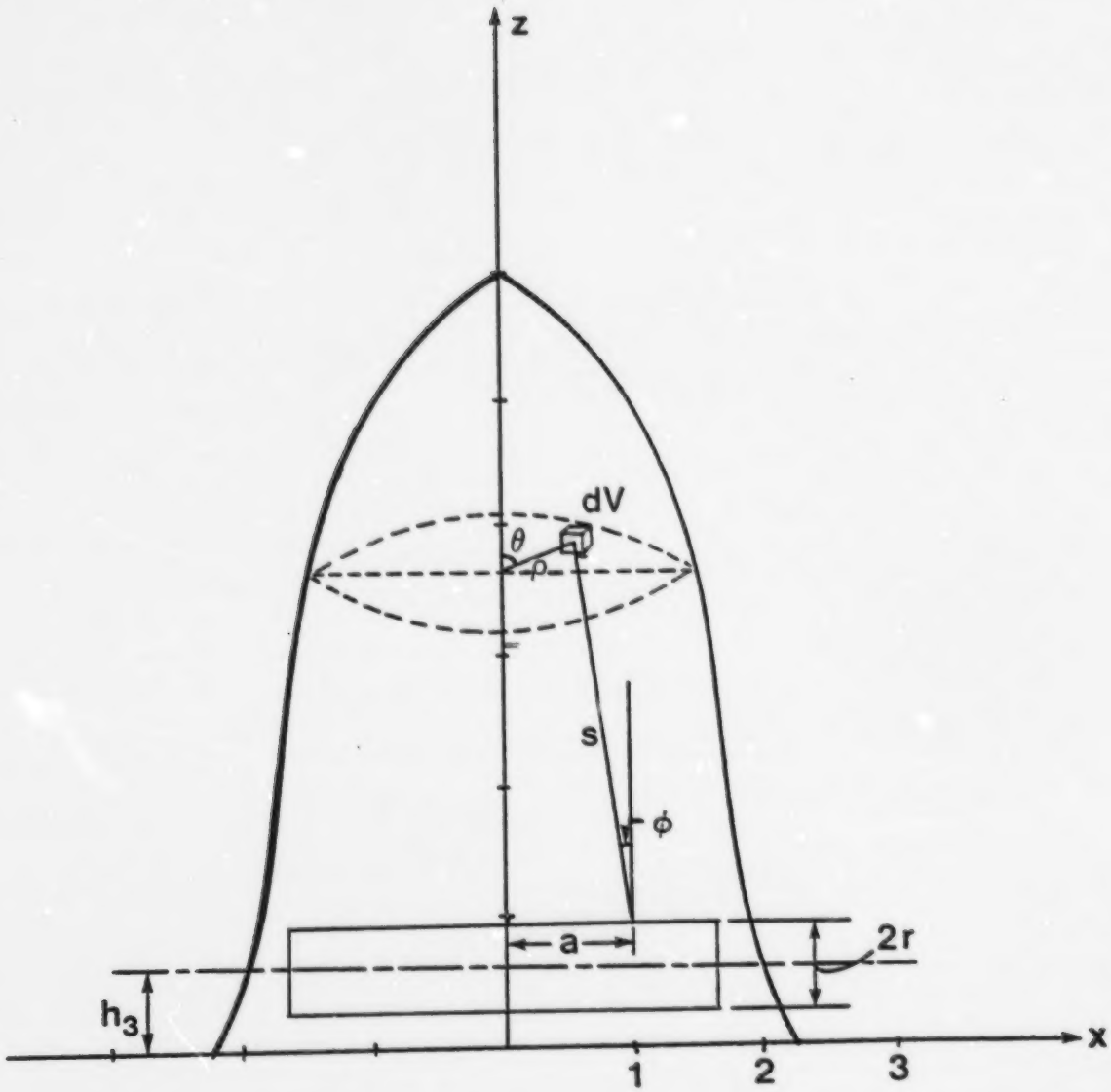
z
dV
θ
ρ
s
ϕ
a
2r
h3
x
1
2
3

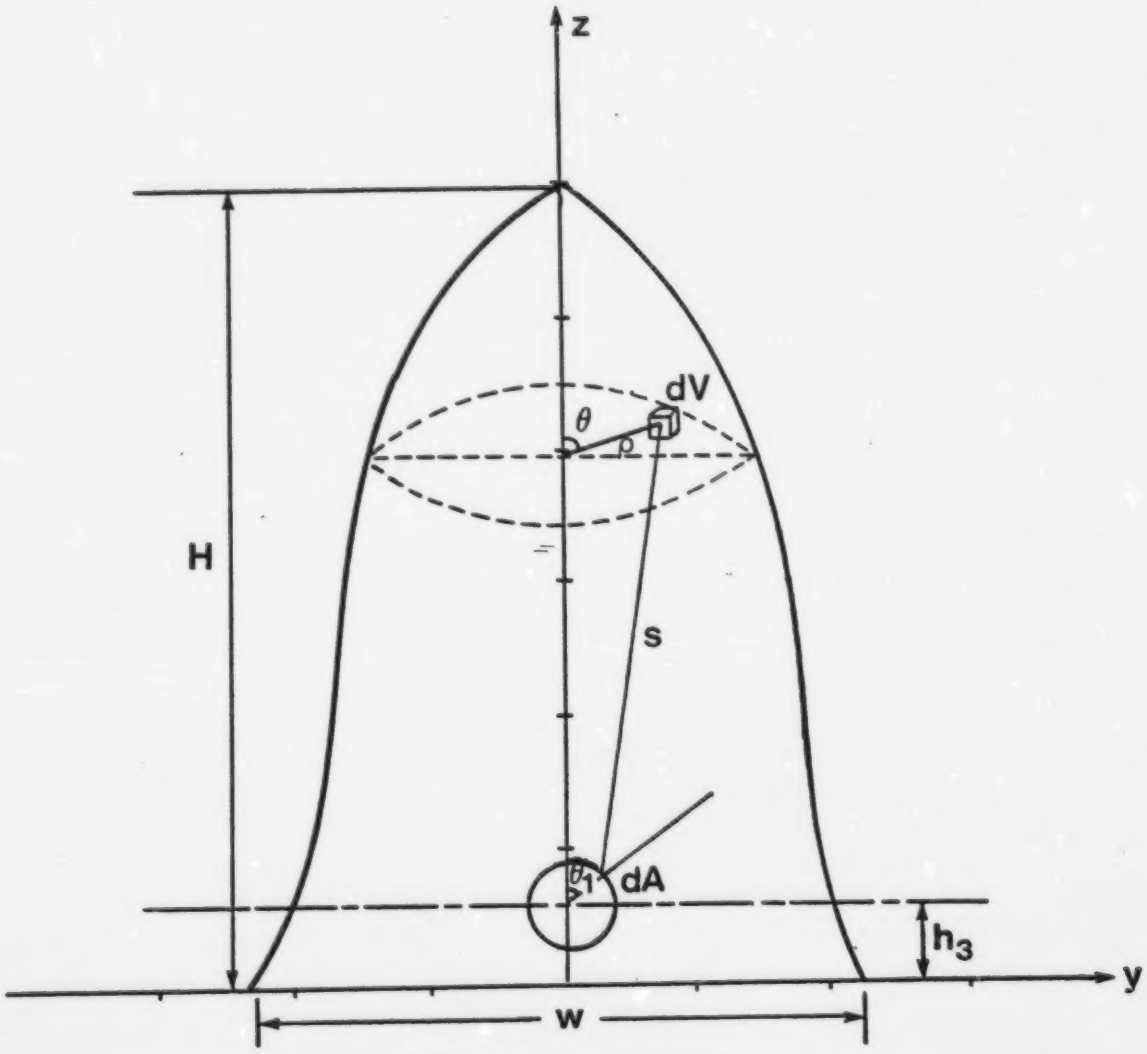
z
dV
θ
ρ
H
s
θ1
dA
h3
y
w

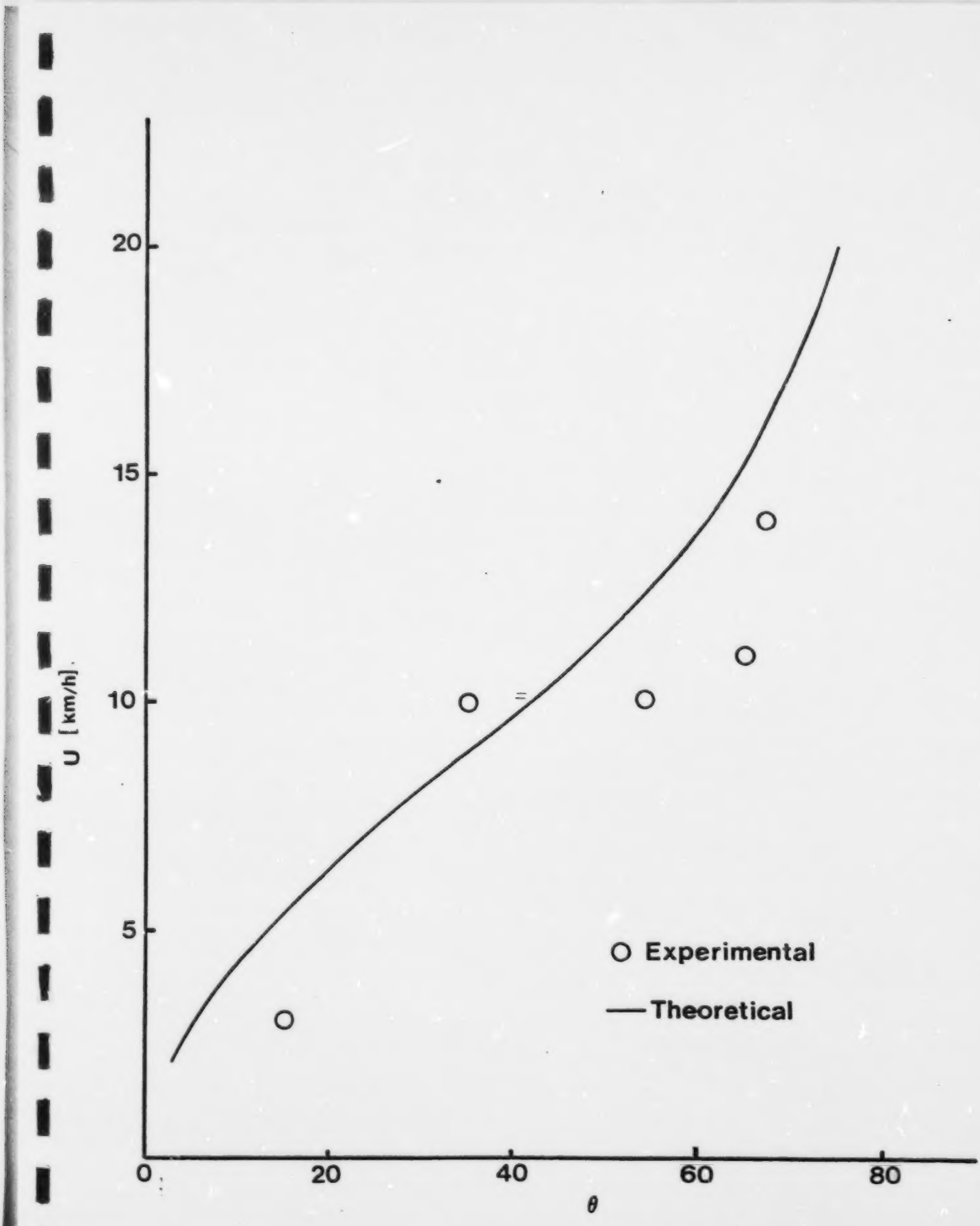
20
15
10
5
U [km/h]
0
20
40
60
80
θ
O Experimental
Theoretical

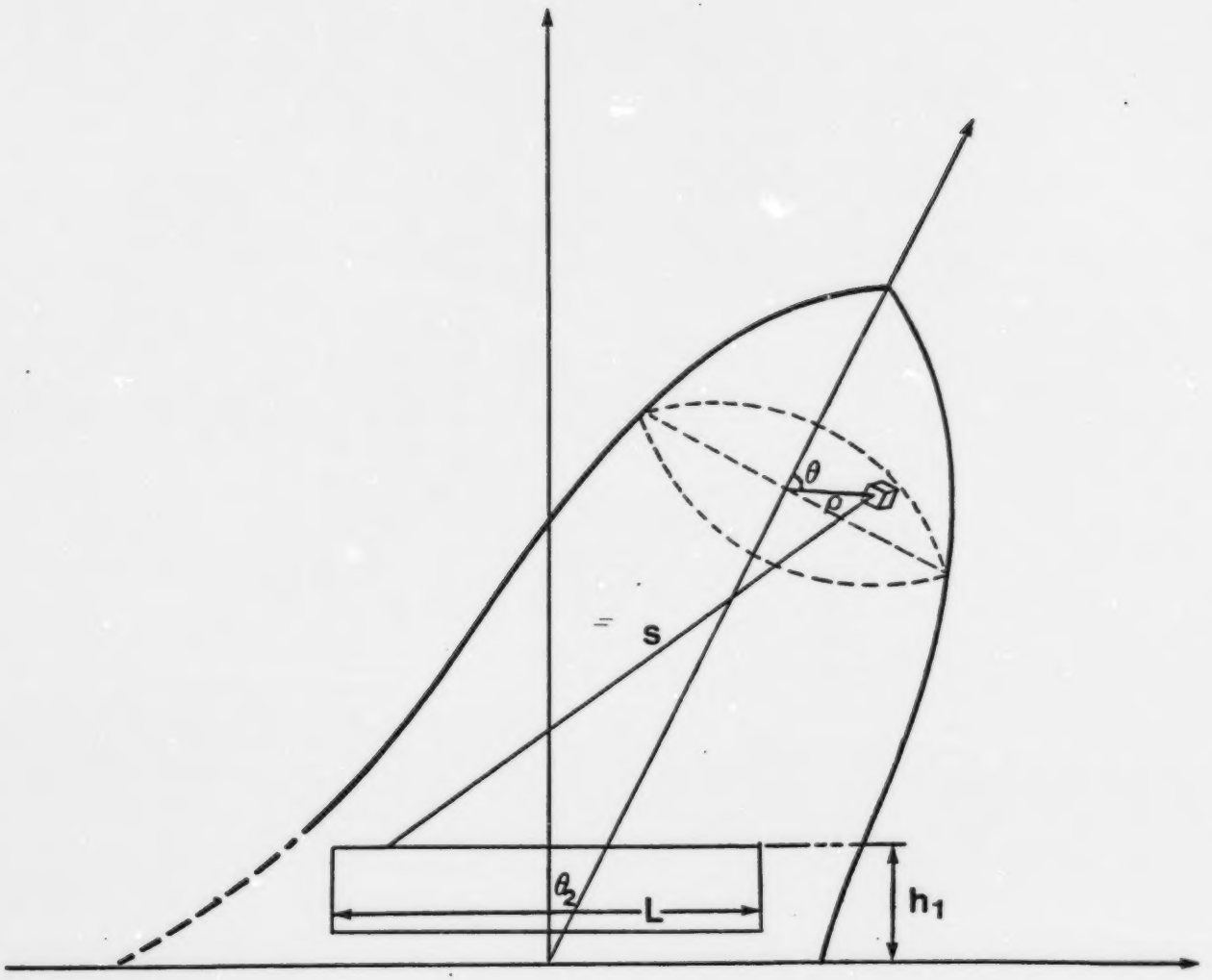
θ
ρ
s
θ2
L
h1

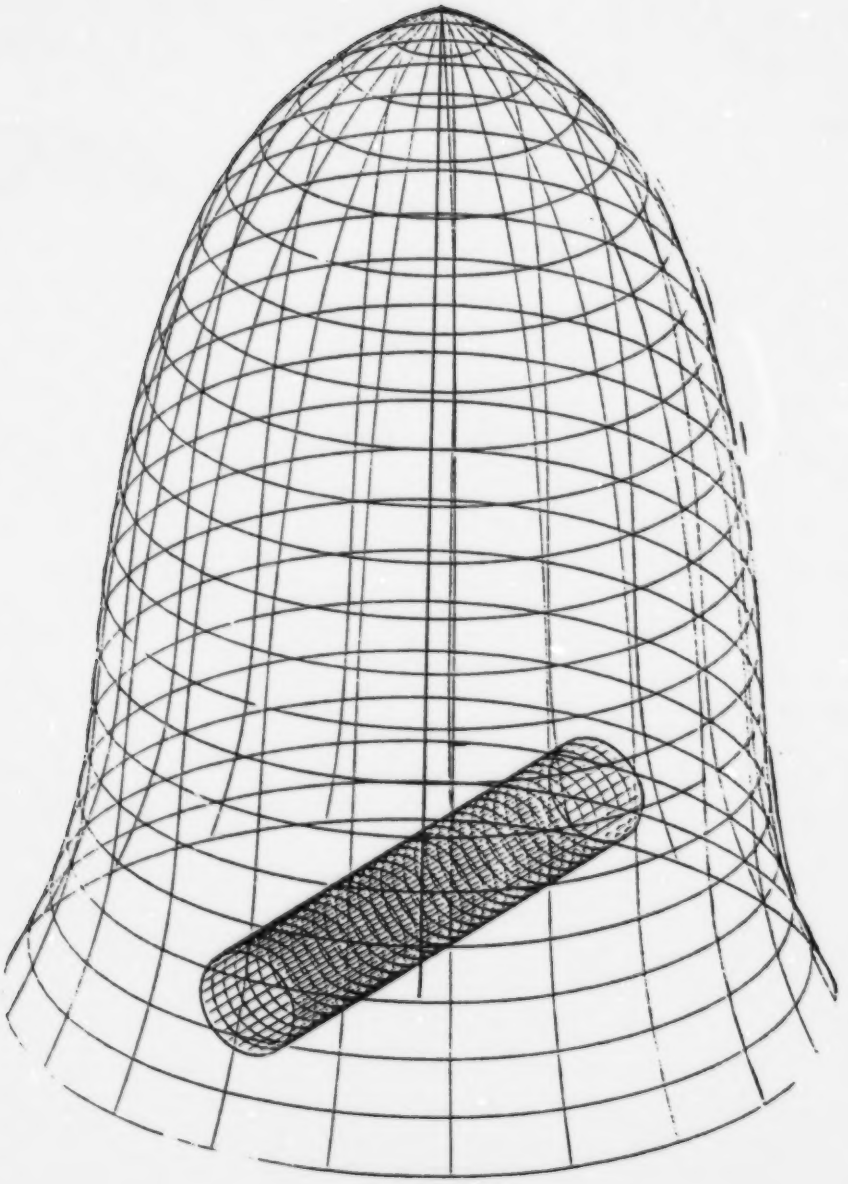

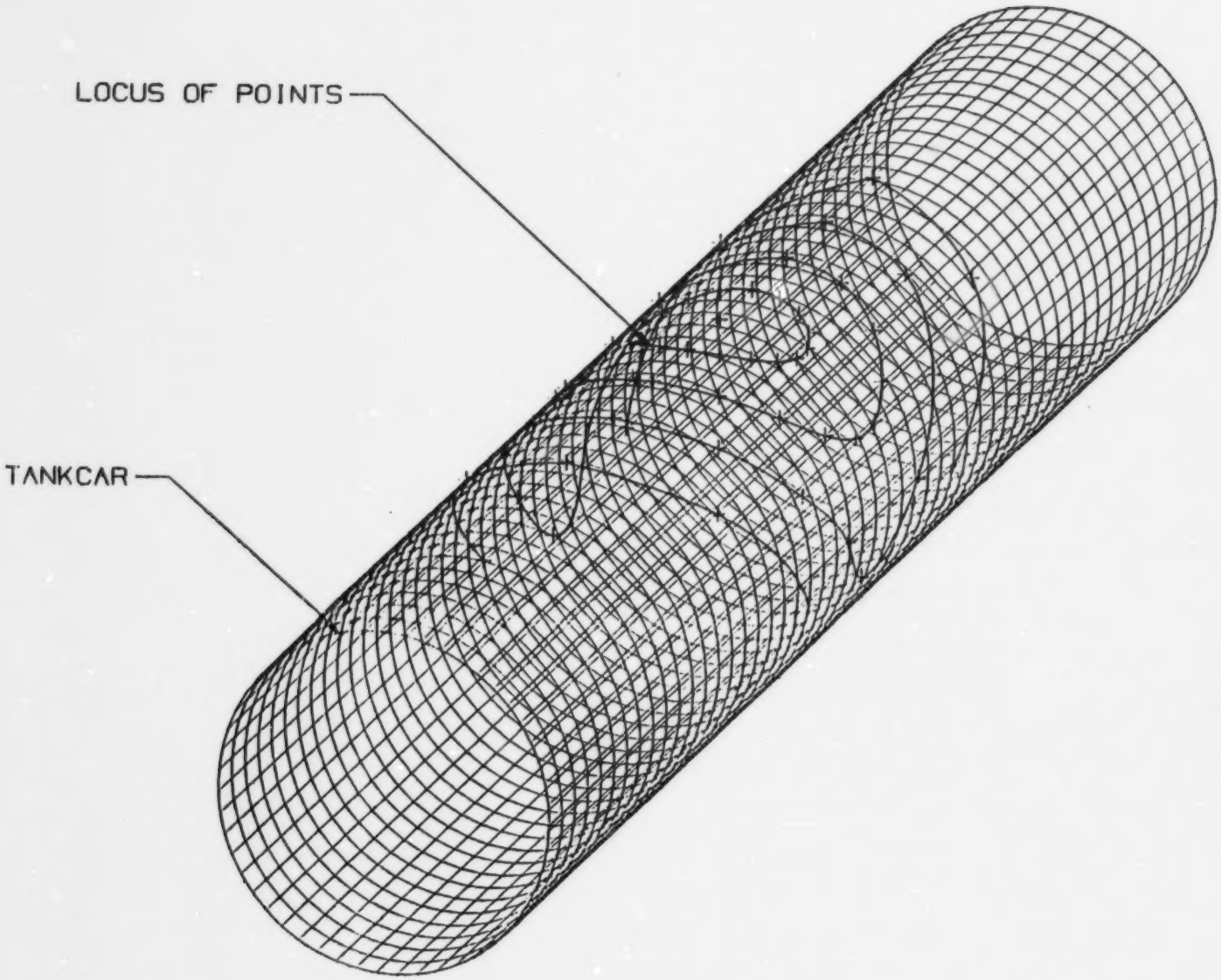
LOCUS OF POINTS
TANKCAR

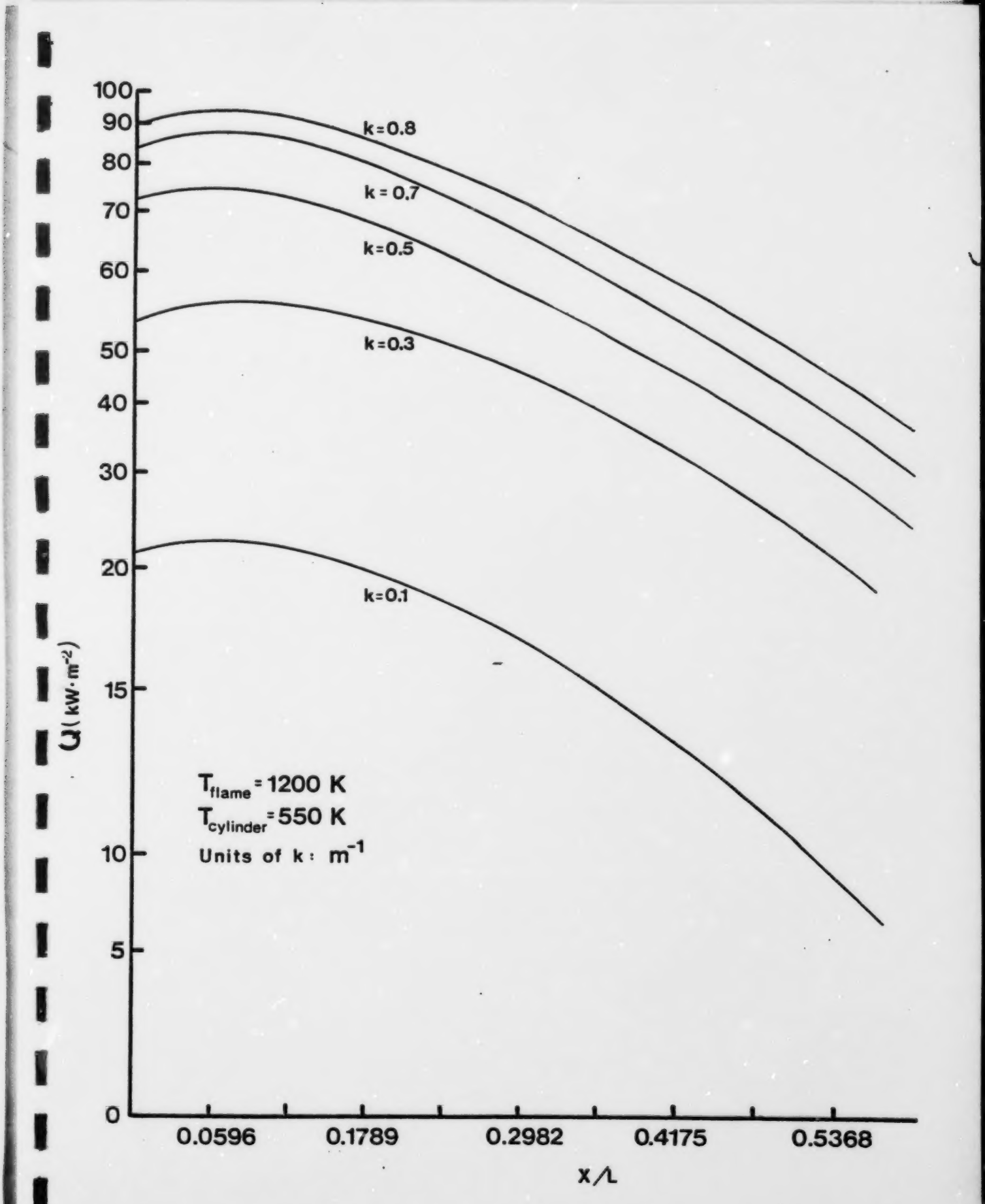
100
90
80
70
60
50
40
30
20
15
10
5
0
k=0.8
k = 0.7
k=0.5
k=0.3
k=0.1
Q(kW·m⁻²)
T_flame = 1200 K
T_cylinder = 550 K
Units of k: m⁻¹
0.0596
0.1789
0.2982
0.4175
0.5368
x/L

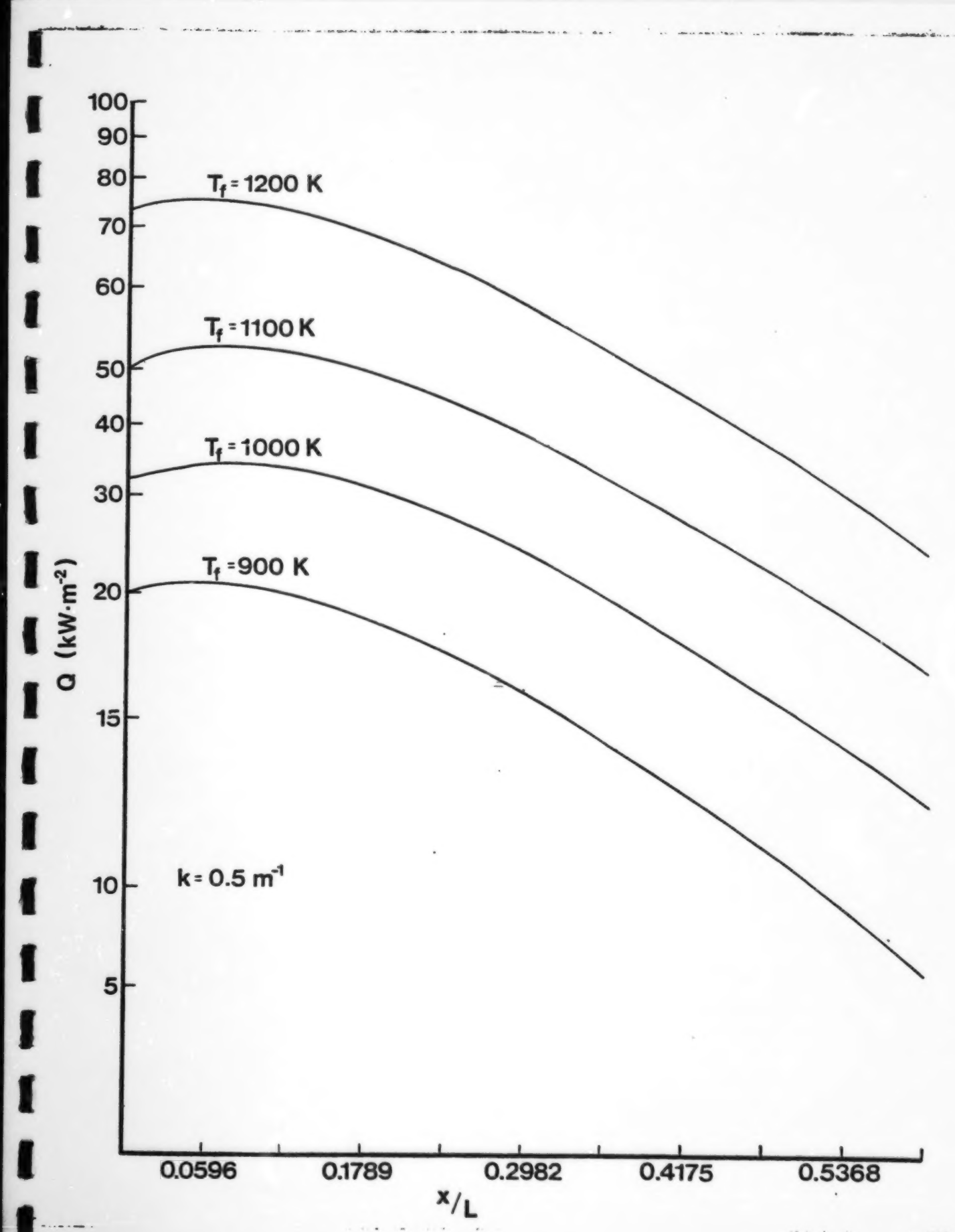
100
90
80
70
60
50
40
30
20
15
10
5
Q (kW·m⁻²)
T_f = 1200 K
T_f = 1100 K
T_f = 1000 K
T_f = 900 K
k = 0.5 m⁻¹
0.0596
0.1789
0.2982
0.4175
0.5368
x/L

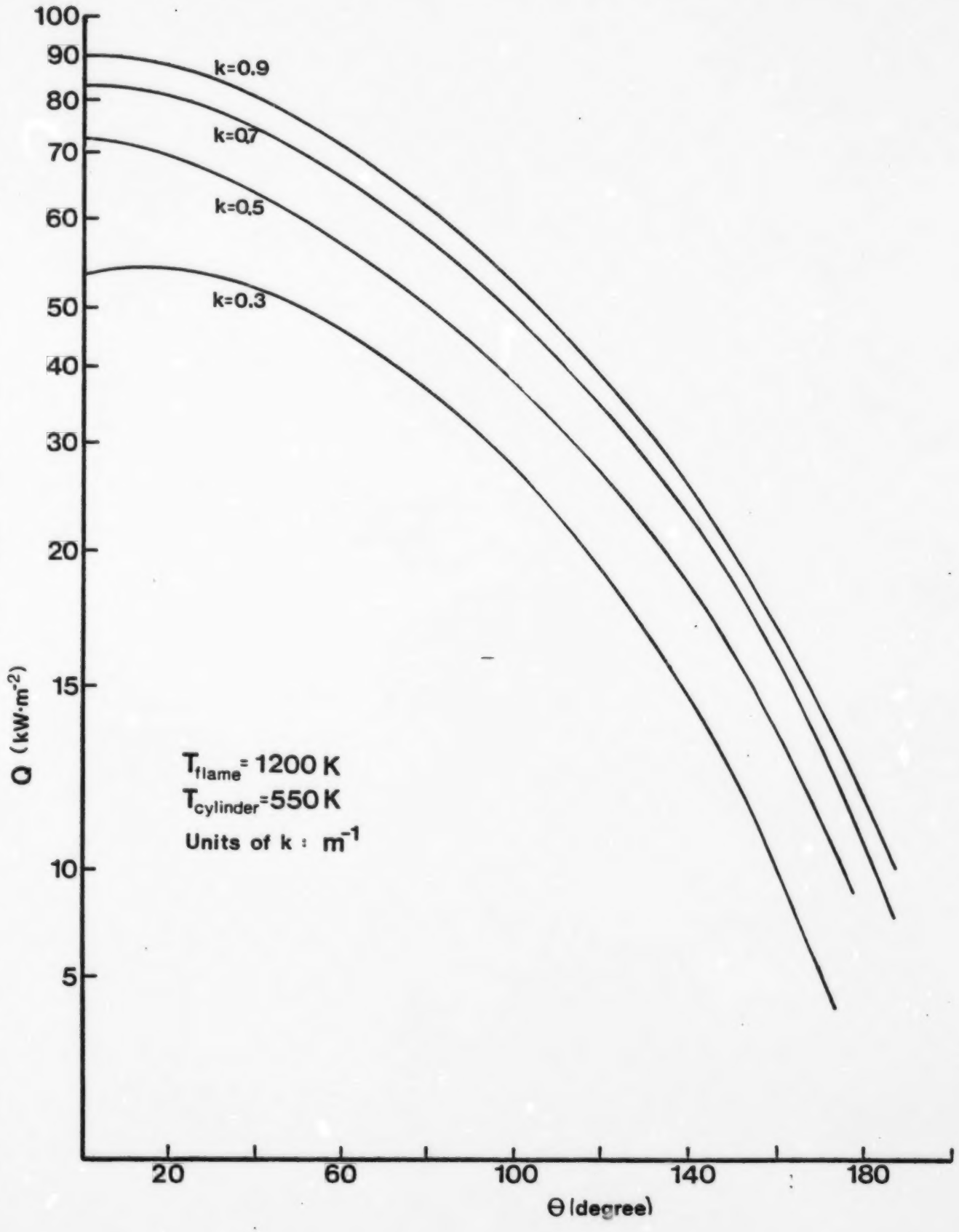
100
90
80
70
60
50
40
30
20
15
10
5
k=0.9
k=0.7
k=0.5
k=0.3
Q (kW·m⁻²)
T_flame = 1200 K
T_cylinder = 550 K
Units of k : m⁻¹
20
60
100
140
180
Θ (degree)

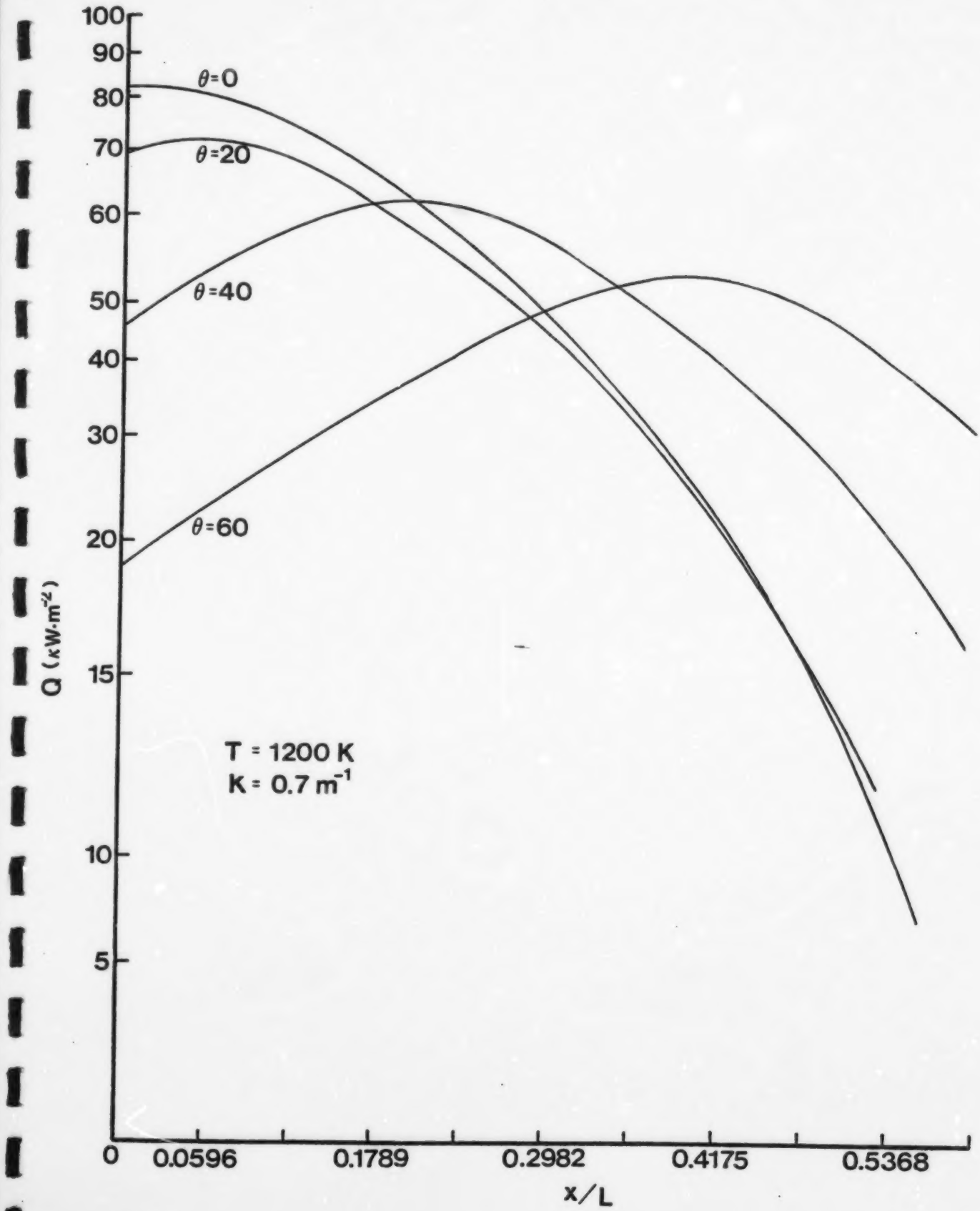
100
90
80
70
60
50
40
30
20
15
10
5
0
θ=0
θ=20
θ=40
θ=60
Q (kW·m⁻²)
T = 1200 K
K = 0.7 m⁻¹
0.0596
0.1789
0.2982
0.4175
0.5368
x/L

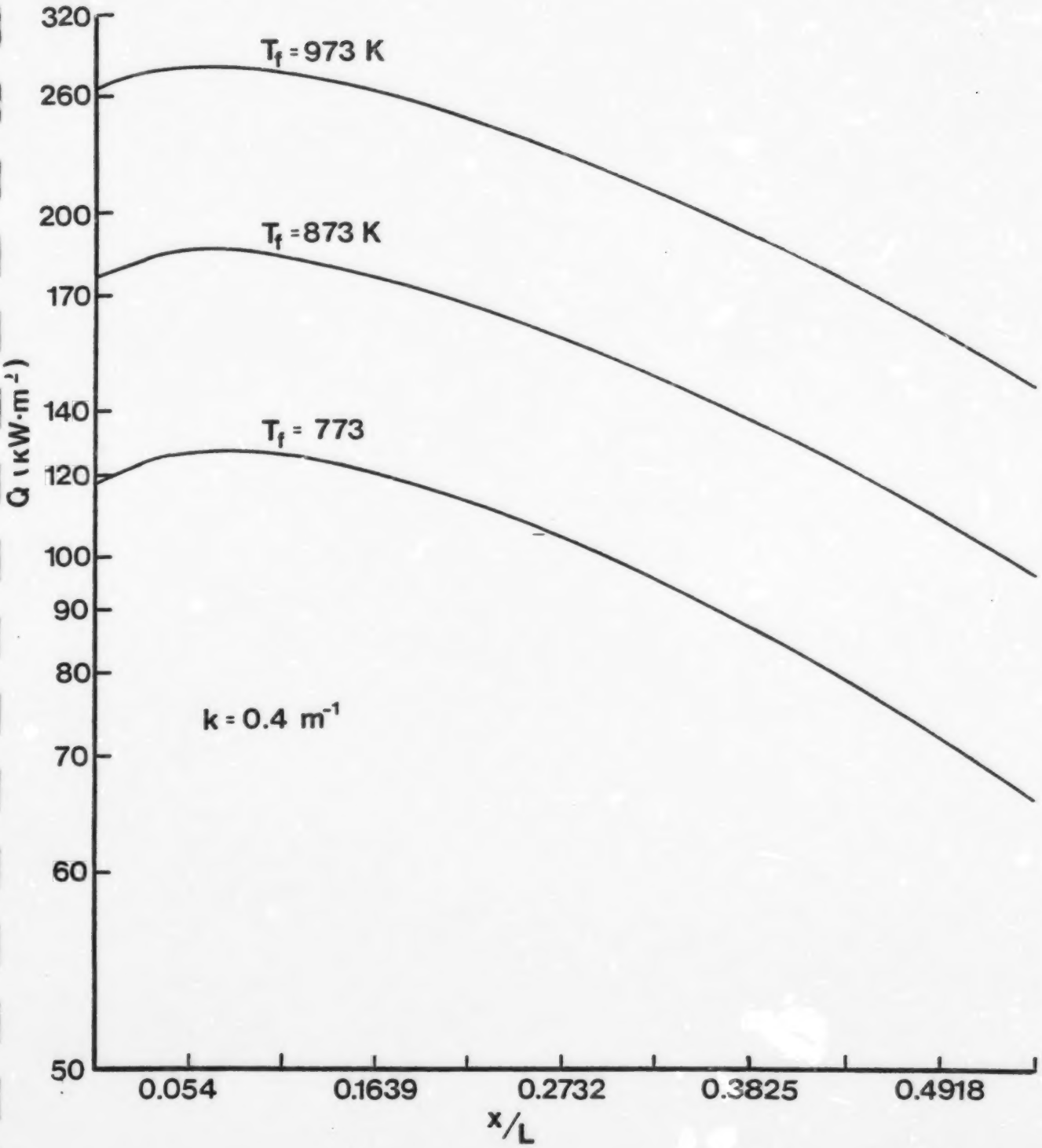
320
260
200
170
140
120
100
90
80
70
60
50
T_f = 973 K
T_f = 873 K
T_f = 773
k = 0.4 m^{-1}
Q (kW·m^{-2})
0.054
0.1639
0.2732
0.3825
0.4918
x/L

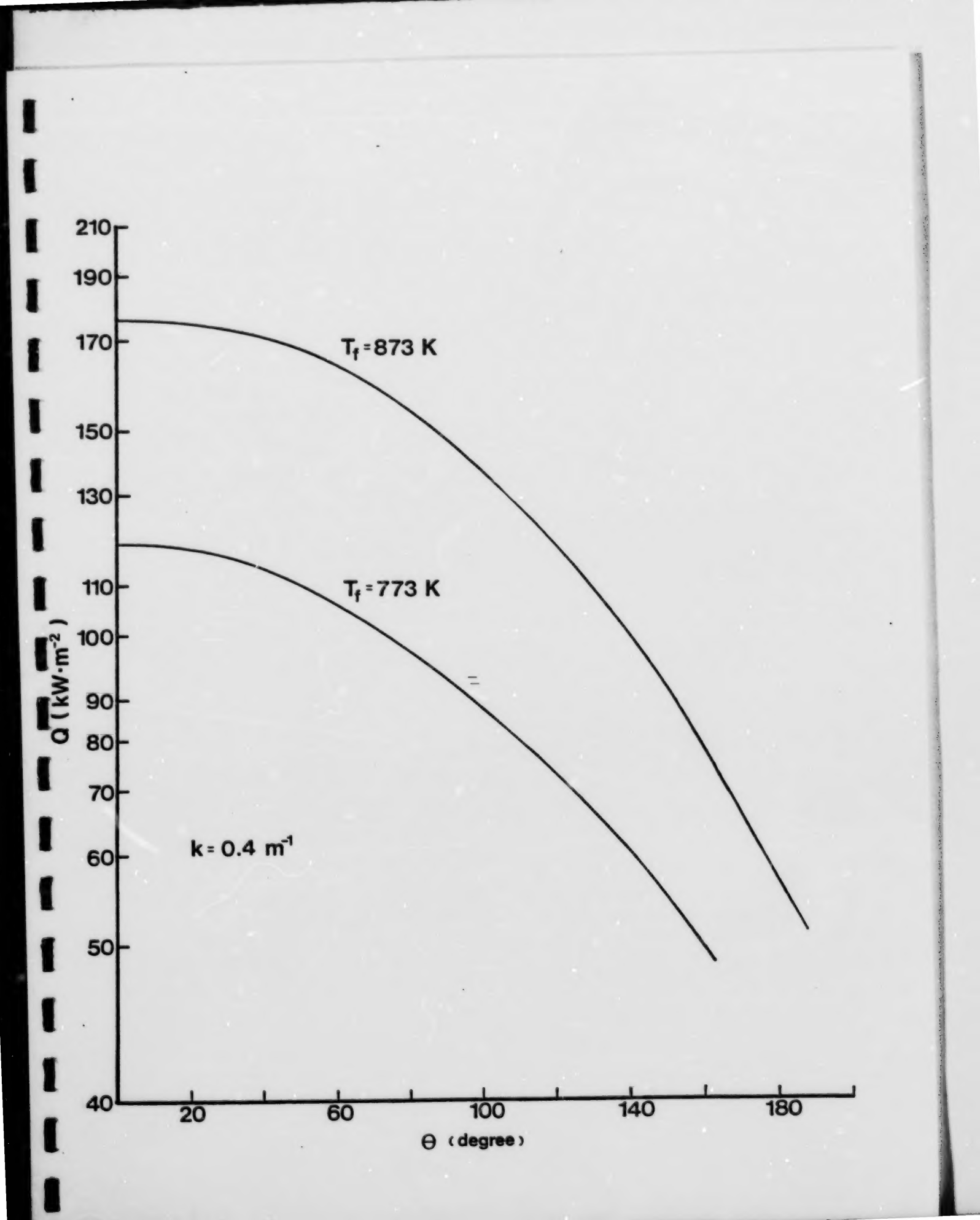
210
190
170
150
130
110
100
90
80
70
60
50
40
Q (kW·m⁻²)
T_f = 873 K
T_f = 773 K
k = 0.4 m⁻¹
20
60
100
140
180
Θ (degree)

INCIDENT RADIATION FROM A FLARE TO A HORIZONTAL CYLINDER PART II

M. Tunc*

J.E.S. Venart

Department of Mechanical Engineering,

U.N.B., Fredericton, N.B., Canada

*Address after Oct. 1, 1983

Technical University of Istanbul
Thermodynamics Department
Mechanical Eng. Faculty
Gumussuyu, Istanbul, Turkey

ABSTRACT

The total radiative heat transfer from a pressure relief valve to a rail tank car surface was calculated. The flame was regarded as a radiating surface. The variation of the incident heat flux on the cylindrical surface due to the inclination of the flare in cross wind conditions was investigated. The results of full and fifth scale fire tests conducted on real tanks filled with LPG were utilized to compare the analytical results obtained here (Part II) and from Part I. Reasonable agreement was obtained between the analyses and experiments.

NOMENCLATURE

a	blow off distance, m
A	area, m^2
c_L	fuel concentration at the lean flammability limit, kg/m^3
$\bar{C}_L$	dimensionless lean - limit concentration of fuel
C_T	fuel concentration in stoichiometric fuel-air mixture, kg/m^3
D	diameter of the relief valve, m
L	flame length, m
m	mass flow rate, kg/s
M_a	molecular weight of air, kg/kg.mol.
M_f	molecular weight of jet fuel, kg/kg.mol.
Q	incident radiant heat flux, W/m^2
R	the ratio of the jet momentum flux, to the cross-wind momentum flux
r	distance between interchanging elements, m
r_1	radius of the flare, m
r_f	radius of the flame in the conical part, m
$\bar{S}_L$	dimensionless coordinate
T_i	temperature of jet fluid, K
T_F	adiabatic flame temperature, K
U_a	average velocity, m/s
U_o	sonic velocity, m/s
u_j	discharge velocity, m/s

u_∞ wind speed, m/s

x distance from the origin of the flare stack to the element of area exchanging radiation, m

W width of the pool fire, m

z distance along the flame centerline, m

z_1 height of the flare stack, m

z_2 total height of the combustion zone, m

α conical angle, rad.

β angle locating the surface element dA_2, rad.

θ angle between the vertical and the centerline of the flame, rad.

ρ_j fuel density, kg/m^3

ρ_∞ air density, kg/m^3

σ Stefan-Boltzmann constant, $5.66 \cdot 10^{-8}$ W/m^2K^4

ϕ angle between connecting vector and the vector normal to the surface, rad.

INTRODUCTION

After a very short period of time, rail tank cars containing LPG, accidentally exposed to an enveloping fire, vent their contents through a relief valve(s) which forms a large flare, some 10-50 m high, depending on the size of the tank, the quantity of LPG and the intensity of the fire surrounding. These flares cause additional radiant heat flux on the cylindrical tank surface.

There are many studies concerning the prediction of radiant heating from flares. Brzustowski [1] discussed the accuracy of the corrected point-source formula for predicting the geometrical distribution of flare radiation. He also showed a new procedure for predicting the shape and length of a very large open flame in a crosswind.

Kent [2], [3] and Kovacs [4] considered the flare as a point source, in determining radiation effects.

Recently Becker [5] calculated the amount of heat radiated to the surroundings from a vertical flare, by considering the flame as a point source and also as a radiating surface. He compared these results with measured values and demonstrated that considering the flame as a radiating surface satisfies the measurements with better accuracy, even if the emissivity was assumed to be $\varepsilon = 1$.

In the present study:

(a) The dimensions of vertical flares and bent over flares under crosswind conditions have been determined.

(b) The radiant heat emitted to the surroundings from the burning flares has been calculated by regarding the flame as a radiating surface. The effects of the bent flares on the emitted radiant heat have been investigated.

(c) The analytical results obtained from Part I and Part II are combined and verified with experiments.

All calculations were performed for two flare sizes with dimensions approximating those of full and fifth scale fire test conducted on real tanks [6, 7].

The shape of the flare and the effects of the wind

The gas velocities at the exit of the pressure relief valve are generally above 0.2 Mach [6]. Combustion takes place at some distance from the exit where the velocity is reduced sufficiently to allow stable combustion. This distance is called the blowoff distance [2]. The actual length of the flare therefore, is the sum of the blowoff distance and the length of the flame.

The blowoff distance may be calculated by using the following relationship [2]:

$$a = \frac{6.4\pi D}{4} \frac{U_o}{U_a} \qquad (1)$$

and the flare length [8] by:

$$\frac{L}{D} = \frac{5.3}{C_T} \frac{T_F}{\alpha_T T_i} \left[C_T + (1 - C_T) \frac{M_a}{M_f}\right]^{1/2} \qquad (2)$$

For propane, $C_T = 0.038$, $T_F/T_i = 7.6$ and $\alpha_T = 0.96$ [9].

The shape of the bent over flare is defined in terms of the vertical flame angle as it is shown in Fig. 1 [1].

The variation of this angle with wind velocity is shown in Fig. 2 and the evaluation procedure is explained in Appendix A, following the work of ref. [1].

Radiative heat exchange between a bent flame surface and the tank surface

The flame is assumed to be a uniformly emitting black radiating surface. A geometrically exaggerated model of the flame contour above the flare vent is shown in Fig. 3.

The total energy per unit time leaving the flame surface and incident upon dA_1 is

$$Q = \frac{2\sigma T_F^4}{\pi} \int_{z_1}^{z_2} \int_{0}^{\cos^{-1}(r_f/x)} \frac{\cos\phi_1 \cdot \cos\phi_2}{r^2} \, dA_2 \qquad (3)$$

The limits of the integration for the angle β are from zero to the value $\cos^{-1}(\frac{r_f}{x})$ which can be derived from simple geometrical considerations. The angle β is shown in Fig. 3 which locates the element dA_2 is subtended by a radius vector, r, passing through the element and pointing in the positive x direction to dA_1. The cone element area dA_2 is given by:

$$dA_2 = \frac{r_f \cdot d\beta}{\cos\alpha} \tag{4}$$

where $r_f = (z - z_1)\tan\alpha + r_1$ is the radius of the conical portion of the flame;

$$\cos\phi_1 = \frac{z\cos\theta + (2\beta/\pi - 1) r_f \cdot \sin\theta}{r} \tag{5}$$

$$\begin{aligned} r^2 = {} & (x - z\sin\theta)^2 + \{r_f\cos\theta + \frac{2 \cdot r_f \cdot \beta}{\pi}(1 - \cos\theta)\}^2 \\ & - 2(x - z\cdot\sin\theta)\{r_f\cos\theta + \frac{2 r_f \cdot \beta}{\pi}(1 - \cos\theta)\}\cos\beta \\ & + \{z\cos\theta - r_f\sin\theta + \frac{2 r_f \cdot \beta}{\pi}\sin\theta\}^2 \end{aligned} \tag{6}$$

and

$$\cos\phi_2 = \frac{(r^2 - x^2)\alpha_1}{2r\, r_f} + \frac{2x\alpha_1 \cdot \cos\beta}{2r\,\alpha_2} + \frac{r_f}{2r}\left(\frac{1}{\alpha_1} - \frac{1}{\alpha_2^2}\right) \tag{7}$$

where $\alpha_1 = \sin\alpha \cdot \tan(\theta + \alpha)$

$\alpha_2 = \sin\alpha \cdot \sin(\theta + \alpha)$

The incident heat flux from the flame surface to dA_1 has been evaluated by substituting equations (5), (6) and (7) into equation (3) and carrying out the necessary integrations.

Results for the one-fifth linear scale are presented in Fig. 4. It is very clear from this figure that the incident

radiant heat flux on the cylinder surface increases considerably, as the angle of inclination changes. Fig. 5 shows similar results for a full scale tank.

The importance of the selection of the model for the flame contour above the flare stack is shown in Fig. 6, where the flame contours are represented by a cylindrical surface as distinct from a cone. The volume of the flare was maintained constant for both geometries. The radiant heat flux, from the bottom surfaces was also included. Depending on the diameter of the cylinder, this heat flux may become very large. A comparison with flame photographs shows that the conical representation is more realistic (Table 1).

EXPERIMENTS

1/5 scale experiments

Six tests have been conducted under pool fire conditions. A pool fire (3 m x 5.45 m) has been used to simulate a typical accident. The flames totally engulfed the test vessels [6]. Flame temperatures were measured by fire thermocouples constructed from 1.5 mm diameter stainless steel sheathed closed junction type with K calibration. Circumferential internal cylinder wall temperatures, vapour space temperature distribution, internal pressures, and liquid temperature distribution were also recorded. The thermocouple data was recorded by a 60 channel fluke model 2240 Datalogger. The

tests were visually recorded on 16 mm colour film by a Locam camera. Wind directions for all six experiments are shown in Fig. 7.

Detailed experimental comments

Experiment number 1: The test was conducted under clear skies with a 12 kmph breeze from the west and an ambient temperature of 0°C. After ignition, the fire spread rapidly across the fire tray and within seconds the area defined by the wind shields was engulfed in flames. Approximately 2 minutes after ignition the relief valve opened for about 5 seconds and the venting propane gas formed a large flare some 15 meters tall. After closing for about 12 seconds the valve opened again and remained open. Tank failure at 12 minutes began with a thermal rupture at top dead center located downwind from the relief valve as is shown in Fig. 8.

Experiment number 2: Weather conditions were again good with clear skies, a 10 kmph breeze from the west and ambient temperature of -22°C. This tank was equipped with a special type of internal thermal protection called EXPLOSAFE [6]. After a 30 second ignition period the pressure rose steadily within the tank until about 2.5 minutes when the relief valve opened at 1.93 MPa and vented for about 13 seconds. Closure was followed by a further opening after which the valve vented continuously until closure at 7 minutes after ignition caused by a lack of fuel at the 5 minute mark. After activating the fuel pump,

re-establishing the fire and following an open-close-open cycle, the valve closed. It was concluded that all propane had been released. The vessel had not ruptured, however, a severe longitudinal temperature gradient with the east end hotter than the west was observed.

Experiment number 3: Weather conditions were clear with an 11 kmph breeze from the WNW and an ambient temperature of -7°C. At approximately 10 minutes the valve closed and an open-close-open cycle of the valve observed. By 15 minutes all propane had been released and the test was terminated. The east end of the vessel was hotter than the west and the vessel had bulged on the upper portion of the far east end.

Experiment number 4: A 4 kmph breenze from the SSW and an ambient temperature of -2°C. The test was terminated at 15 minutes after ignition when all the propane had been vented. The south side of the vessel being cooler than the north side.

Experiment number 5 was approximately the same as experiment number 4 with similar results.

Experiment number 6: The wind speed was 3 kmph from the south with an ambient temperature of 0°C. This vessel was not fitted with explosafe. Approximately 2 minutes after ignition the relief valve opened at 1.83 MPa, cycled 3 times and then continuously vented. Pressure again peaked at 6 minutes after ignition and was falling steadily when the

tank ruptured. The fire ball was estimated to be 60-70 m high and some 15 m in diameter. Fig. 9 shows the vessel lying on its side after the test with the rupture at the left higher portion. Table 2 presents the time weighted average heat fluxes for all experiments. Fig. 10 shows the average fire temperatures determined.

FULL SCALE EXPERIMENT

A full scale tank car was positioned in a large excavation which measured 45.7 m in length, 30.5 in width, and 7.92 m in depth [7]. A fuel dike to contain the JP-4 fuel was constructed at the center of the excavation, and measured 24.4 m by 9.14 m. The fire thermocouples were placed in the fire and chromel-alumel thermcouples were positioned on the interior wall of the tank shell and inside the tank at different locations. Six CEC pressure gauges were mounted inside the tank car. Radiation heat flux calorimeters were located 1.2 m and 7 m above the pool surface respectively.

The tank car, filled with 60,000 L. of LPG (Propane 98%), was subjected to a severe fire environment, and catastrophically ruptured 24.5 minutes after ignition. The relief valve opened at 1.96 MPa and remained open. During the first three quarters of the experiment, there was little or no wind, then a slight wind arose about three quarters of the way through the test blowing from east to west. The sudden release of pressure with an additional energy release

of combustion propane broke the tank into approximately 63 fragments. The metallurgical investigation of the fragments has shown that failure was initiated along the main longitudinal fracture path, 3.5 m from the west head to shell weld in the west end of the car [10].

The JP-4 pool fire and propane torch temperatures and heat flux averages are presented in Table 3.

DISCUSSION

The presented analytical results from Parts 1 and 2, have been compared with the experiments. The reasonable agreement has been found between them.

In the analytical parts of the study, it was concluded that those parts of the cylinder surface which are under the inclined (pool fire and flare), received more radiation than the rest of the cylinder surfaces. From the experimental results it is observed that cylinder surface temperatures increase considerably in the wind direction and in addition failure or incipient failure also occurred downwind of the pressure relief valve.

APPENDIX A

(1) The dimensionless lean-limit concentration of fuel is given by [11]:

$$\bar{C}_L = C_L \left(\frac{U_j}{U_\infty}\right) \left(\frac{M_f}{M_a}\right)$$

where U_j = 220 m/s and $1/C_L$ = 45.5 are given in ref. [12]:

(2) The dimensionless coordinate $\bar{S}_L$ of the concentration $\bar{C}_L$ on the axis of the jet and from it the downwind coordinate $\bar{X}_L$ are calculated by using the following relationships [11]:

a) $\bar{C}_L < 0.5$ $\bar{S}_L = 2.04\ (\bar{C}_L)^{-1.03}$

$\bar{X}_L = \bar{S}_L - 1.65$

b) $\bar{C}_L > 0.5$

$\bar{S}_L = 2.51\ (\bar{C}_L)^{-0.625}$

if $\bar{S}_L > 2.35$ $\bar{X}_L = \bar{S}_L - 1.65$

if $\bar{S}_L < 2.35$ $\bar{S}_L = 1.04\ \bar{X}_L^2 + 2.05\ \bar{X}_L^{0.28}$

(3) The dimensionless rise $\bar{Z}_L$ of the flame tip above the flare tip is given as follows [11]:

$$\bar{Z}_L = 2.05\ \bar{X}_L^{0.28}$$

(4) The ratio R of the jet momentum flux to the crosswind momentum flux:

$$R = \frac{\rho_j U_j^2}{\rho_\infty \cdot U_\infty^2}$$

(5) The dimensional coordinates of the flame tip relative to the flare tip [11]:

$$Z_L = \bar{Z}_L, DR^{1/2}$$

$$X_L = \bar{X}_L \; D \cdot R^{1/2}$$

TABLE 1

Quantity	Full Scale [7]	Fifth Scale [6]
a (m)	4	1
D (m)	3.05	0.61
Z_2 (m)	52	11.5
W (m)	17	4.5
α	20°	14
T (K)	1600	1400
m (kg/s)	33.1	1

TABLE 2

Time Weighted Average Heat Fluxes

Test Vessel Code	Mean Fire Temperature °C	Overall W/m^2	Up to Point of Vessel Failure W/m^2
2	578	64291	64228
3	765	51815	52092
4	627	50389	29143
5	610	60286	50298
6	727	45924	45924

TABLE III

Radiative Fluxes and Temperatures of the Fire and the Propane Torch

Time Interval Minutes	Recorded Flux (kW/m^2)	T_{Fire} °C	Fire Flux (kW/m^2)	Torch Flux (kW/m^2)	T_{Torch} °C
5.0 - 11.5	90.12	871	60.28	171.8	1120
11.5 - 15.0	68.7	816	49.4	134.28	1040
15.0 - 24.5	29.65	802	46.94	159.22	1090
Maximum Reading (6.5 Min)	104.8	871	60.28	203.4	1180

LIST OF FIGURES

Figure 1 - The definition of θ and X_L, Z_L.

Figure 2 - The variation of the inclination angle of the flare with the wind velocity.

Figure 3 - A geometrically exaggerated model of the flame contour above the flare stack.

Figure 4 - The variation of the incident radiant heat flux on the cylinder surface for several flare inclinations (1/5 scale).

Figure 5 - Full scale similar results as Figure 4.

Figure 6 - The incident radiant heat fluxes for different flame contours.

Figure 7 - Wind directions during (1/5) scale experiments.

Figure 8 - The raptured 1/5 scale rail tank car (experiment number 1).

Figure 9 - The vessel lying on its side after the test with the rapture at the left higher portion.

Figure 10 - Measured flame temperature during the 1/5 scale experiments.

REFERENCES

1. T.A. Brzustowski, Flares, Norwegian Society of Chartered Engineers, Stayanger, Norway, November 19-21, 1980.
2. Kent, G.R., "Find radiation effects of flares", Hydrocarbon Processing and Petroleum Refiner," Vol. 47, No. 6, 1968, pp. 120-130.
3. Kent, G.R., "Practical Design of Flare Stacks," Hydrocarbon Processing and Petroleum Refiner, Vol. 43, No. 8, 1964.
4. Kovacs, F. and Honti, G., "Secondary Heat Effect on LPG Storage Spheres in Cases of Fire," AICHE Symposium Series, No. 198, 1980.
5. Becker, R., "Mathematical model of luminous flame radiation for the determination of safety zones," Ger. Chem. Eng., Vol. 3, 1980, pp. 229-333.
6. Appleyard, R.D., "Testing and Evaluation of the Explosafe System as a Method of Controlling the Boiling Liquid Expanding Vapour Explosion (BLEVE)," Vulcan Industrial Packaging Ltd., 1980.
7. Charles, A., "The effects of a fire environment on a rail tank car filled with LPG", U.S. Department of Transportation, PB-241358, 1974.
8. Hawthorne, W.R., Weddell, D.S. and Hottel, H.C., "Mixing and combustion on turbulent gas jets," Third Symposium on Combustion, Flame and Explosion Phenomena, Williams and

Wilkins, Baltimore, 1949, pp. 266-288.

9. Brzustowski, T.A., "A new criterion for the length of a gaseous turbulent diffusion flame," Combustion Science and Technology, Vol. 6, 1973, pp. 313-319.
10. Charles, A. and Norris, E.B., "Fragmentation and Metallurgical Analysis of Tank Car Rax 201," U.S. Department of Transportation, FRA/R8D 7530, 1974.
11. Brzustowski, T.A., Collahalli, S.R. and Sullivan, H.F., "The turbulent hydrogen diffusion flame in a crosswind," Combustion Science and Technology, Vol. 11, 1975, pp. 29-33.
12. Prasad, R. and Reid, J.W., Report on significance of flare radiation on railway cars containing LPG. Unpublished report, University of New Brunswick, 1981.
13. Steward, F.R., "The distribution of radiation on a horizontal surface surrounding a uniformly emitting gray gas cone," ASCE, 57 Annual Meeting, Boston, 1964.
14. Gradshteyn, I.S. and Ryshik, I.M., "Table of Integrals, Series and Products," Academic Press, 1965.
15. Brzustowski, T.A., "Flaring in the Energy Industry," Prog. Energy Combust. Science, Vol. 2, pp. 127-141, Pergamon Press, Great Britain, 1976.
16. Brzustowski, T.A., et al., "Radiant Heating from Flares," ASME Paper 75-HT-4, 1976.
17. Anderson, C., et al., "The Effects of a Fire Environment on a Rail Car Filled with LPG," Ballistic Research Laboratories, prepared for Federal Railroad Administration, September 1974.

18. Van Elbe, L., "Combustion, Flames and Explosions of Gases, 2nd Ed.," p. 486, Academic Press Inc., New York, 1961.

19. Sonntag, R.E. and Van Wylen, G., "Fundamentals of Classical Thermodynamics, 2nd Ed." John Wiley & Sons, New York, 1978.

20. Steward, F.R., "Prediction of the Height of Turbulent Diffusion Boyant Flames," Combustion Science and Technology, Vol. 2, pp. 203-212, 1970.

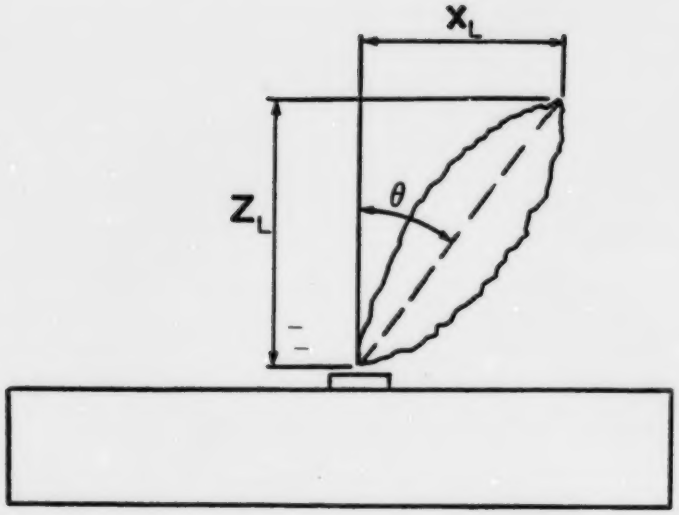
X_L
Z_L
θ

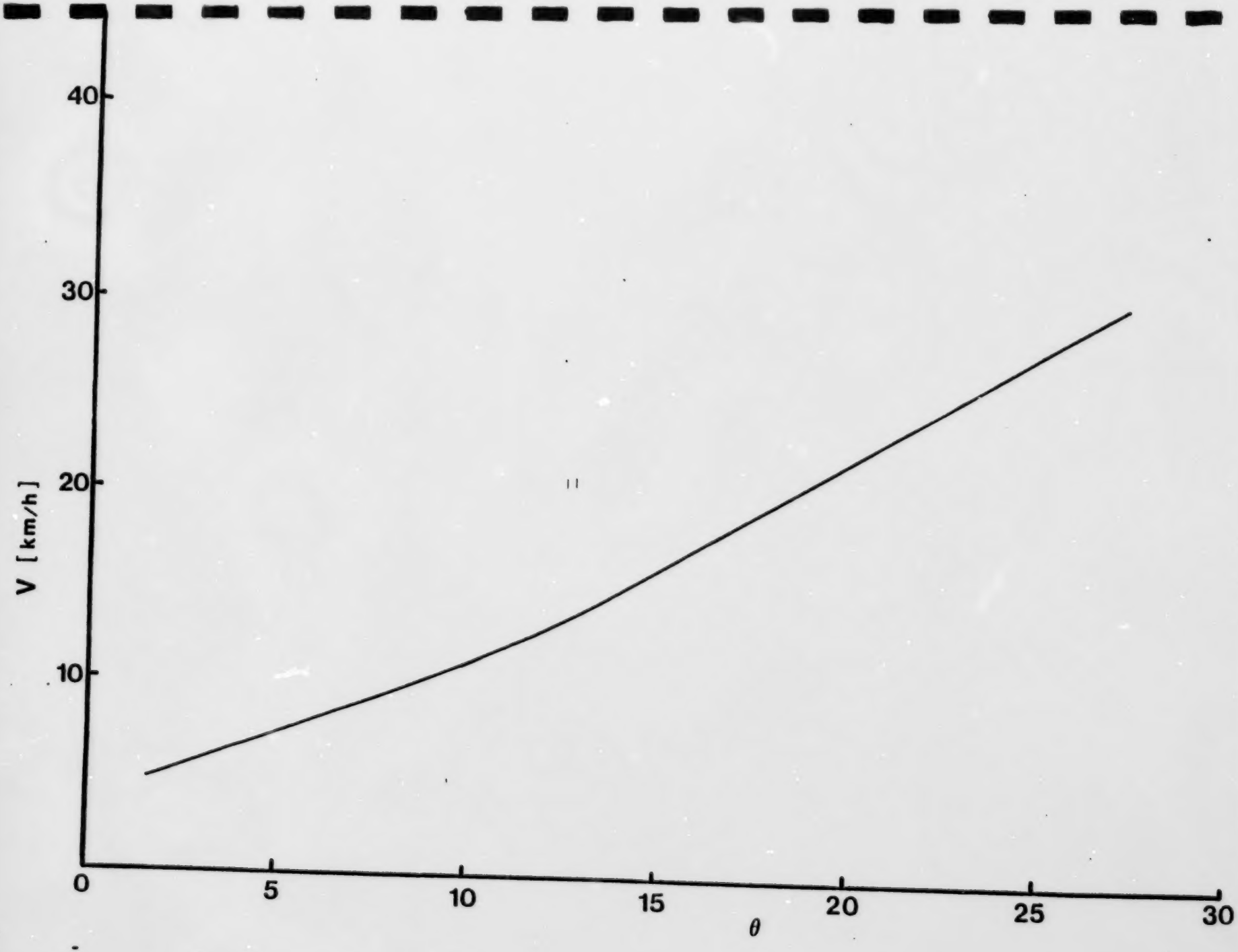
40
30
20
10
V [km/h]
0
5
10
15
20
25
30
θ

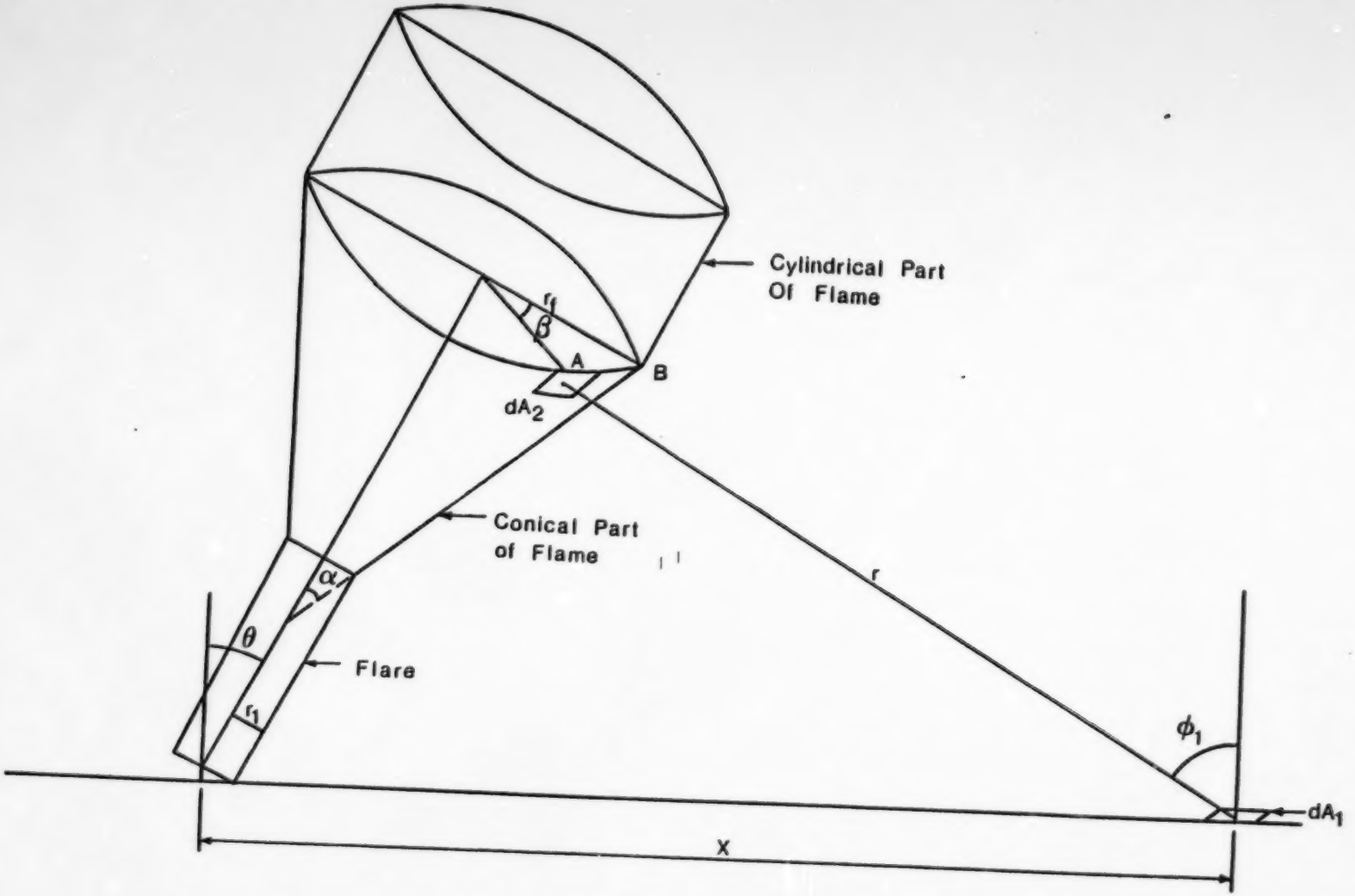
Cylindrical Part
Of Flame
r_1
β
A
B
dA_2
Conical Part
of Flame
r
α_1
θ
Flare
r_1
ϕ_1
dA_1
X

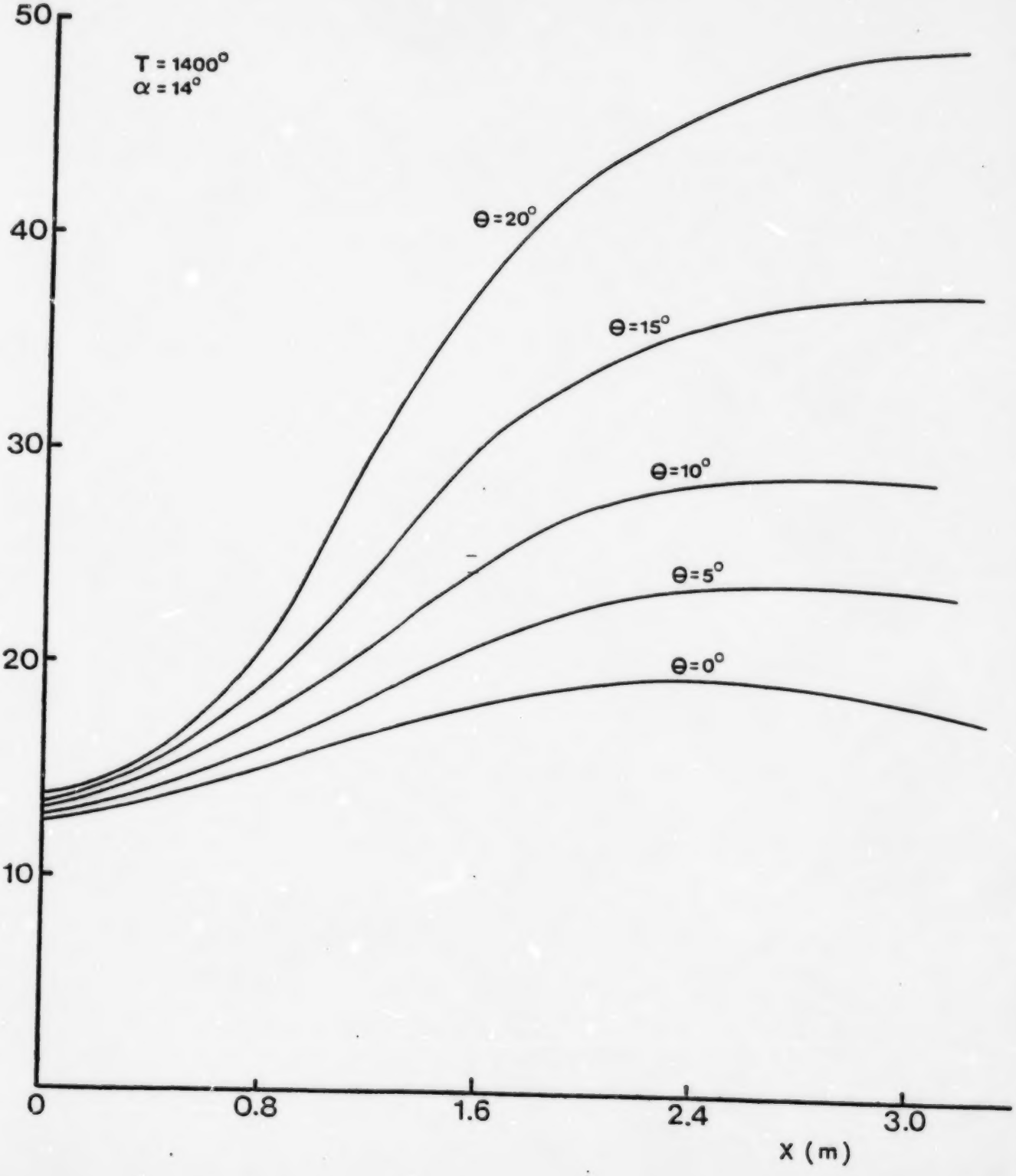
T = 1400°
α = 14°
Θ=20°
Θ=15°
Θ=10°
Θ=5°
Θ=0°
50
40
30
20
10
0
0.8
1.6
2.4
3.0
X (m)

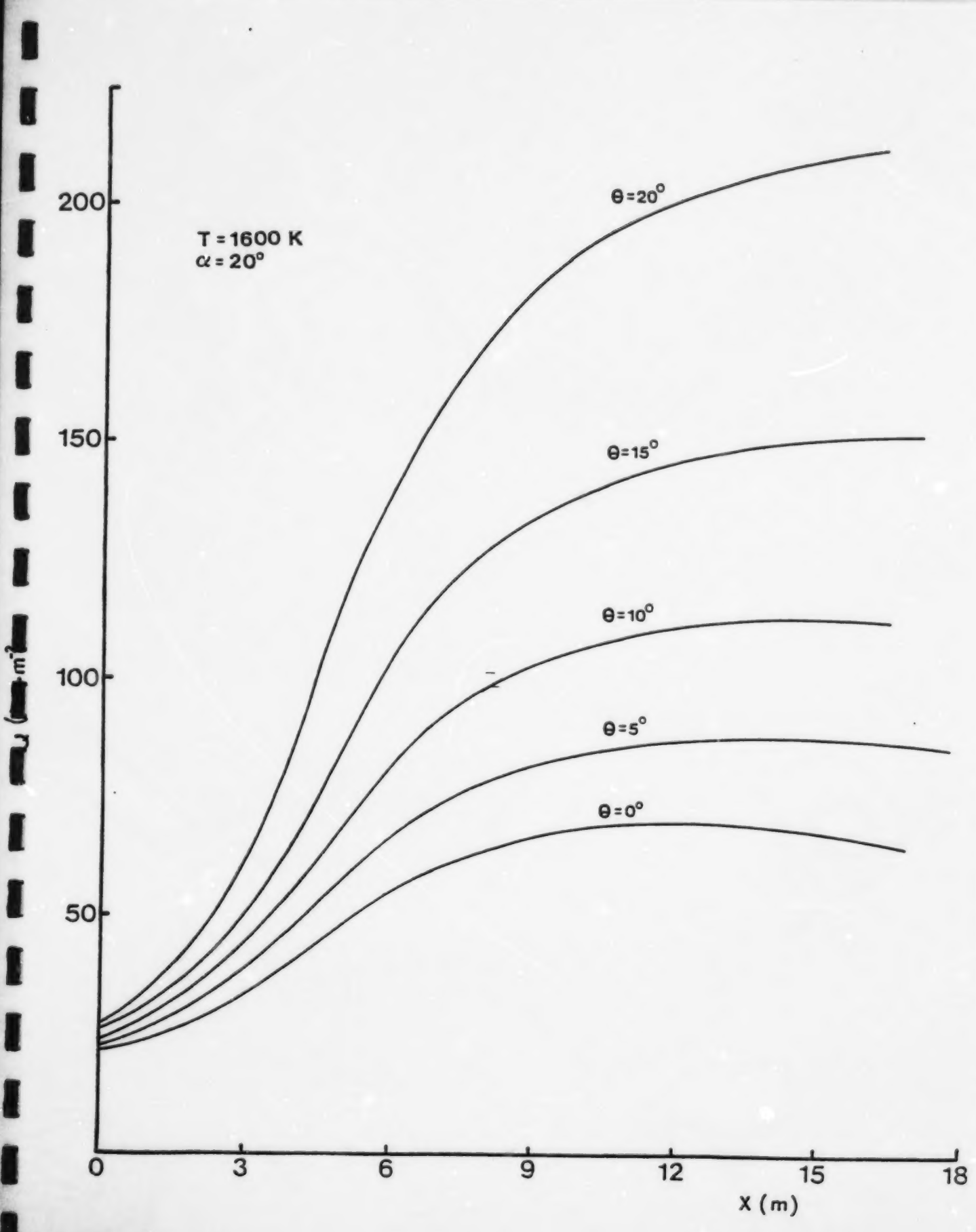
T = 1600 K
α = 20°
θ=20°
θ=15°
θ=10°
θ=5°
θ=0°
200
150
100
50
0
3
6
9
12
15
18
X (m)

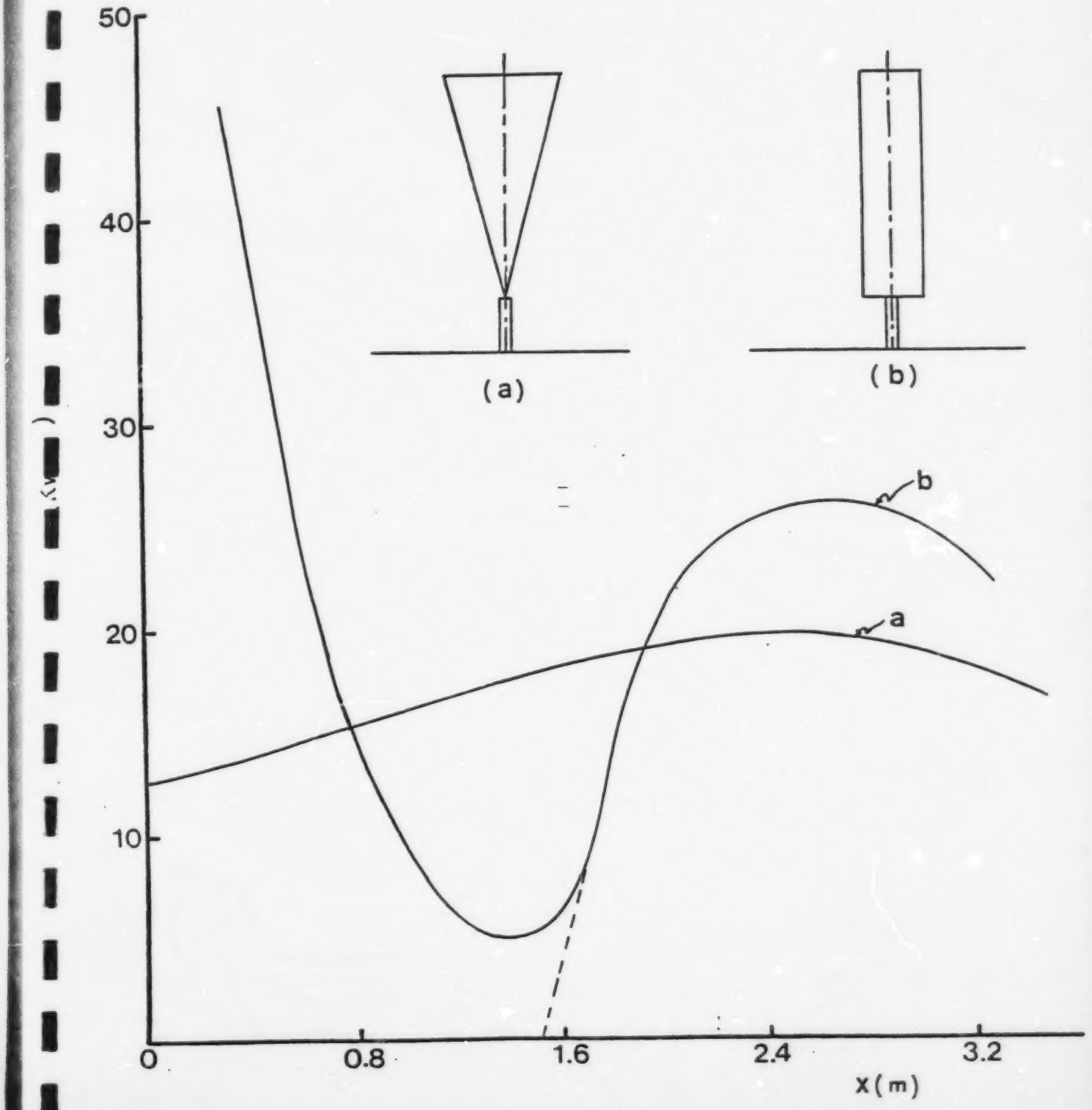
50
40
30
20
10
0
0.8
1.6
2.4
3.2
x(m)
(a)
(b)
a
b

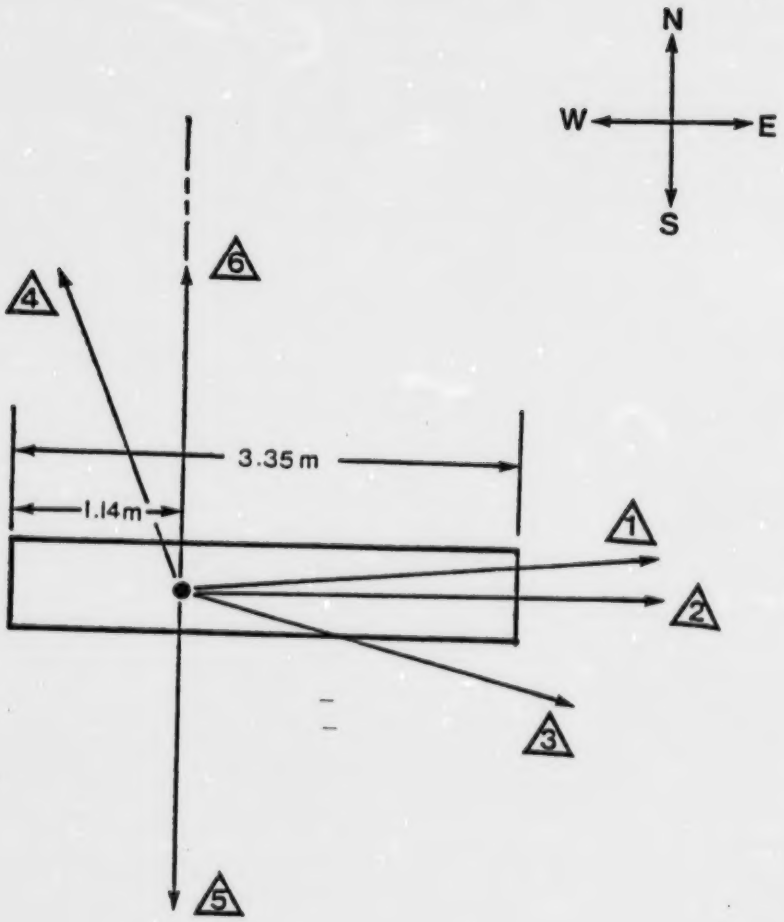
N
W
E
S
6
4
3.35 m
1.14 m
1
2
3
5

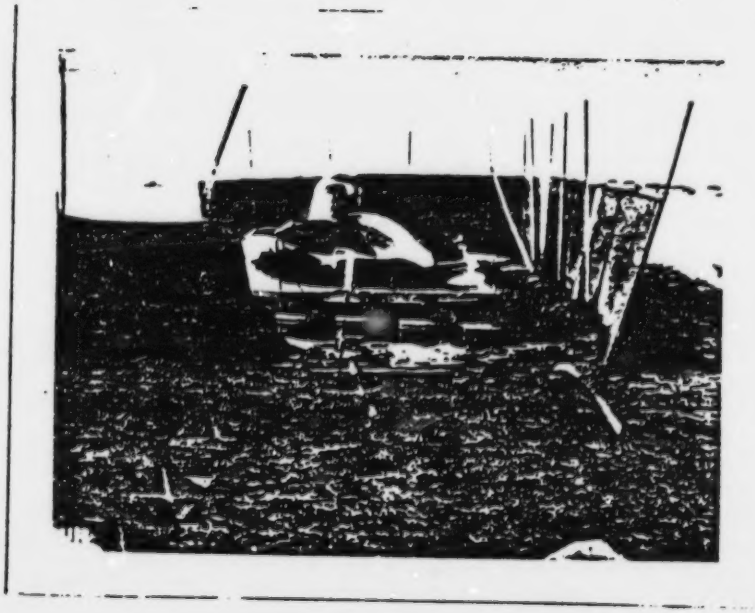

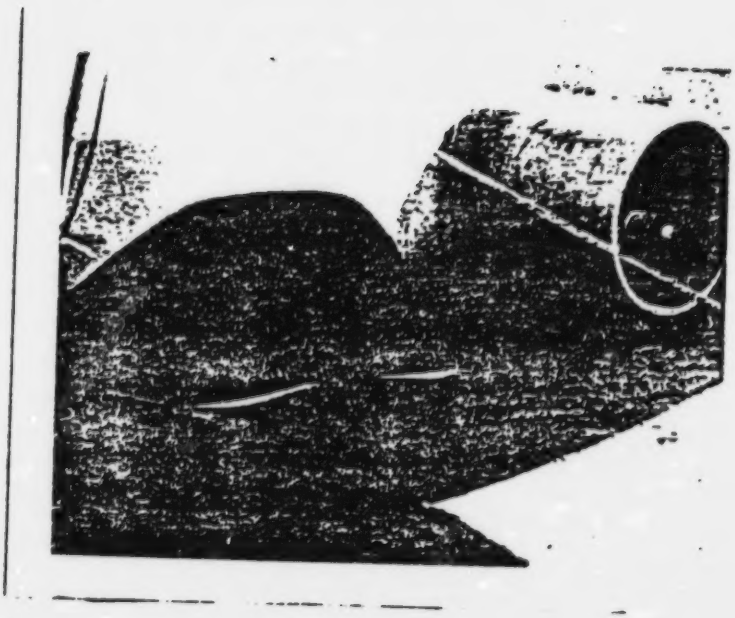

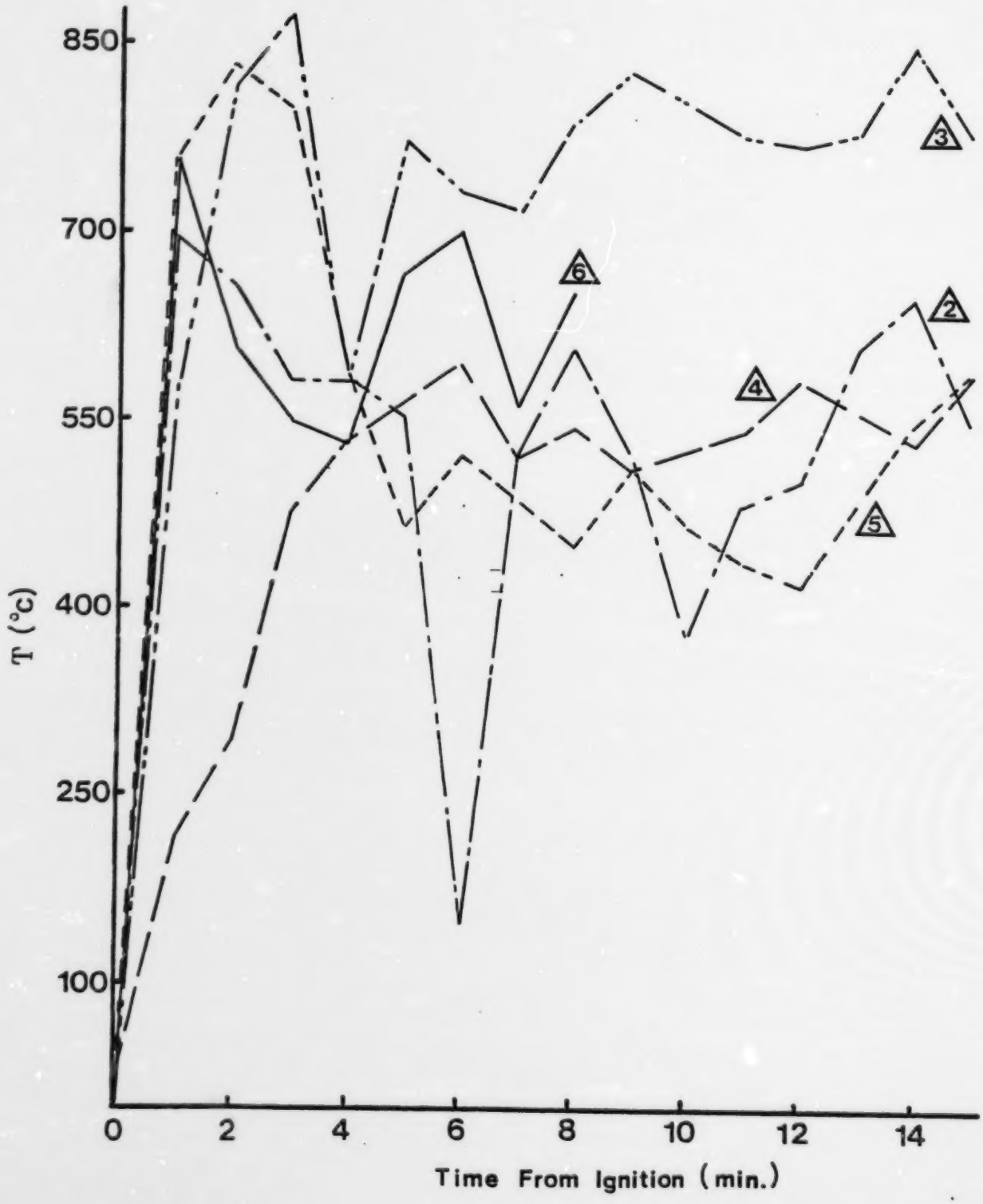
850
700
550
400
250
100
T (°C)
0
2
4
6
8
10
12
14
Time From Ignition (min.)
3
6
2
4
5